JAERI-Tech
94-007

DESIGN STUDY OF PROTOTYPE ACCELERATOR AND MeV TEST FACILITY FOR DEMONSTRATION OF 1 MeV, 1 A NEGATIVE ION BEAM PRODUCTION

August 1994

Takashi INOUE, Masaya HANADA, Shuichi MAENO*
Kenji MIYAMOTO, Yoshihiro OHARA
Yoshikazu OKUMURA and Kazuhiro WATANABE

日本原子力研究所
Japan Atomic Energy Research Institute

本レポートは，日本原子力研究所が不定期に公刊している研究報告書です。
入手の問合わせは，日本原子力研究所技術情報部情報資料課（〒319-11 茨城県那珂郡東海村）あて，お申し越しください。なお，このほかに財団法人原子力弘済会資料センター（〒319-11 茨城県那珂郡東海村日本原子力研究所内）で複写による実費頒布をおこなっております。

This report is issued irregularly.
Inquiries about availability of the reports should be addressed to Information Division, Department of Technical Information, Japan Atomic Energy Research Institute, Tokai-mura, Naka-gun, Ibaraki-ken 319-11, Japan.

編集兼発行　日本原子力研究所
印　　刷　㈱原子力資料サービス

Design Study of Prototype Accelerator and MeV Test Facility for Demonstration of 1 MeV, 1A Negative Ion Beam Production

Takashi INOUE, Masaya HANADA, Shuichi MAENO* Kenji MIYAMOTO
Yoshihiro OHARA, Yoshikazu OKUMURA and Kazuhiro WATANABE

Department of Fusion Engineering Research
Naka Fusion Research Establishment
Japan Atomic Energy Research Institute
Naka-machi, Naka-gun, Ibaraki-ken

(Received June 9, 1994)

In fusion reactors such as ITER, a neutral beam injector of MeV class beam energy and several tens MW class power is required as one of candidates of heating and current drive systems. However, the beam energy of existing high power accelerators are one order of magnitude lower than the required value. In order to realize a neutral beam injector for the fusion reactor,"Proof-of-Princeple" of such high energy acceleration is a critical issue at a reactor relevant beam current and pulse length. An accelerator and an accelerator facility which are necessary to demonstrate the Proof-of-Principle acceleration of negative ion beams up to 1 MeV, have been designed in the present study. The accelerator is composed of a cesium-volume type ion source and a multi-stage electrostatic acceleration system [Prototype Accelerator]. A negative hydrogen ion beam with the current of about one ampere (1 A) can be accelerated up to 1 MeV at a low operating pressure. Two types of acceleration system, a multi-multi type and a multi-single type, have been studied. The test facility has sufficient capability for the test of the Prototype Accelerator [MeV Test Facility]. The dc high voltage generator for negative ion acceleration is a Cockcroft-Walton type and capable of delibering 1 A at 1 MV (= 1 MW) for 60 s. High voltage components including Prototype Accelerator are installed in a SF_6 vessel pressurized at 6 kg/cm^2 to overcome high voltage gradients. The vessel and the beamline are installed in a X-ray shield.

Keywords: Accelerator, Ion Source, Ion Beam, Negative Ion, H^- , Neutral Beam, NBI, High Voltage, Cockcroft-Walton, X-ray

---

* Nissin Electric Co. Ltd.

１ＭｅＶ，１Ａ負イオンビーム生成実証のための原型加速器とＭｅＶ級イオン源試験装置の設計検討

日本原子力研究所那珂研究所核融合工学部
井上多加志・花田磨砂也・前野　修一*・宮本　賢治
小原　祥裕・奥村　義和・渡辺　和弘

（1994年６月９日受理）

ＩＴＥＲ等の核融合炉では，加熱電流駆動システムの候補として，ＭｅＶ級ビームエネルギー，数十MW級パワーの中性粒子入射装置が必要とされる。しかしながら既存高パワー加速器のビームエネルギーは必要とされるエネルギーより１桁以上低い。核融合炉に適した電流，パルス幅において，このような高エネルギー加速の「原理実証」を行うことが，核融合炉用中性粒子入射装置を実現する上で急務である。本研究では，１ＭｅＶまでの負イオンビームの加速原理実証のために必要な加速器と加速器試験施設の設計検討を行った。「原型加速器」はセシウム添加体積生成型負イオン源と多段静電加速系から構成される。低ガス圧力運転条件において約１アンペア（１Ａ）の水素負イオンビームを１ＭｅＶまで加速することができる。２種類の加速系，すなわちマルチーマルチ型とマルチーシングル型が検討された。「ＭｅＶ級イオン源試験装置」は原型加速器の試験を行うために十分な性能をもつ試験施設である。負イオン加速のための直流高電圧発生器は１ＭＶ，１Ａ（＝１MW）を60秒間発生しうるコッククロフトワルトン型電源である。原型加速器を含む高電圧機器は、高電界に耐えるために６kg/cm^{2}に加圧されたＳＦ$_6$ガス容器中に設置される。本装置は厚さ80cm以上のコンクリート製しゃへい内に据え付けられ，負イオンに付随して電子が加速された場合のＸ線に備える。

那珂研究所：〒311-01　茨城県那珂郡那珂町大字向山801-1
＊日新電気㈱

Contents

目　　次

1. INTRODUCTION

In fusion reactors, a neutral beam injector of MeV class beam energy and several tens MW class power is required as one of heating and current drive systems. For example in the Outline Design prepared for the TAC-4 (4th Technical Advisary Comittee meeting of ITER), the Neutral Beam Injection (NBI) is proposed as a back-up option which is compatible or competitive with the Ion Cyclotron Radio Frequency waves (ICRF) in heating and current drive. The NBI system is required to deliver a neutral deuterium beam of 50 MW, using four tangential beamline units. Each beamline unit has one ion source and accelerator which can accelerate an intense deuterium ion beam of around 30 A up to 1 MeV.

In the mean time, acceleration of several tens of milliamperes ion beam above 1 MeV is within a conventional technology in the high energy accelerator area. Additionally, a hydrogen negative ion beam of 0.18A has been accelerated up to 400 keV electrostatically[1]. However, acceleration of multi-ampere negative ion beams above 1 MeV has never been tried yet. As an intermediate step toward the full-current and full-energy acceleration, it is believed to be important to demonstrate stable acceleration of one-ampere level negative ion beams up to 1 MeV, namely, Proof-of Principle Acceleration demonstration. This demonstration would promise the realization of 1 MeV NBI systems. The present status and the goal for ITER of the negative ion source/accelerator development is shown in Fig. 1 together with the intermediate step.

The objective of the present task is to make a detailed design of a prototype of the full-energy 1A negative ion source /accelerator [Prototype Accelerator] and a test facility [MeV Test Facility] to demonstrate the Proof-of-Principle acceleration. The following R&Ds can be carried out in this test facility;

To develop a 1MeV electrostatic acceleration system which can produce a negative hydrogen ion beam stably with good beam optics,
To develop power supply components including a surge blocker and a high voltage transmission line which is compatible with the reactor relevant design, and
To test an accelerator insulator at a high voltage.

The detailed design of the Prototype Accelerator is described in Chapter 2, together with the ion source structure, accelerator structure and their design basis. In Chapter 3, the detailed design of the MeV Test Facility including a beamline system, a power supply system, and a layout will be described followed by a summary in Chapter 4.

Reference

[1] K. Watanabe, et al.; Private communication, attained at the JAERI 400keV test stand in January 1994.

940326

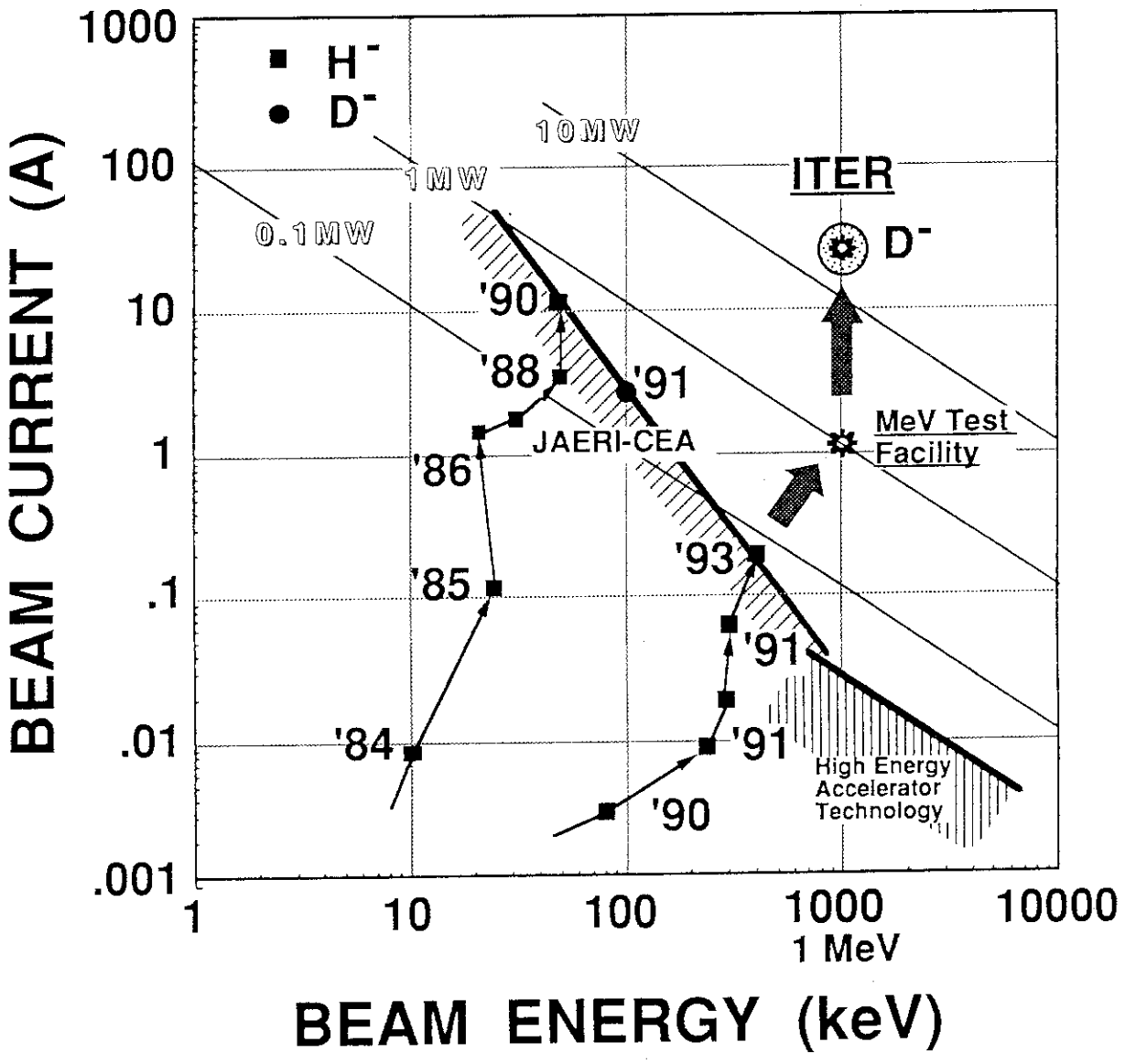

Fig.1 Negative ion source/accelerator development for the ITER neutral beam injection system

2. Design of Prototype Accelerator

2.1 Overview

The objective of the full energy test is to demonstrate stable, full energy acceleration at an intermediate current, but full current density. For this purpose, the Prototype Accelerator is designed so as to produce 1 MeV, 1 A hydrogen negative ion beams for a pulse length of 60 s with a current density of 13 mA/cm^2. The current density will be increased to 26 mA/cm^2 by masking the 1/2 section of the extractor. The major specifications of the Prototype Accelerator are listed in Table 2.1-1.

Table 2.1-1 Specifications of the Prototype Accelerator

Beam Energy:	1.0 MeV
Beam Current:	<1.0 A
Current Density:	13 - 26 mA/cm^2
Pulse Length:	60 s
Ion Species:	H^-
Beam Divergence:	5 mrad
Beam Size:	128 mm x 140 mm
Dimensions:	2.08 m in outer diameter
Weight:	4 ton

Figure 2.1-1 shows a cross-sectional view of the Prototype Accelerator. It consists of a plasma generator or a negative ion source, an extractor, an accelerator and an insulator column. Hydrogen negative ions are produced in the plasma generator via both volume and surface processes and extracted from the multi-aperture extractor. In the extractor, the H^- ions are pre-accelerated up to the energy of 10 keV, while the electrons extracted from the plasma are deflected magnetically and removed from the beam. Only the negative ions are accelerated up to 1 MeV in the multi-stage electrostatic accelerator. The accelerator has five-stages, each has 200 keV acceleration capability.

In the design of the Neutral Beam System for ITER, two types of the electrostatic accelerator are proposed by JAERI. One is called "Multi-Single" type, and the other is "Multi-Multi" type. In the Multi-Single type, multiple beamlets formed in the multi-aperture extractor are merged into a

single acceleration channel, while each beamlet is accelerated individually in a multi-aperture accelerator. Both types of the accelerator will be tested in the Prototype Accelerator. The Prototype Accelerator is to be installed in a SF6 gas vessel for high voltage insulation. Since the SF6 gas vessel is pressurized, the accelertor column is designed so as to sustain the pressure difference up to 0.7 MPa.

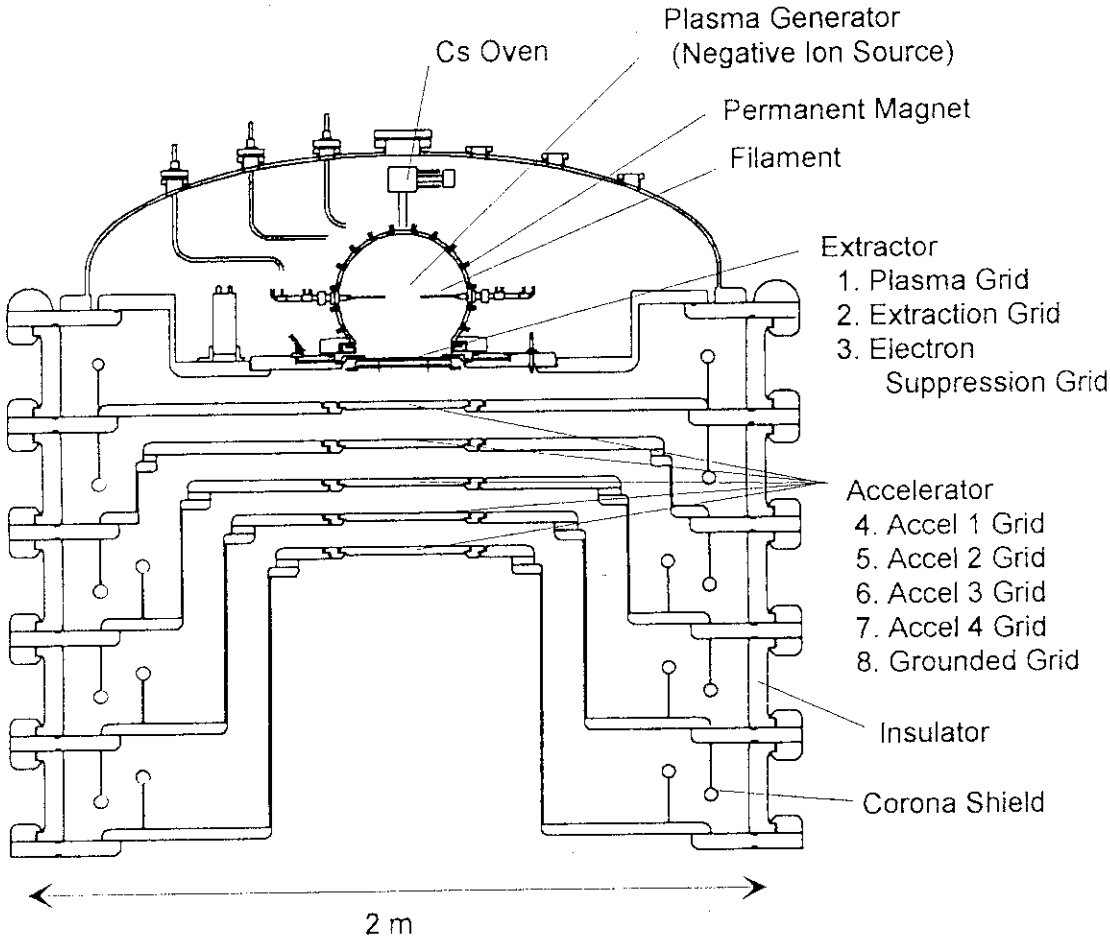

Fig.2.1-1 Cross-sectional View of the Prototype Accelerator

2.2 Plasma Generator (Ion Source)

The acceleration test should be conducted at the equivalent condition to the design specification of the ITER NB system. The requirements and specifications for the plasma generator, as the source of the negative ion, are listed below.

Table 2.2-1 Specification of the plasma generator

Type:	Magnetically Filtered Multicusp Plasma Generator
Negative Ion Production Method:	Cesium Seeded Volume Production
Cathode:	Tungsten Filament (1.2 mm dia. x eight)
Arc Input Power:	120 V x 400 A
Dimensions:	34 cm inner diameter, 34 cm in length (Semi-cylindrical; KAMABOKO)
Work Gas:	Hydrogen
Operational Pressure:	Typically 0.13 Pa
Ion Species:	H^-
Current Density:	13 - 26 mA/cm^2

A cesium seeded volume production type source is adopted as a plasma generator for the present test. In recent researches of negative ion production in the source of this type[1, 2], it is believed that the negative ion is produced by backscattering or desoption of neutral atoms at a surface with low work function, i.e. surface production. Keys of enhancing the surface production are in both decrease of work function[3] and generation of source plasma containing high ratio of atoms.

On designing the plasma generator, scaling of the plasma generator of this type[4] was studyed. A result of the scaling study is shown in Fig. 2.2-1 for various negative ion sources developed at JAERI. The figure indicates that the ion current density obtained is linearly corelated with the arc power density, i.e. arc power in the source plasma divided by the surface area of the plasma generator. This suggests that the negative ion production is dependent on the surface process.

Taking capacity of the arc power supply and the current density required into account, the surface area of the plasma generator was decided to be 5400 cm^2 from the figure. Choosing a semi-cylindrical shape for the surface/volume ratio to be a minimum, the dimension of the plasma generator was arranged as the dimension listed in the Table 2.2-1.

A merit of the plasma generator of the cesium seeded volume production tyoe is in reduction of operational gas pressure. The reduction of the pressure results in pressure decrease in the accelerator, which is essential to suppress stripping loss of negative ions due to the collision with gas molecules. To realize a reasonably efficient NB system, the source pressure should be below 0.3 Pa[5] to suppress the stripping loss below 30 % in the accelerator. Production of free charged particles (electron and positive ions), as a result of the stripping process, may trigger electric breakdown in the voltage holding parts of the accelerator. The operational gas pressure in the plasma generator was decided to 0.13 Pa in the presentr design of the plasma generator.

Figure 2.2-2 and 2.2-3 shows the plasma generator. The plasma generator is made of copper with water cooling pipes brazed on the outer surface. Arrangement and size of the the water pipes are designed on a basis of long pulse operation of the same type of sources[6, 7].

The plasma generator is designed to minimize loss area of primary electron, which generate highly dessociated plasma, by the shape and confinement magnets. Dimensions of the discharge chamber is 34 cm dia and 34 cm long (semi-cylindrical shape, KAMABOKO shape) to generate the discharge plasma of a high volume/surface ratio.

Equipped on the discharge chamber wall are permanent magnets in line cusp configuration. The same type of magnet as those in other JAERI negative ion sources are used in the plasma generator. The magnets are Sm2Co17 type, of which residual magnetic flux density (remanence) is 1.1 T. Size of the magnet are chosen to be 10 mm x 20 mm in cross sectional area. The magnetic line cusps are arranged every 18 degree on the side wall (cylindrical part). The line cusps are also arranged on the both end plugs in the same polarities as those in the neighbor line cusps on the side wall. The external magnetic filter[8] is formed by a pair of large permanent magnet embedded in the bottom flange of the plasma generator.

A result of three dimensional calculation of the magnetic field is shown in Fig. 2.2-4. Strong magnetic field is formed near the wall to prevent the primary electron loss to the wall, while large volume of field free region is formed in the center of the plasma generator. A transverse magnetic field is formed in the bottom of the plasma generator, which is to be faced to an extractor. A result of primary electron trajectory simulated in the computation is shown in Fig. 2.2-5. The primary electron is contained in the center region of the plasma for an efficient plasma generation. Negative ion is produced in the magnetic filter field, where the electron temperature is kept to be low to prevent destruction of the negative ion.

A cesium oven[9] is mounted on the top of the plasma generator. It is known in the experiment of this type of sources[2, 9] so far that introduction of a few hundreds milli-grams of cesium vapor is normally enough to reduce the work function on metal surface of this type of plasma generators. It is also proven that the cesium consumption rate[6] in a plasma generator of this type is small and the cesium effect lasts for more than a week.

A source of identical geometry / configuration was build in a domestic program and used in US-Japan collaboration experiment[10]. A result of the source is shown in Fig. 2.2-6. This figure shows the negative ion current density as a function of source filling pressure. The source could be operated stably at 70 V x 250 A arc discharge with the gas filling pressure of 0.13 Pa. In the low pressure, low power operation it was succeeded to produce a H^- ion beam of 10 mA/cm^2. By optimization of the plasma generator, required current density will be attained in the plasma generator.

Reference

[1] Y. Okumura et.al., Proc. 5th Symp on Production and Neutralization of Negative Ions and Beams, AIP conf. Proc. Series No. 210, Upton NY, (1989).
[2] T. Inoue et.al., Proc. 6th Symp on Production and Neutralization of Negative Ions and Beams, AIP conf. Proc. Series No. 287, Upton NY, (1992).
[3] Y. Suzuki et.al., "Measurement of Work Function of a Plasma Grid in a Cesium Seeded Negative Ion Source", JAERI-M 92-168 (1992) in Japanese.
[4] Y. Okumura et.al., private communication.
[5] M. Hanada et.al., "Estimation of Stripping Losses in an Accelerator of a High Energy Negative Ion Source", presented in 10th Annual Meeting of the Japan Society of Plasma science and Nuclear Fusion Research, Kawagoe, March 25-27 (1993).
[6] Y. Okumura et.al., Rev. Sci. Instrum. 63/4, 2708 (1991).
[7] M. Hanada et.al., "Long Pulse Operation of Multi-Ampere Negative Hydrogen Ion Source -2 A/10 s H- Beam Production-", presented in 9th Meeting of the Japan Society of Plasma science and Nuclear Fusion Research, Sendai, October 29-31 (1992).
[8] T. Inoue et.al., Nucl. Instrum. Meth. in Phys. Res. B37/38, 111-115 (1989).
[9] T. Inoue et.al., to be published in Plasma Devices and Operations Vol.2.
[10] T. Inoue et.al., to be published in Proc. 15th Symp. on Fusion Engineering, Hyannis MA, Oct 11-15 (1993).

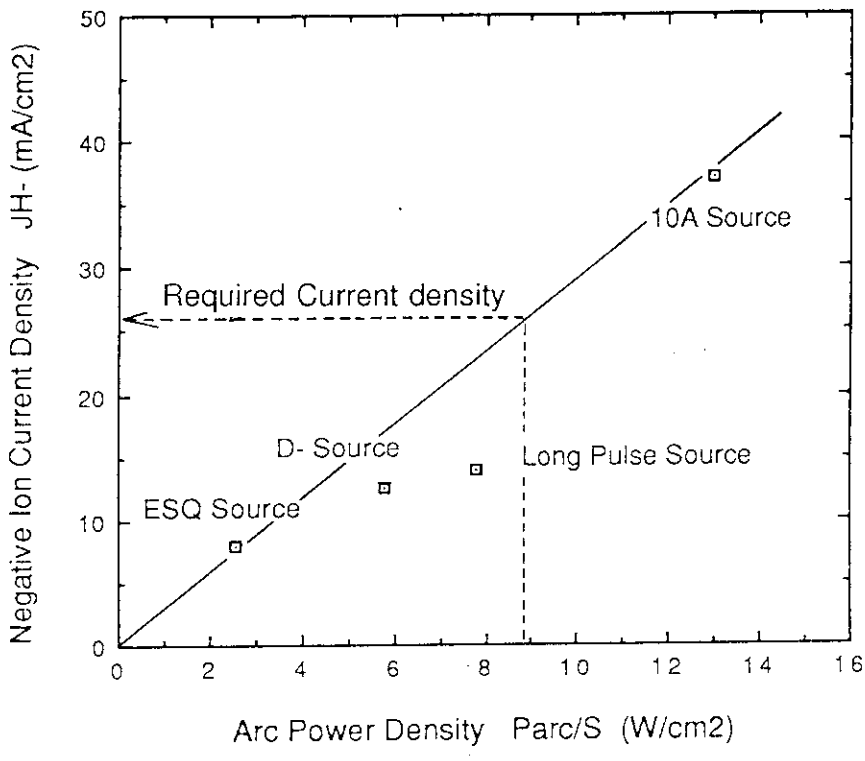

Fig.2.2-1 A scaling of the plasma generator performance for various sources developed at JAERI

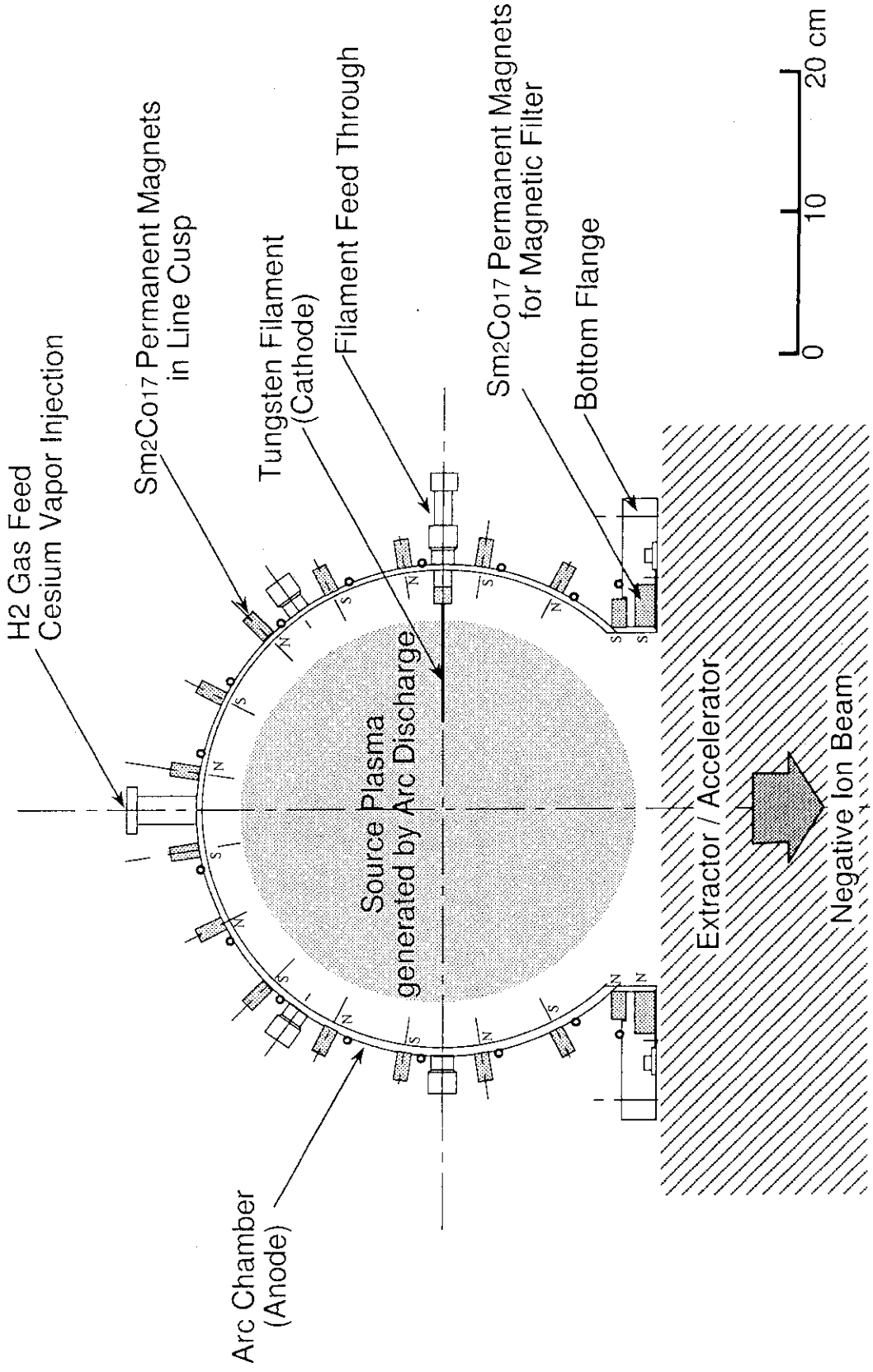

Fig.2.2-2 A cross-sectional view of the plasma generator for the prototype accelerator

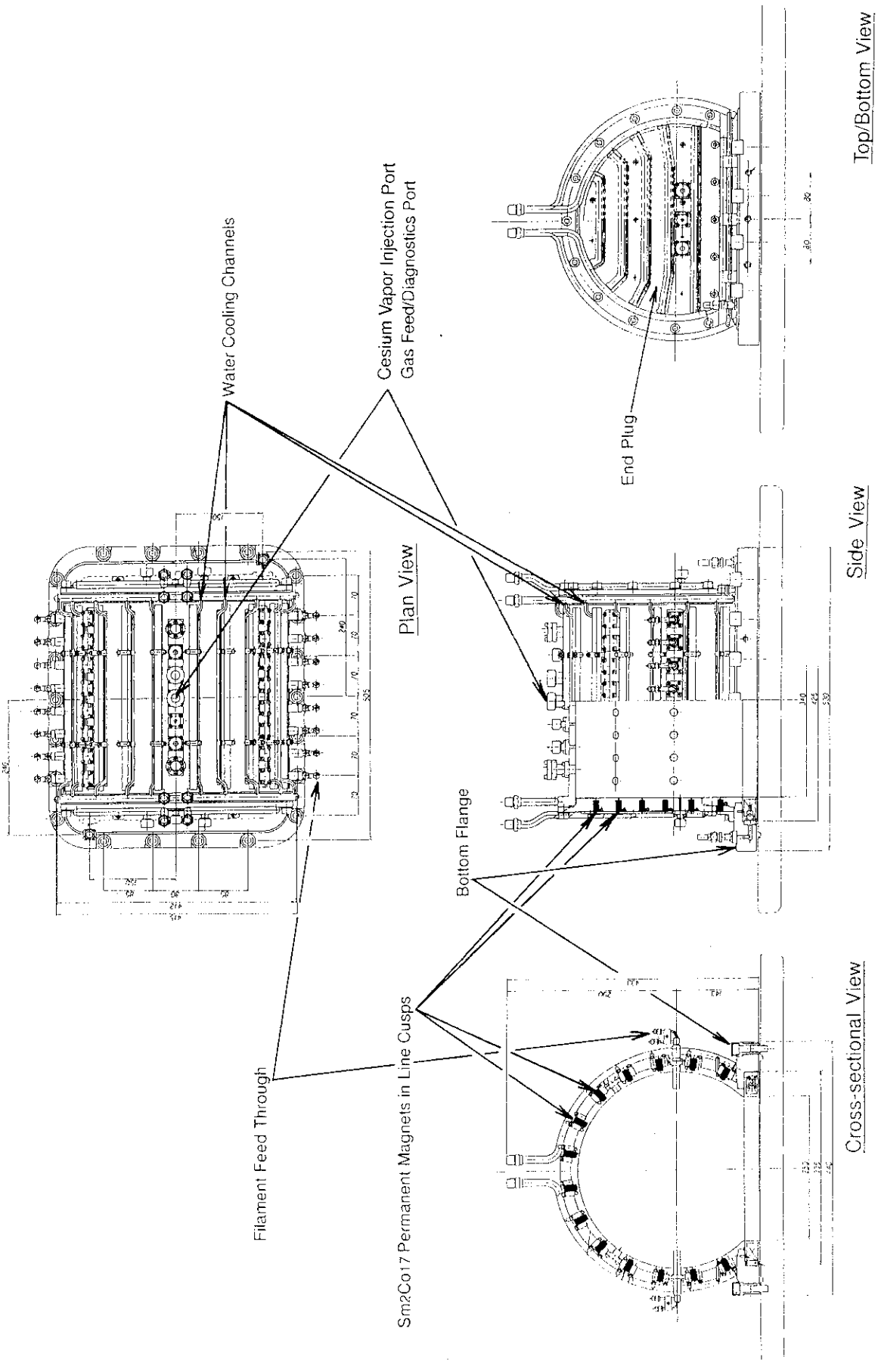

Fig.2.2-3 The plasma generator for the Prototype Accelerator

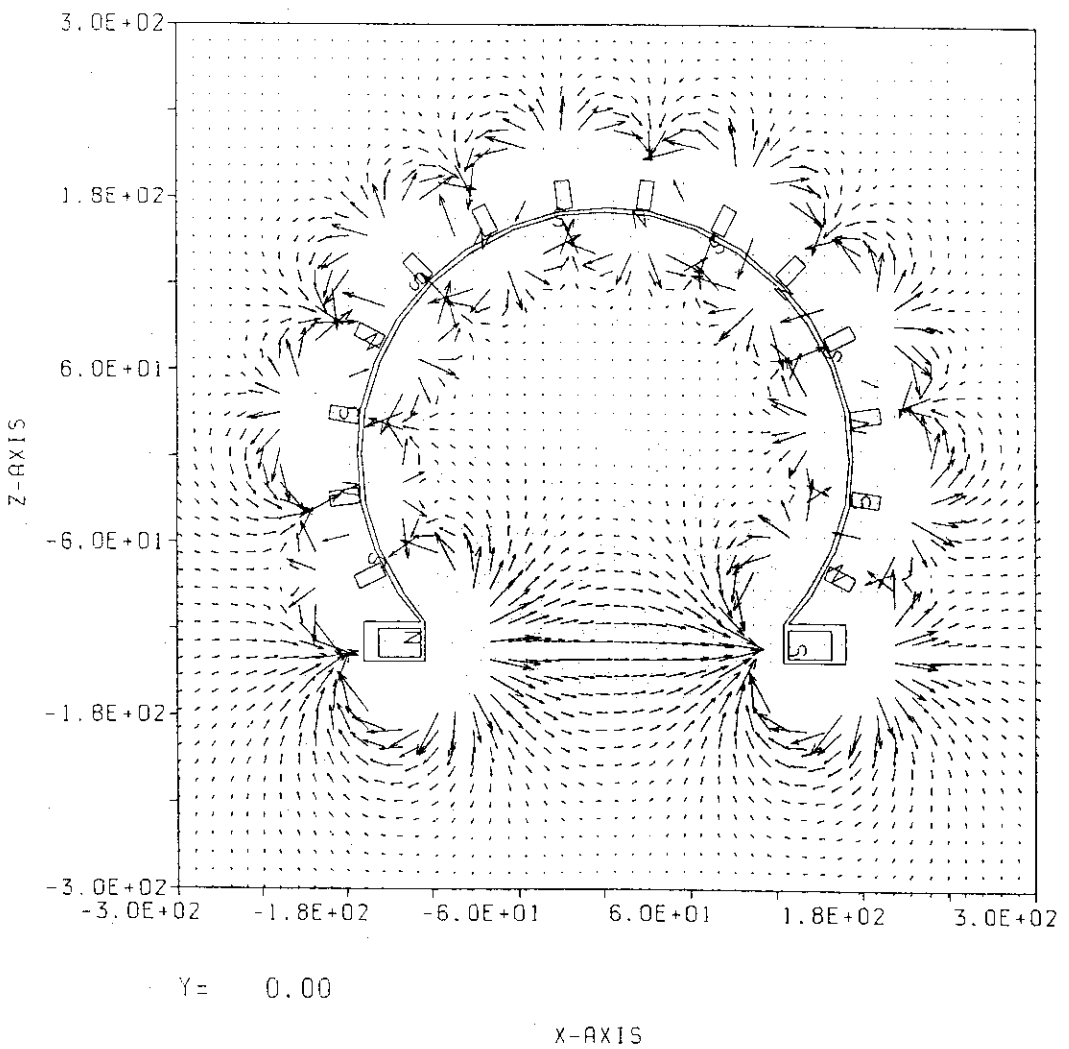

Fig.2.2-4 Magnetic field in the plasma generator

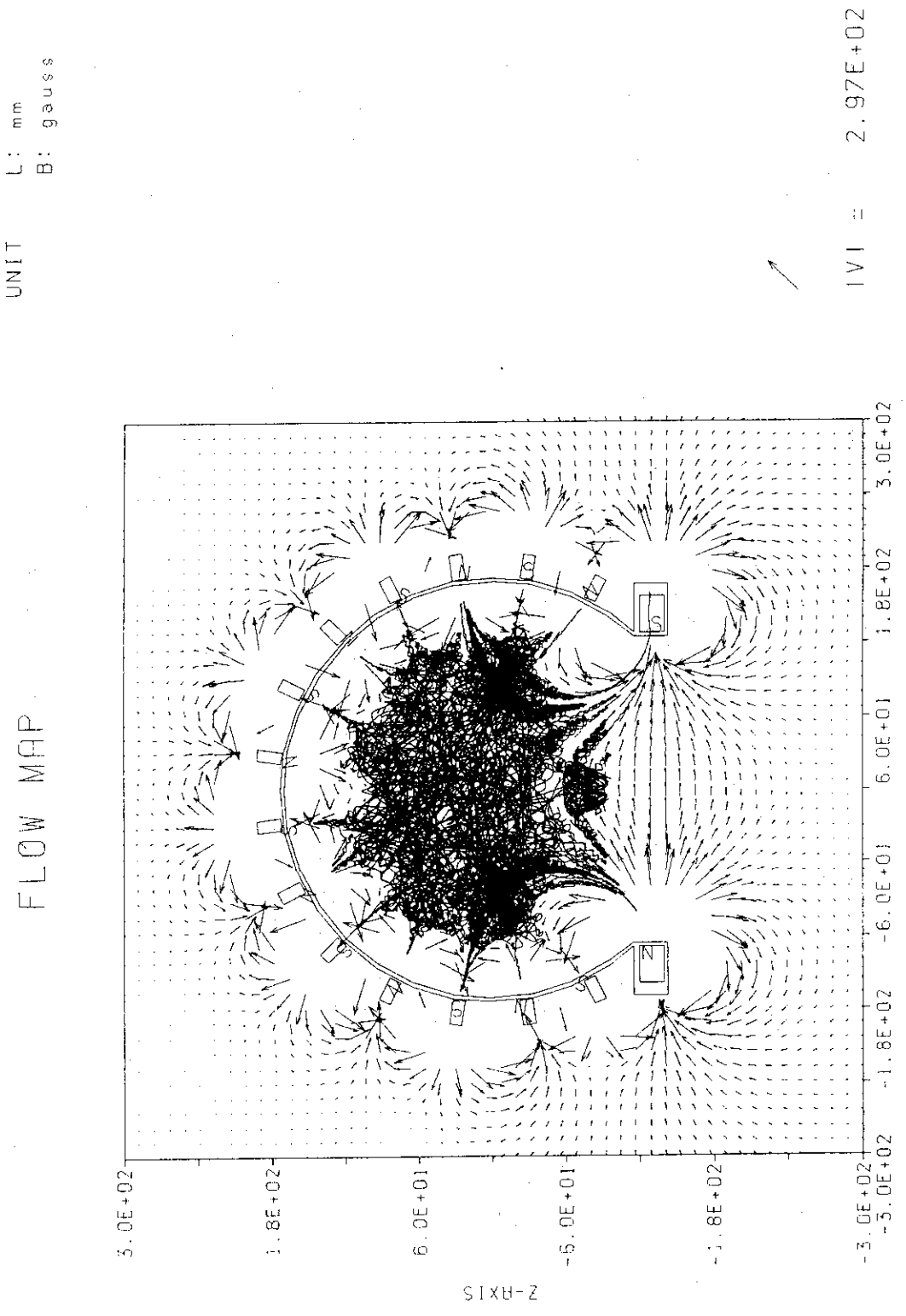

Fig.2.2-5 Primary electron trajectory in the plasma generator

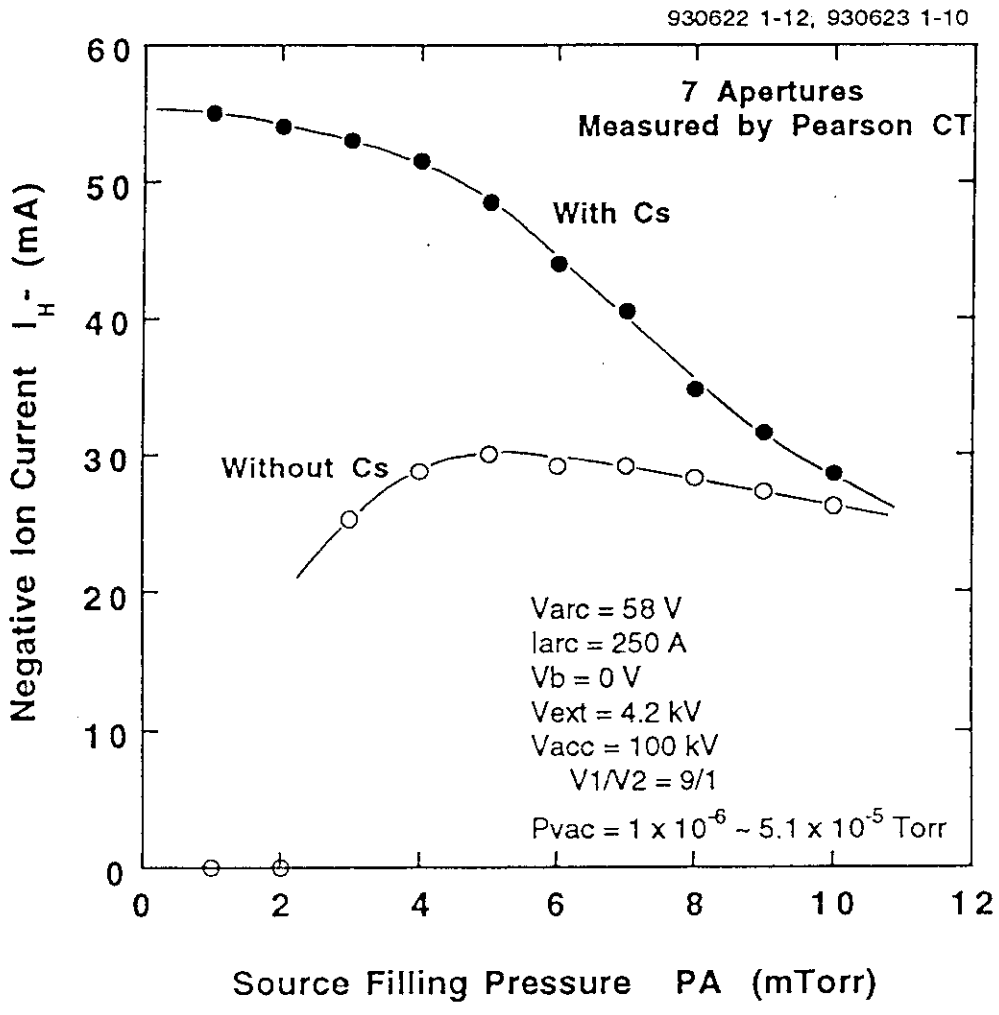

Fig.2.2-6 Negative ion current as a function of gas pressure

2.3 Exractor / Accelerator

The negative ions produced in the plasma generator are extracted electrostatically through multi-apertures in the extractor together with electrons from the source plasma. The electrons are deflected by a magnetic field in the extractor and inpinged on the second grid. While the ions are injected to the electrostatic accelerator, then accelerated up to a high energy.

The specifications of the extractor / accelerator are summarized in Table 2.3-1.

Table 2.3-1 Specifications of the extractor and the prototype accelerator

Extractor

Type:	Electrostatic with multi-apertures
Extraction voltage:	< 10 kV
Aperture:	7 x 7 array, 49 apertures of 14 mm dia.
Electron suppression:	Electron deflection by dipole magnetic field
	formed by pairs of magnets embedded in extraction grid
	Geometric and electrostatic trap on electron suppression grid
Heat removal:	Water cooling channel between apertures

Accelerator

Type:	Five stages electrostatic with multi-apertures
Acceleration voltage:	200 kV in each stage, 1MeV total
Aperture:	7 x 7 array, 49 apertures of 16 mm dia. ("multi-multi")
	Single aperture of large bore ("multi-single")
Electron suppression:	Electron deflection
	Magnet grooves in acceleration grids available
	Geometric trap may also available beneath acceleration grids
Heat removal:	Water cooling channel around each grid

Two types of extractor / accelerator have been proposed by JAERI for NB system of ITER EDA. One is called conventional "multi-multi (MM)" type extractor / accelerator, and the other is called as new "multi-single (MS)" type one. Concepts of these extractor / accelerators are illustrated in Fig. 2.3-1

MM type is designed in a conventional ES extractor / accelerator concept of fusion application. Negative ions are extracted through the multi-apertured extractor to form multi-beamlets. Each beamlet is injected directly into a corresponding apertures in the accelerator grids. Then the

beamlets are accelerated in the form of the multi-beamlets up to a high energy.

While in MS type, the beamlets extracted through the extractor are merged into a single, parallel beam of a high current. Then the merged beam is injected into the accelerator with relatively simple structure of single, large bore.

The beam cross-sectional area can be reduced in MS type extractor / accelerator. This enables to design the beamline of NB system to be slender and compact. A merit of such a system is, for example, in the decrease of neutron flux streaming back through the beamline to the ion source / accelerator, which lighten activation and degradation of functional materials due to neutron irradiation.

2.3.1 Multi-Multi Type Extractor / Accelerator

R&D of the extractor / accelerator of this type has been carried out for more than ten years at JAERI. The results were all utilized in the present design for MM type extractor / accelerator of the proof of principle test.

Extractor

The extractor assembly is shown in Fig. 2.3-2. The extractor consists of three grids, namely, plasma grid (PLG), extraction grid (EXG), and electron suppression grid (ESG). Each grid has 7 x 7 array of 49 apertures of 14 mm in diameter drilled within an area of 128 mm x 130 mm. The pattern of the multi-aperture and cross-sectional view of the aperture shape are shown in Fig. 2.3-3 and 2.3-4, respectively. The negative ion is extracted by electrostatic field between PLG and EXG together with electron.

PLG is faced to the source plasma in the plasma generator. In the cesium seeded condition, negative ion is produced on PLG by the surface process, and extracted through the apertures. Negative ion yield increases exponentially as decrease of work function of the PLG surface[1]. The work function of PLG surface is reduced by cesium coverage[2] of PLG metal substrate. Once an amount of cesium is seeded in the plasma generator, the cesium coverage on PLG is controlled by regulating the PLG temperature[3] heated by discharge power. Optimum temperature of PLG is normally 200 ~ 300 degreeC in the existing JAERI sources. Hence PLG is made of molybdenum for the high pemperature operation. To keep PLG temperature around these values, PLG is mounted on a support structure via ceramic thermal insulator. The temperature of PLG is monitored by a

thermocouple.

EXG is a 11 mm thick copper grid with water cooling pipes and magnet grooves. Embedded in the grooves are small permanent magnets for electron suppression. Size of the magnets are 5.4 mm x 4.9 mm in cross-sectional area. The magnet type is the same as used on the plasma generator. The magnet is arranged to form a dipole magnetic field[4], as shown in Fig. 2.3-5, for electron suppression. A part of the dipole field penetrate into the source plasma. The electron density near the emittion surface is decreased by the magnetic field. Adopting the dipole field negative ion is extracted accompanying electron of reduced current due to decrease of the electron density. Then electron extracted from PLG aperture is deflected by the dipole magnetic field and impinged on upper surface of EXG. The negative ion also affect the magnetic field slightly, however the deflection is compensated by another dipole field of the other polarity formed bottom of EXG.

ESG is the third grid made of copper to collect the leakage electron flowing through EXG apertures. The leakage electron is thought that secondary electron or stripped electron produced in EXG aperture. ESG works primarily as a geometric trap for such a low energy electron. By applying decceleration voltage of a few keV, electron leakage from the extractor to the accelerator is suppressed efficiently.

Accelerator

The accelerator has five acceleration stages which consist of four acceleration grids (A1G, A2G, A3G, and A4G from extractor side to downstream) and a grounded grid (GRG). Negative ion beam is electrostatically accelerated by 200 kV in each stage, to obtain a 1 MeV beam at the accelerator exit. A schematic of the accelerator is shown in Fig. 2.3-6. In each grid there are 49 apertures within an area of 130 mm x 142mm which is arranged as shown in Fig. 2.3-7. The diameter of apertures is 16 mm except for 4 apertures the corners. Each grid has a water cooling channel around the aperture area.

In the present design of the accelerator, (1) Optics of the beam, (2) Stripping loss in the accelerator, are evaluated. Acceleration efficiency and heat load on the acceleration grids are also discussed in the end of this section.

(1) Optics of the negative ion beam

In extraction / acceleration experiments at a relatively low energy it is known that the negative ion beams with remarkably small divergent angle can be obtained. The minimum beam divergent

angle of 1.5 mrad[5] was obtained from a single stage ES accelerator at JAERI. Such a small divergence is thought that original temperature of negative ion is very low[6] in volume production type source. Including the beam aberration in the accelerator into the value, 1.5 mrad, the temperature is estimated to be 0.2 eV. Thus the negative ion beam has a potential to form a fine, focussed beam.

Then next importance is in acceleration of the ion beam with good beam optics.

One of optical issues in the ES acceleration is expansion of accelerating beam due to the space charge. In ES accelerators of this type developed at JAERI, electrostatic lens formed in the grid aperture has been optimized to focus the expanding beam. The gap length between grids and high voltage applied in each grid are regulated so as to form a stronger electrostatic field in downstream. Consequently a convex focussing lens is formed in the aperture to compensate the expanded beam to be converging.

An example of the effectiveness of such a method is shown in Fig. 2.3-8. The result was obtained with 350keV Ion Source which consists of two stage ES accelerator[7]. Figure 2.3-8 shows the beam divergence angle as a function of the ratio of V_{A1} to V_{ACC}. Here V_{ACC} the acceleration voltage, and V_{A1} is electric potential of the Acceleration Grid, which is equal to the voltage in the second stage. As V_{A1} is higher, i.e, the electric field in the second stage becomes stronger with respect to that in the first stage, resulting in a formation of stronger focussing lens in the aperture. As in the figure the divergence angle is smaller in higher V_{A1}.

The each gap length of the MeV prototype accelerator is designed to be shorter in downstream stage to form a focussing electrostatic lens mentioned above.The gap length of the downstream stage is designed to be 85, 80, 75, 70, 65 mm, in each stage from extractor to downstream.

As for the ES accelerator of this type, 500 keV three stage acclerator[8] has been developed at JAERI. An example of the beam trajectory computation in the accelerator is shown in Fig. 2.3-9. Figure 2.3-10 and Figure 2.3-11 show the beam divergence angle obtained through a parameter survey in the accelerator as a function of J_{D^-} , Vext , respectively. the smallest beam divergence angle of 3.3 mrad was obtained at a condition that the extraction voltage Vext is 8 kV, the D^- current density J_{D^-} is 20 mA / cm^2. From this result an optimum condition of acceleration in the MeV prototype accelerator is scaled as follows;

Taking the mass effect of H^- / D^- into consideration, the current density J_{D^-} is converted to J_{H^-} by multiplying by $\sqrt{2}$. The optimum perveance P in the hydrogen operation is scaled as;

$$P = (20 \times 10^{-3}) \times \sqrt{2} / (8 \times 10^{3})^{3/2} = 3.95 \times 10^{-8}\ A / V^{3/2}$$

The beam optics is kept in the optimum in the MeV prototype accelerator at the same perveance. Taking J_{H^-} to be 26 mA / cm^2 as a typical current density, the extraction voltage at the scaled optimum condition is estimated as follows;

$$V_{ext} = (26 \times 10^{-3} / 3.95 \times 10^{-8})^{2/3} = 7.5\ kV$$

An example of the computation of the beam trajectory in acceleration up to 1MeV is shown in Fig. 2.3-12.

(2) Stripping loss in the accelerator

Much amount of stripping loss of negative ions in the accelerator is a serious problem because not only the ion current decreases but also stripped electrons / produced positive ions may cause such problems.

1) They lower the acceleration efficiency of negative ion beam.
2) They give heat loads on the acceleration grids and the grounded grid.
3) They cause breakdown between acceleration gaps.

The heat load in the acceleration grids were measured with 350keV Ion Source which has two acceleration stages[7]. The heat load as a function of the operational gas pressure in the plasma generator is shown in Fig. 2.3-13. Both in the Acceleration Grid (P_{A1}) and in the Grounded Grid (P_G) the heat loads vary approximately linearly as varying the pressure. The broken lines show an extrapolation of the heat loads to zero (0) Pa at which there is no stripped electron, neutral particle, and positive ion produced by the stripping. The extrapolated value is almost zero in the grounded grid, only 2% in the acceleration grid, respectively. This result indicates that the heat loads are mainly due to these particles rather than the direct incidence of H^- beam or stripped electrons in the extractor. Hence the heat loads will be suppressed significantly by reducing the operational gas pressure.

The solid lines in the figure show the heat loads calculated using a three dimensional Monte-Carlo gas flow code developed at JAERI[8]. The result of the calculation with the experimental are in good agreement in the acceleration grid, while the heat load measured in the experiment is larger than

the analytical prediction in the grounded grid. From this comparision, it is presumed that some of stripped electrons and neutral particles produced in the first stage flow into the second stage through the acceleration grid, then give the heat loads to the grounded grid.

Next the heat loads in the acceleration with three stages[9] were investigated. The heat loads in each acceleration grid and the grounded grid as a function of the extraction voltage are shown in Fig. 2.3-14. The minimum values of heat loads in the Acceleration Grid1 (PA1), the Acceleration Grid2 (PA2), the Grounded Grid (PG) are 4.8%, 5.4%, 2.9%, respectively. Althogh PA2 is larger than PA1 , PA2 does not increases largely in comparison with PA1. On the other hand PG in the three-stages is almost eqaul to in the two-stages (see Fig.2.3-13). This suggests some of the stripped electrons and the neutral particles produced in the first stage flow into the second stage through the Acceleration Grid1, however, do not fiow into the Grounded Grid.

A weak transverse magnetic field is formed in the extractor /accelerator as a leakage field from the plasma generator. The magnetic field is so weak for the ion trajectory, however, it is enough to affect the stripped electrons. Even if the electron is deflected slightly by the leakage magnetic field, they are inpinged on Acceleration Grid after a few stages of acceleration. This is an merit of the multi-stage ES acceleration.

By calculating gas flow in the extractor / accelerator stripping loss of the negative ion in the accelerator was evaluated in the MM type of the present design. Followings are assumed in the calculation;

1) Temperature of the gas: 293 K
2) Apertures in the extractor are modeled as a single aperture of the same diameter.
   length of the modeled aperture was taken as an equivalent thickness of the extractor
3) Beam energy in the accelerator gap was taken as an average energy in the gap

Although all these assumptions give an over estimation, resulting in a safety mergin in the present design of the accelerator. Processes and the result of the calculation is summarized in Table 2.3-2. The total stripping loss is evaluated to be 13.6 %. The pressure is higher in the upstream in the accelerator, subsequently the stripping loss is higher in the upstream stages. The stripping loss is evaluated to be 8.0 % at maximum in the first stage. However the leakage magnetic field is stronger in the stages. It is expected that the stripped electrons in the upstream stages are deflected effectively as found in the experiment.

By extrapolating from this experimental data, the total heat loads in the acceleration grids is estimated to be 22 kW at the maximum. For the one minutes contenious beam production, Water cooling channels are brazed around each grid.

2.3.2 Multi-Single Type Extractor / Accelerator

Concepts of a "multi-single" type extractor / accelerator have been developed at JAERI[12], and LBL[13]. A test[14] of the "multi-single" extractor / accelerator was carried out first under a US-Japan collaboration combining JAERI negative ion source, multi-apertured extractor, and LBL ESQ (electrostatic quadrupole) accelerator. A 100 mA H^- ions are merged into a single parallel beam[14]. Then the merging beam was accelerated up to 200 keV in the ESQ accelerator. Loss or emittance growth of beam in the accelerator was not observed.

From the successful results of the US-Japan collaborative experiment, the merging technique of one ampere class negative ion beam came into a scope of next demonstration.

A schematic of the one ampere class merging system is illustrated in Fig. 2.3-15. Basic structure of the extractor is the same as that used in MM system. One exception to that is a shape of the extractor. The grids in the extractor are curved spherically so as to form the multi-beamlets toward a geometric focal point. Pre-accelerator is located between the extractor and the accelerator to form a merging beam. Focussing grid, with single bore, is located in the pre-accelerator. High voltage ranging 100 ~ 200 kV are applied between the extractor and the focussing grid to accelerate the multi-beamlets to a higher energy. In the meantime, the multi-beamlets are focussed and merged into a single beam in the preaccelerator. The merged beam is formed to be a parallel beam in an electrostatic lens at the focussing grid, then injected into the ES accelerator.

An acceleration of MeV, ampere class negative ion beam is an impotant demonstration in the R&D of prototype accelerator for ITER NB. One of ways to achieve the milestone is to develop a simple accelerator for reseach of pure acceleration physics in the MeV ampere class beam acceleration at a relatively low current density of 13 mA/cm^2. Hence MM type extractor / accelerator is adopted first in the present design as a prototype extractor / accelerator for ITER NB system. Production of one ampere class merging beam is planed at JAERI combining the merging system with an electrostatic accelerator.

Reference

[1] Y. Suzuki et.al., "Measurement of Work Function of a Plasma Grid in a Cesium Seeded Negative Ion Source", JAERI-M 92-168 (in Japanese), (1992).
[2] K. Shinto et.al., "Measurement of Work Functions of a Plasma Grid by Laser", presented in 10th Annual Meeting of the the Japan Society of Plasma science and Nuclear Fusion Research, Kasugai, March 25-27 (1994).
[3] Y. Okumura et.al., Proc. 5th Symp. on Production and Neutralization of Negative Ions and Beams, AIP Conf. Proc. No. 210, Upton NY, (1990).
[4] Y. Okumura et.al., Proc. 11th Symp. on Fusion Eng., Austin, TX, Nov. 18-22 (1985).
[5] T. Inoue et.al., Proc. 14th Symp. on ISIAT '91, 137, Tokyo (1991).
[6] P. Devynk, M. Bacal et.al., Rev. Sci. Instrum., 60/9, 2873 (1989).
[7] K.Miyamoto, et al. Proc. of the Third Workshop on Negative Ion Formation and Beam Handling KEK, August 18-19, 1993
[8] M.Hanada, et al. "A Large Negative Ion Source for JT-60U", presented in 10th Annual Meeting of the the Japan Society of Plasma science and Nuclear Fusion Research, Kasugai, March 25-27 (1994).
[9] K.Watanabe, private communication
[10] K.Watanabe, et al., A Memo of Plasma Research Meeting, The Institute of Electrical Engineers of Japan, EP-93-48, August 24 (1993).
[11] M. Kuriyama et.al., "Design Report of N-NBI System for JT-60, to be published in JAERI-M 93-XXX.
[12] Y. Ohara et.al., "A Review of JAERI R&D Activities on the Negative-Ion-Based Neutral Beam Injection System", JAERI-M 90-154, (1990).
[13] C. F. Chan, O. A. Anderson et.al., "Preaccelerator for Merged Beamlets", Proc. US-Japan workshop on negative-ion-based NBI development, vol. 3, Berkeley CA, Oct. (1990).
[14] T. Inoue et.al., to be published in Proc. 15th Symp. on Fusion Eng., Hyannis MA, Oct. 11-15 (1993).

Table 2.3-2 Calculation of stripping loss in the MM Type ES accelerator.
The extractor grids were modeled to be a single plate with 49 apertures.

	A	B	C	D	E	F	G	H	I	J	K	L	M	N
1	Assumption				Gap	Energy		Cross Section		Gap Length				
2														
3	Source Pressure (PA)	0.13	Pa											
4					Extractor-A1G	100	keV	3.95E-16	cm2	8.5	cm			
5	Pumping Speed (S)	120	m3/S											
6					A1G-A2G	300	keV	2.05E-16	cm2	8	cm			
7	Gas temperature (T)	293	K											
8					A2G-A3G	500	keV	1.3E-16	cm2	7.5	cm			
9	Boltzman Const. (k)	1.3807E-23	JK-1											
10					A3G-A4G	700	keV	1E-16	cm2	7	cm			
11	Extractor Grid													
12	Aperture dia. , d	14	mm		A4G-GRG	900	keV	7.9E-17	cm2	6.5	cm			
13	Grid Thickness, l	25	mm											
14														
15	Acc. Grid													
16	Aperture dia. , d	16	mm											
17	Grid Thickness, l	20	mm											
18														
19	Number of Apertures	49												
20														
21	Grid Conductance	Cn = K1(l/d) C0												
22		K1 Fitting Available: 0<l/d<2.0												
23		C0 = 91 d^2: for Orifis												
24														
25	Mass Coeff.	3.79												
26														
27	Gap		l/d	K1	C0	Conductunce		Pressure		Density		Survived H-	Stripping Loss	
28														
29	Extractor-A1G													
30		C1	1.8	0.37	1.78E-02	1.22468637	m3/s	0.1001237	Pa	2.475E+13	n/cm3	0.92025964	0.0797	
31	A1G-A2G													
32		C2	1.43	0.424	2.33E-02	1.83277408	m3/s	0.08016	Pa	1.9815E+13	n/cm3	0.96802513	0.032	
33	A2G-A3G													
34		C3	1.43	0.424	2.33E-02	1.83277408	m3/s	0.0601962	Pa	1.488E+13	n/cm3	0.98559637	0.0144	
35	A3G-A4G													
36		C4	1.43	0.424	2.33E-02	1.83277408	m3/s	0.0402324	Pa	9.9454E+12	n/cm3	0.99306241	0.0069	
37	A4G-GRG													
38		C5	1.43	0.424	2.33E-02	1.83277408	m3/s	0.0202687	Pa	5.0104E+12	n/cm3	0.99743048	0.0026	
39	A4G (C7)													
40		C6	1.43	0.424	2.33E-02	1.83277408	m3/s	0.0003049	Pa	7.5373E+10	n/cm3	1	0	
41	GRG (C8)													
42														
43					Total C	0.28211606	m3/S						Total Stripping	
44					Q	0.03658907	m3/S						0.1356	
45					PVAC	0.00030491	Pa							

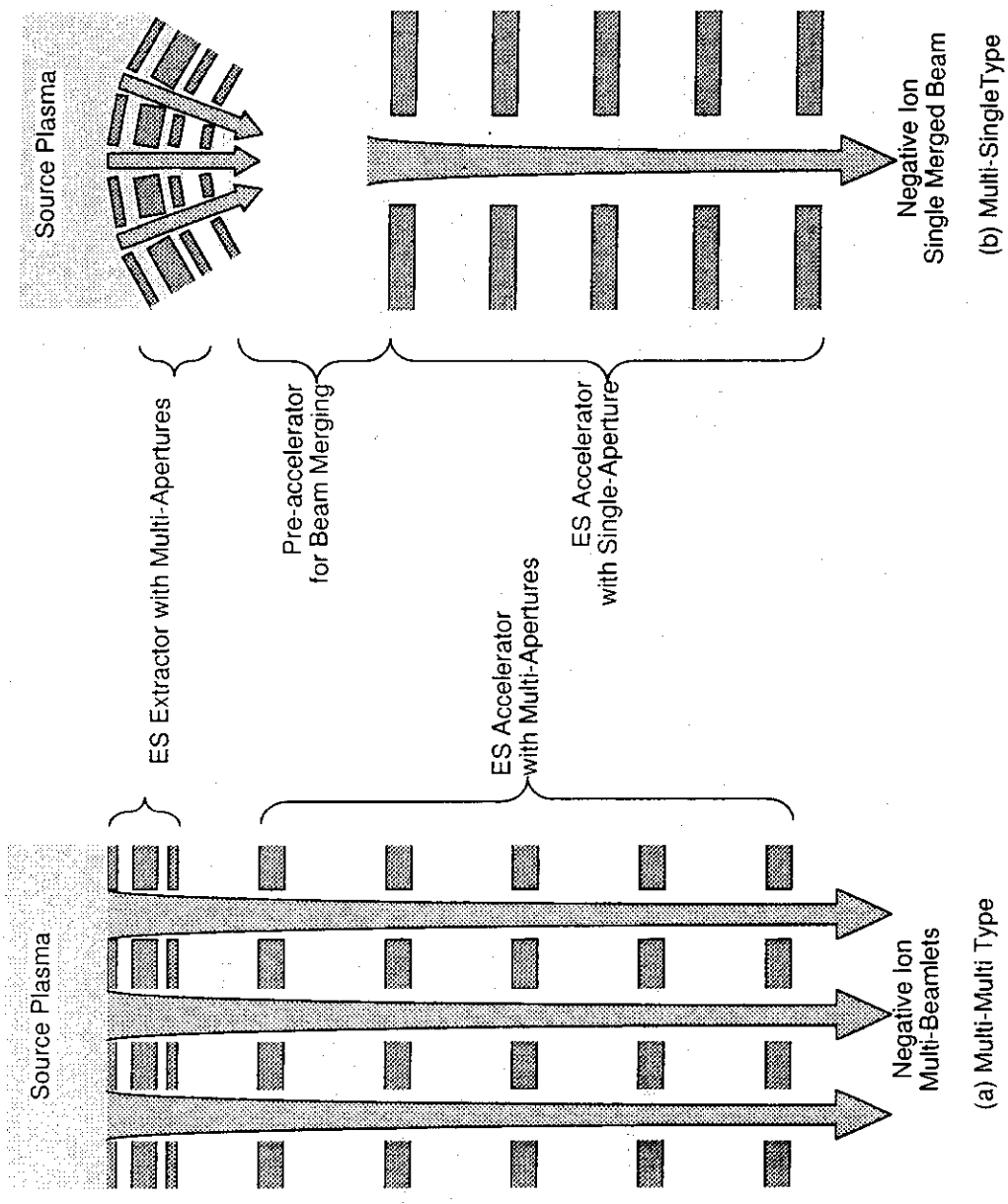

Fig.2.3-1 A conceptual illustration of (a) Multi-Multi Type and (b) Multi-Single Type electrostatic accelerator

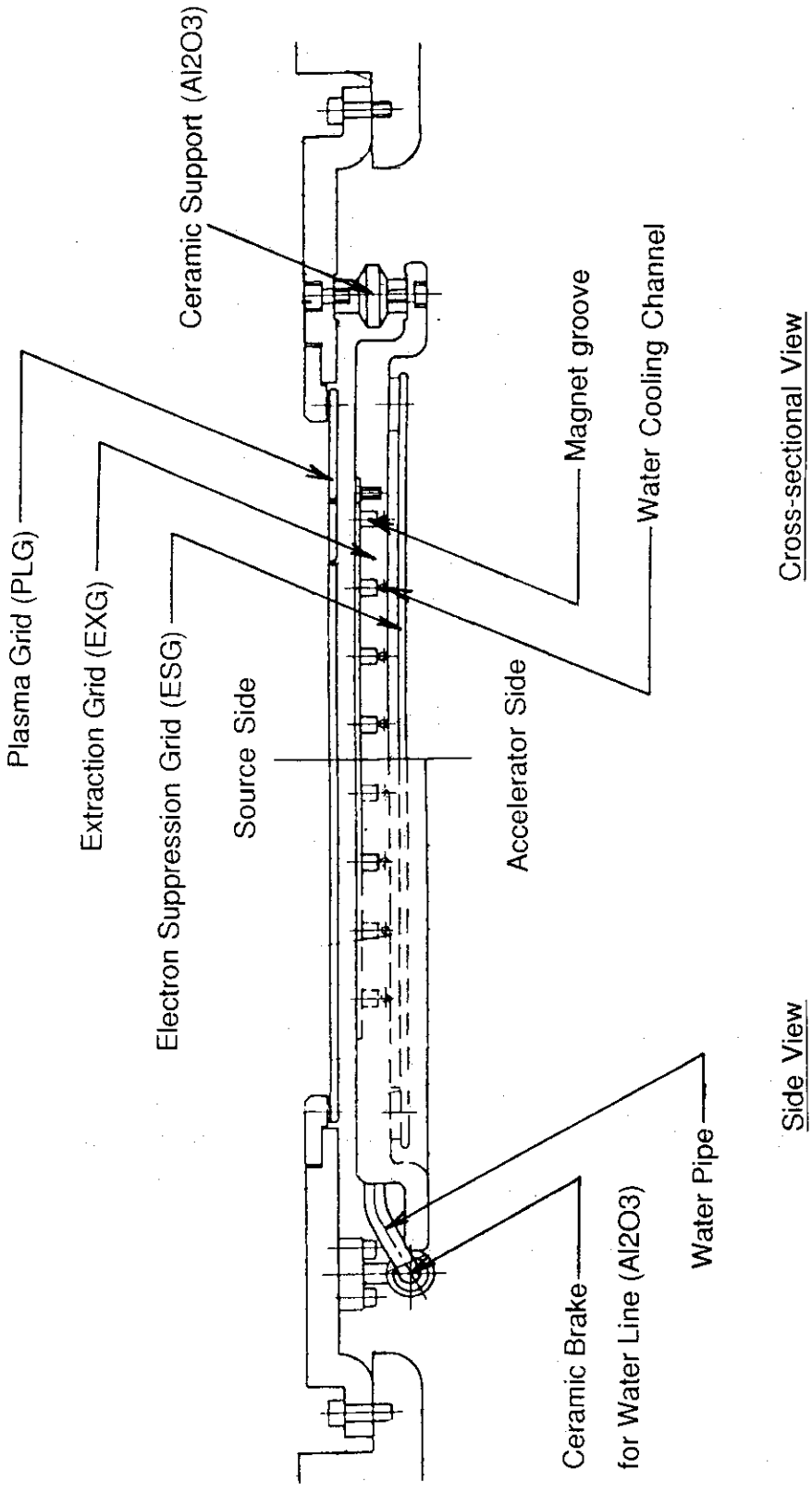

Fig.2.3-2 A side and cross-sectional view of the extractor assembly.

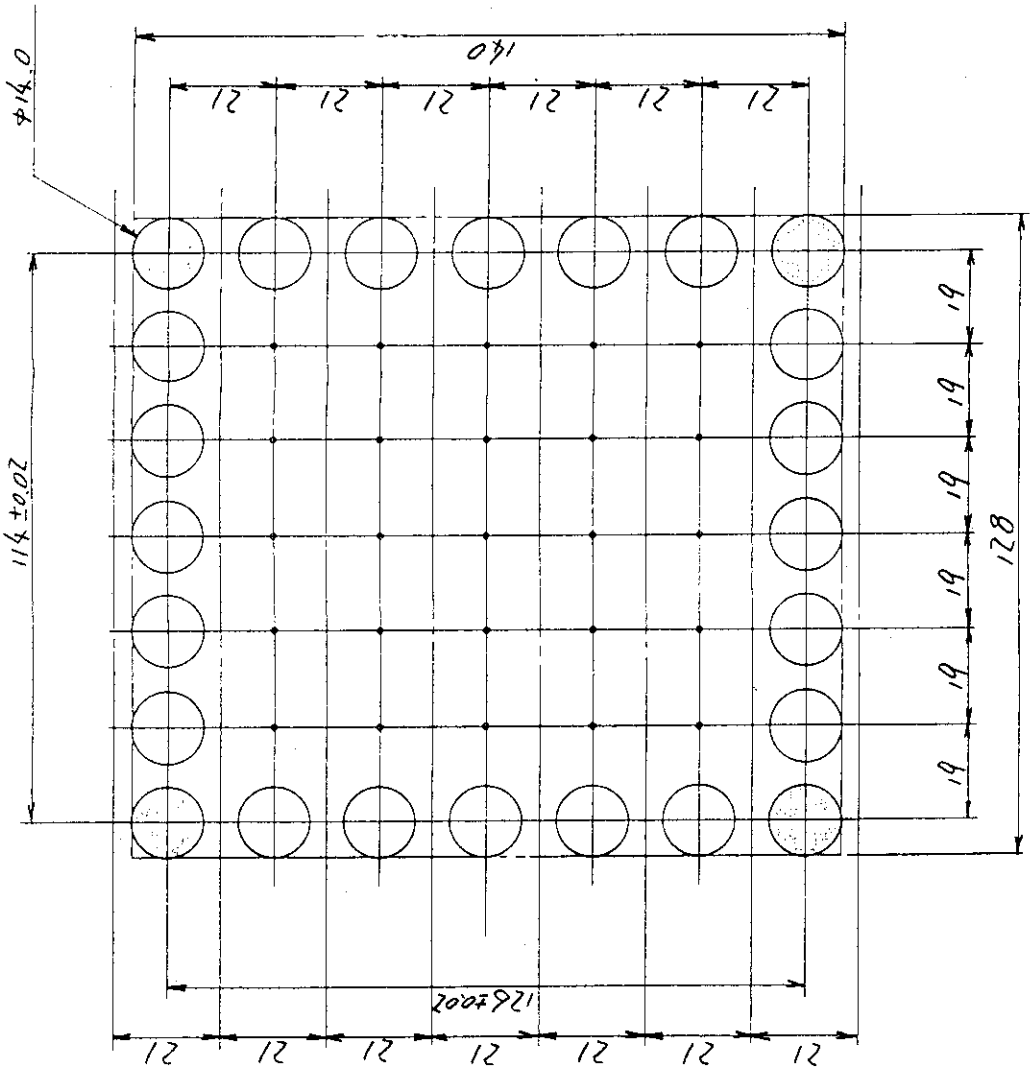

Fig.2.3-3 The pattern of multi-apertures in the extractor.
The 49 apertures in the arrangement of 7×7 array are drilled in an area of 128 mm×140 mm. The aperture diameter is 14 mm.

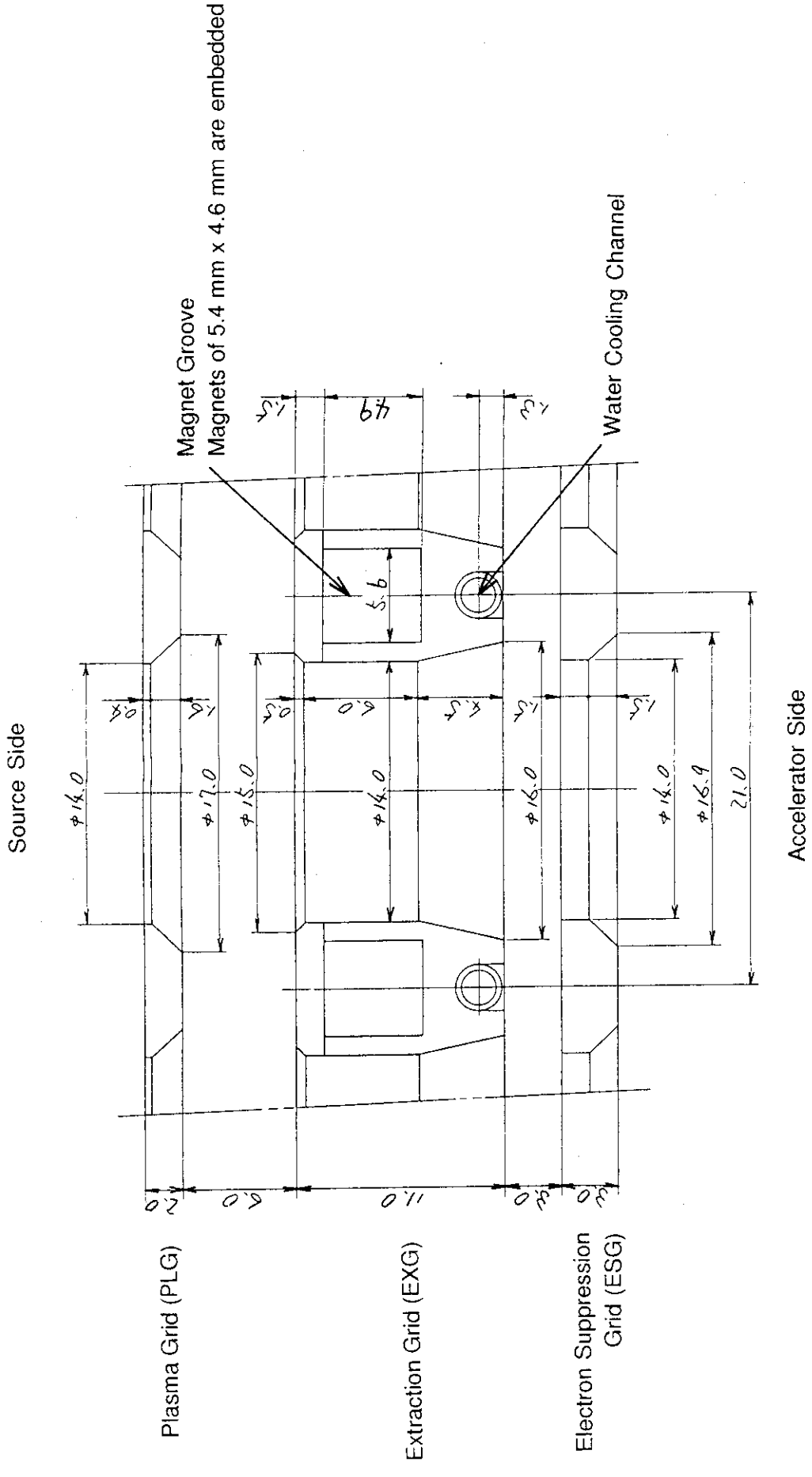

Fig.2.3-4 A cross-sectional view of the apertures in the extractor. The apertures in each grid are shaped so as to reduce the beam divergence by the electrostatic lens formed in the apertures.

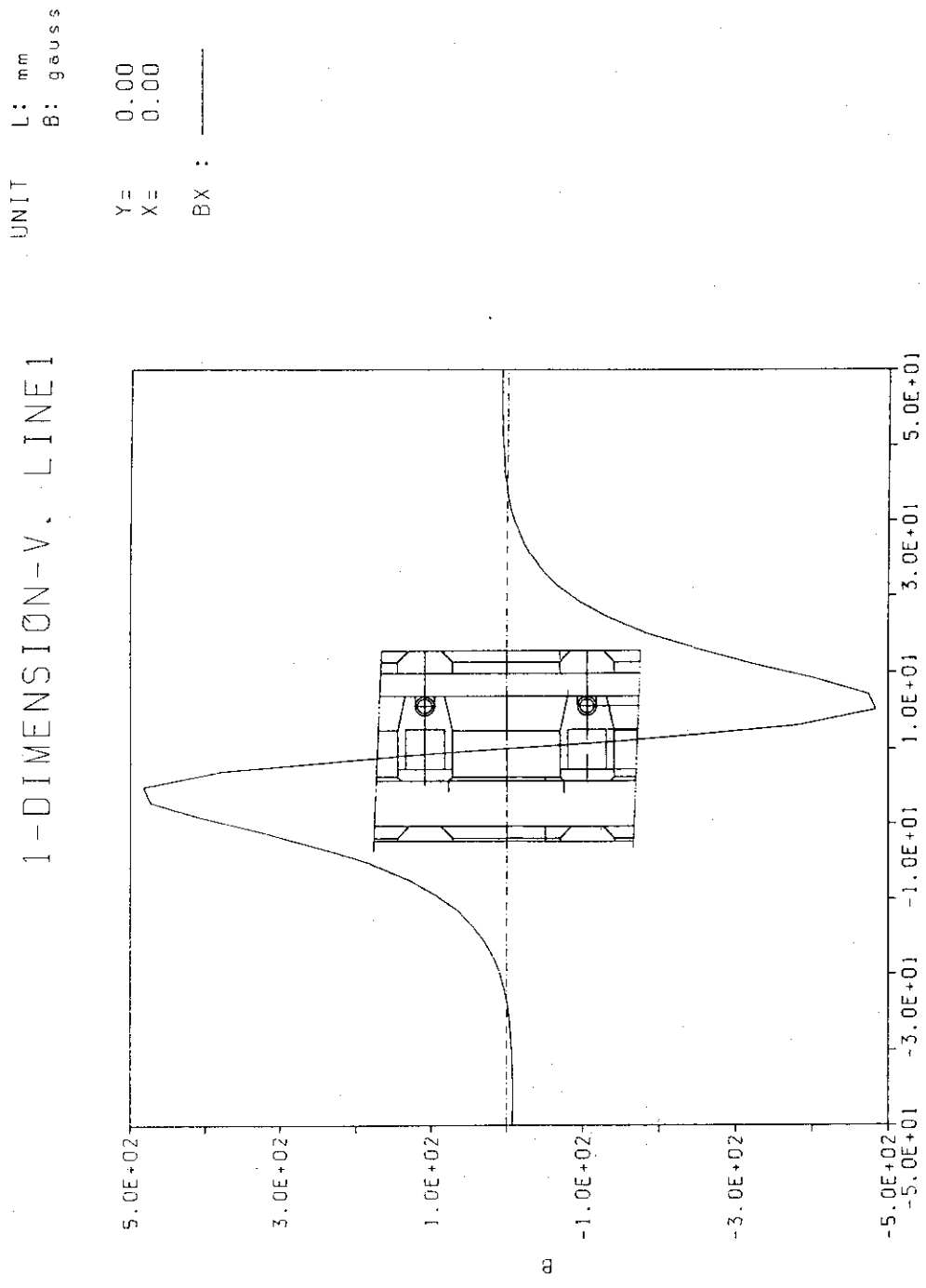

Fig.2.3-5 The dipole magnetic field for electron suppression

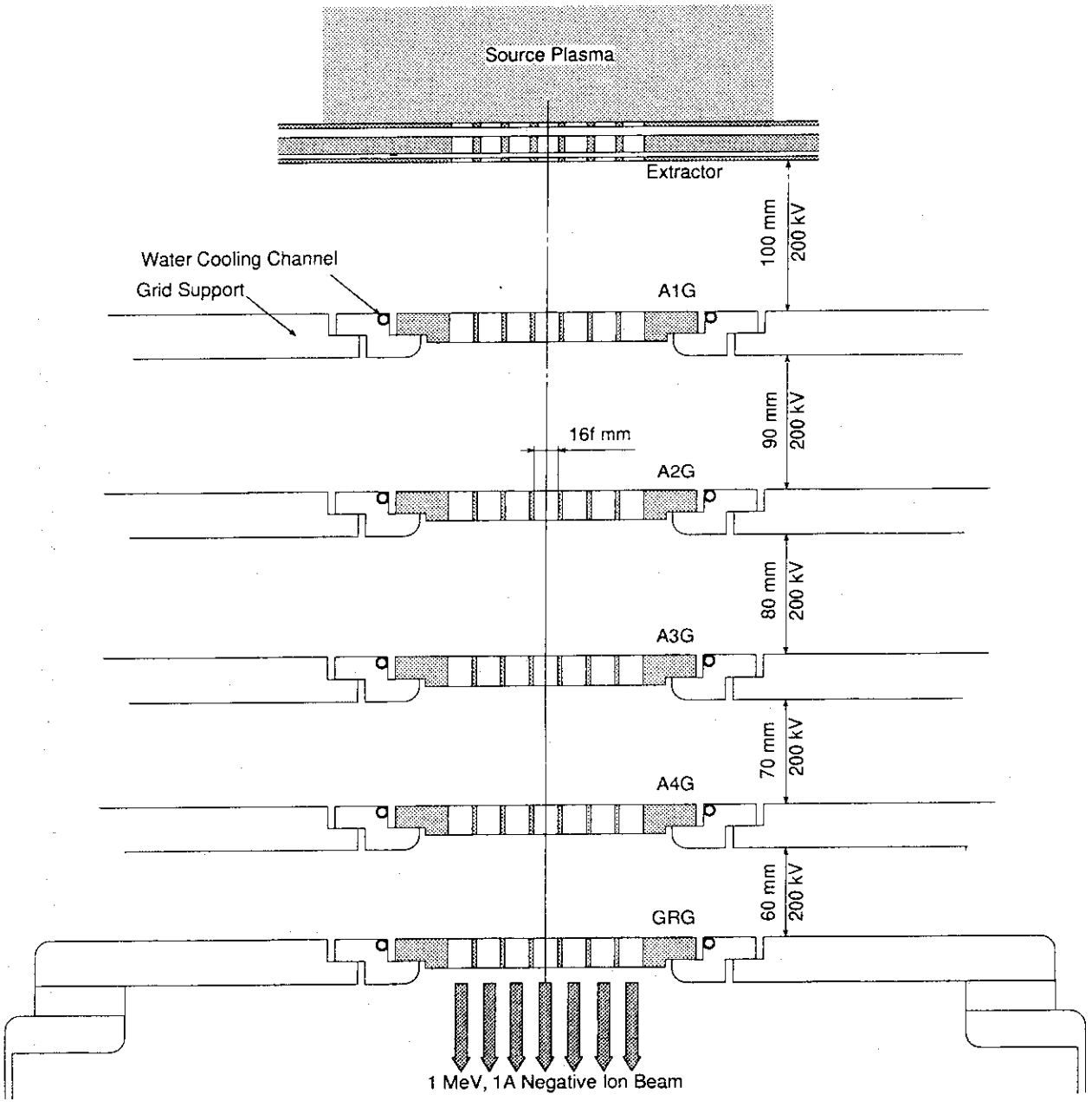

Fig.2.3-6 A schematic of the MM type ES accelerator.
The gap length was taken as an example, corresponding to a computational result of Fig.2.3-12.

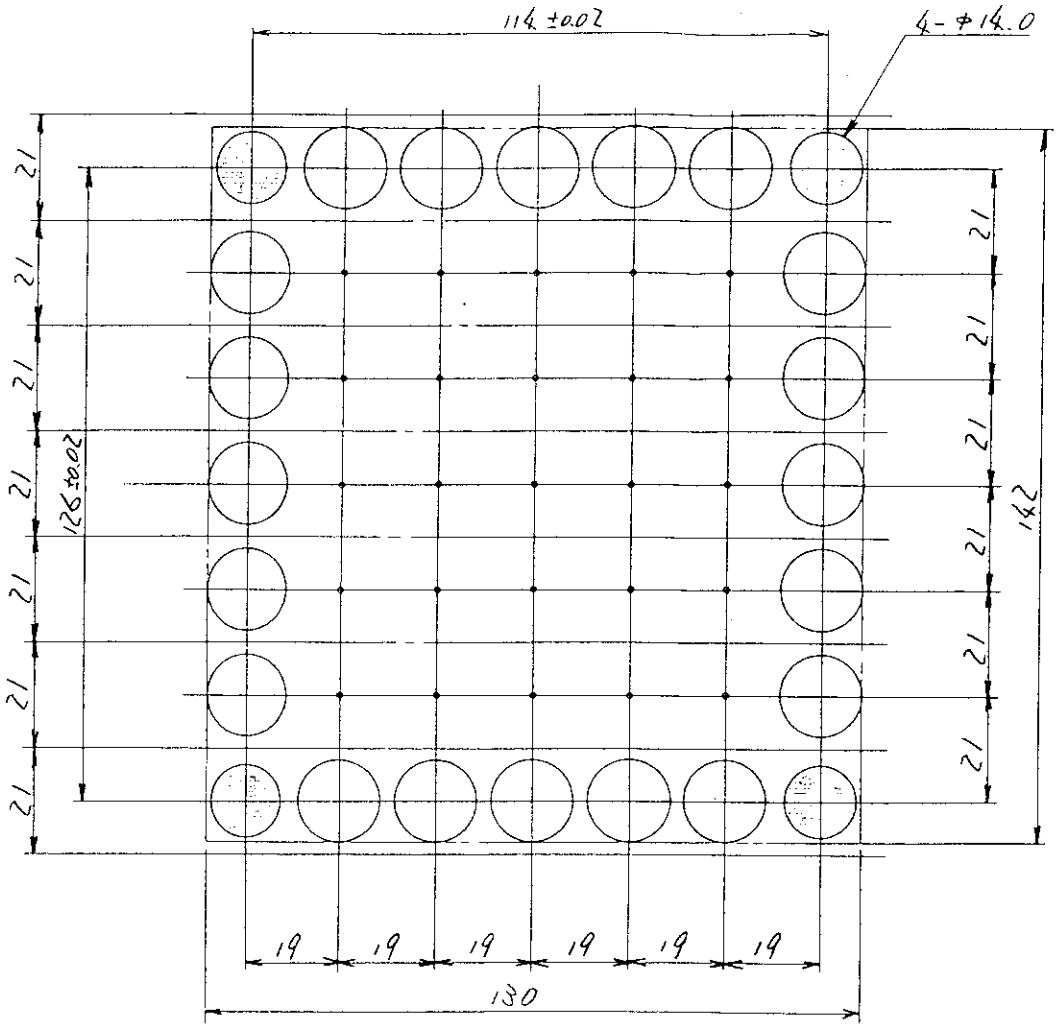

Fig.2.3-7 The pattern of multi-apertures in the accelerator. The 49 apertures in the arrangement of 7×7 array are drilled in an area of 130 mm×142 mm. The aperture diameter is 16 mm except for four apertures of 14 mm dia. on the corners

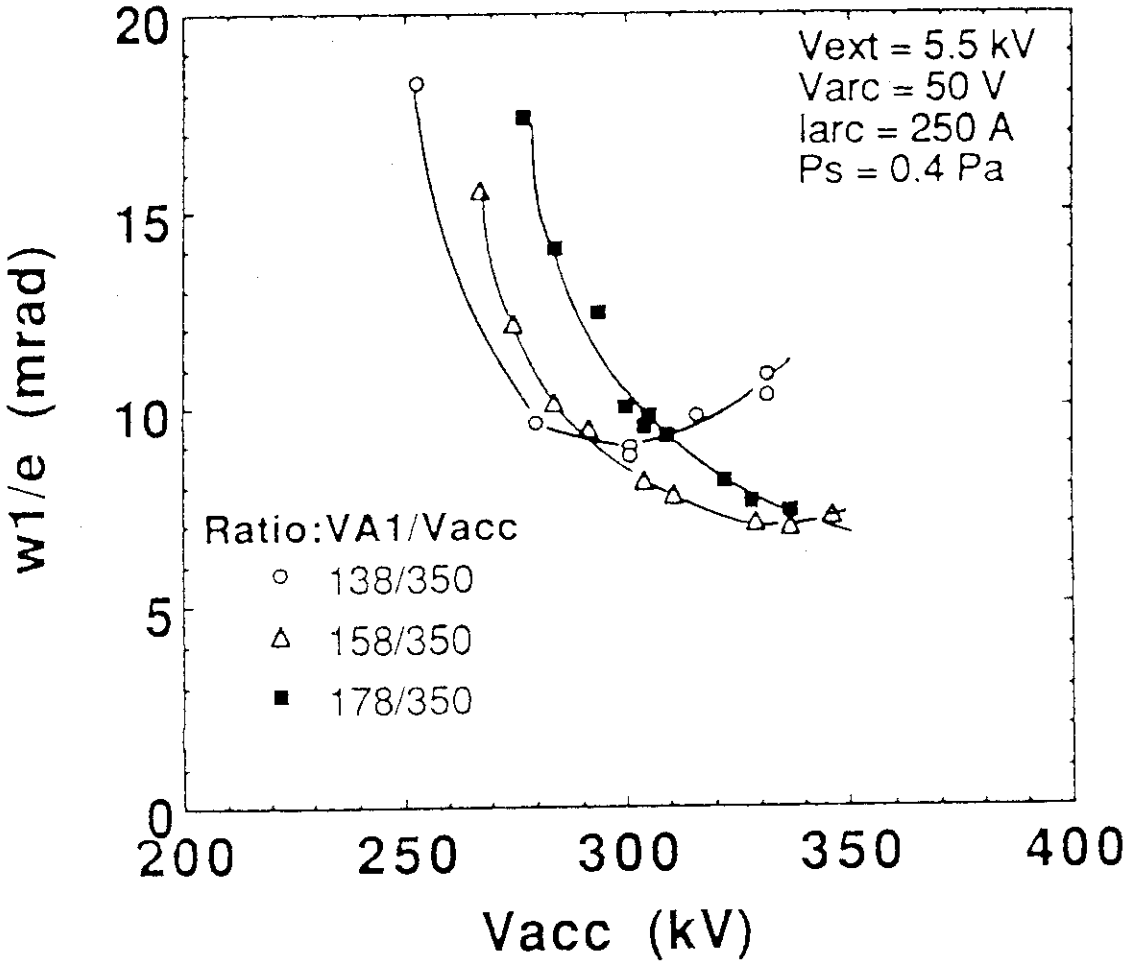

Fig.2.3-8 Beam divergence angle as a function of V_{A1} to V_{acc}

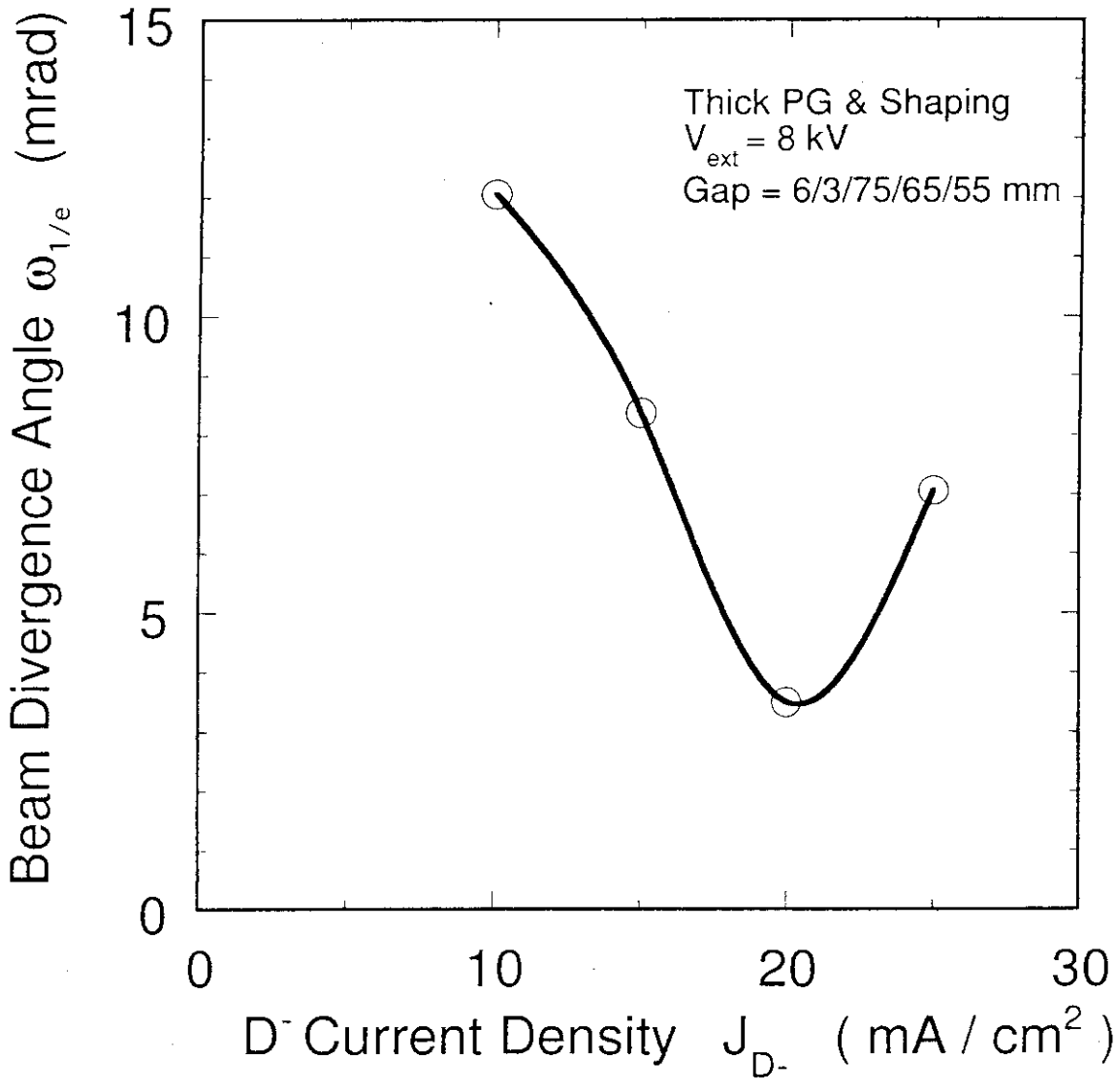

Fig.2.3-9 Beam divergence angle as a function of the D^- current density

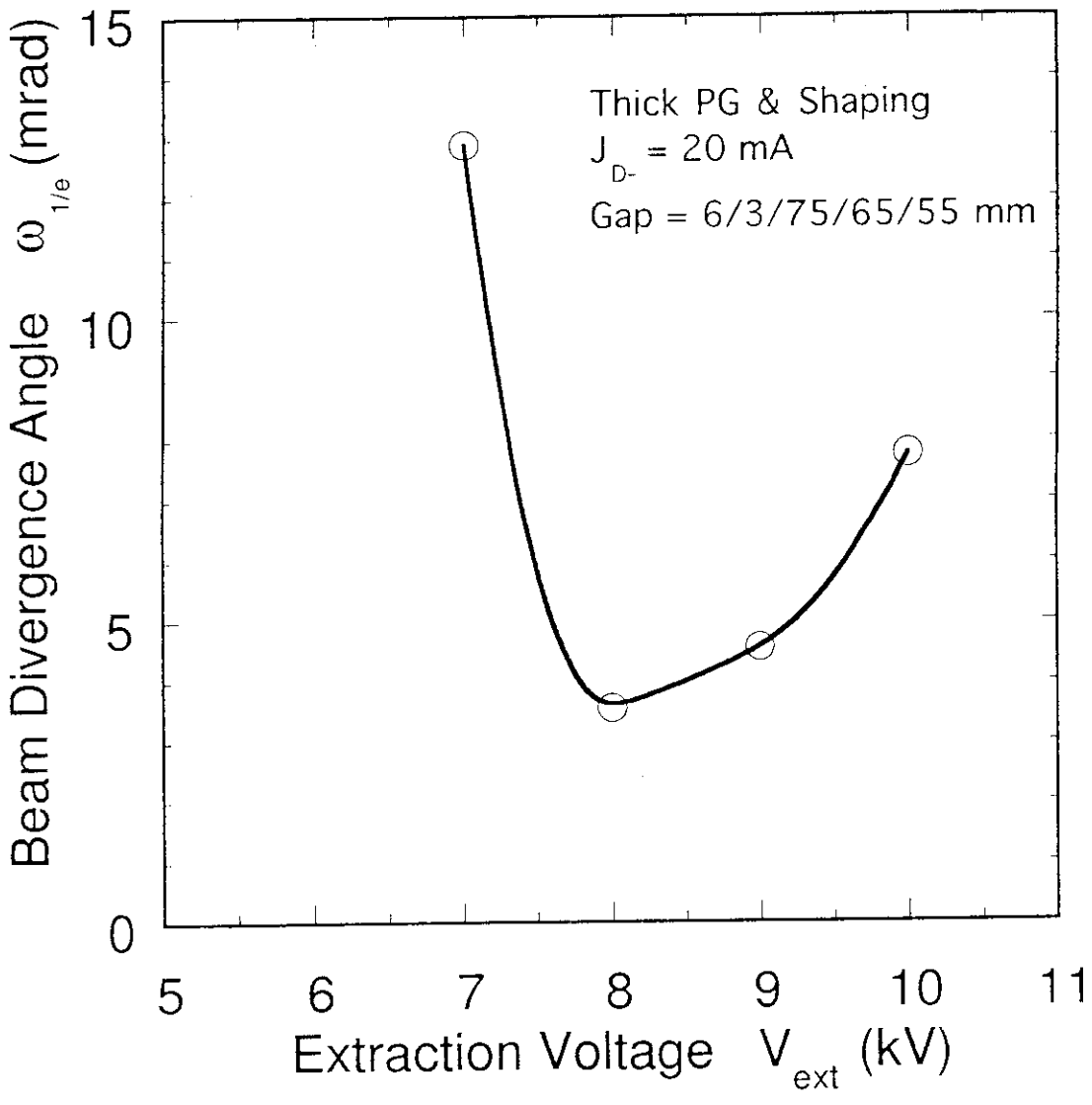

Fig.2.3-10 Beam divergence angle as a function of the extraction voltage

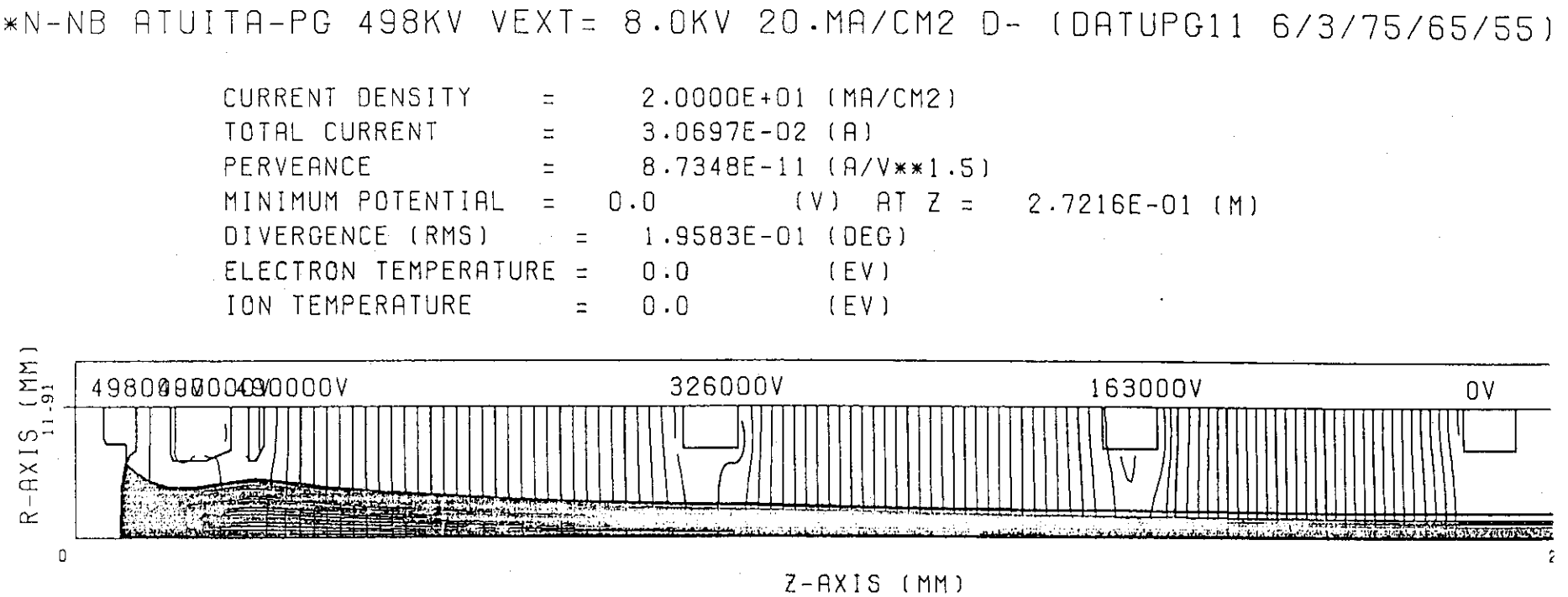

Fig.2.3-11 An example of the computation of the beam trajectory in acceleration up to 500 keV

*MEV VACC=1000KV VEXT= 7.5KV 26.MA/CM2 H- GAP 100/90/80/70/60

Current Density = 2.6000E+01(mA/cm2)
Total Current = 3.8540E-02(A)
Perveance = 3.8111E-11(A/V**1.5)
Minimum Potential = 0.0000E+00(V) AT Z = 5.4068E-01(m)
Divergence (RMS) = 1.8282E-01(Deg)
Electron Temperature = 0.0000E+00(eV)
Ion Temperature = 0.0000E+00(eV)

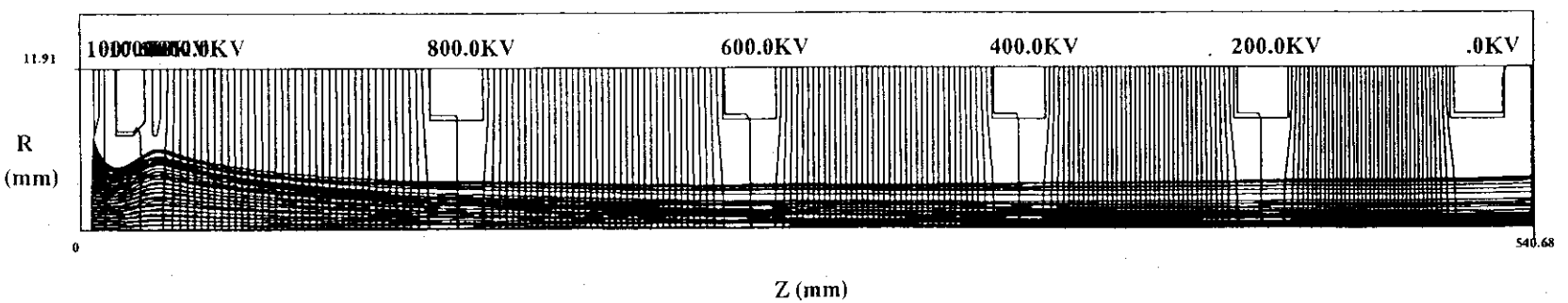

Fig.2.3-12 An example of the computation of the beam trajectory in acceleration up to 1 MeV

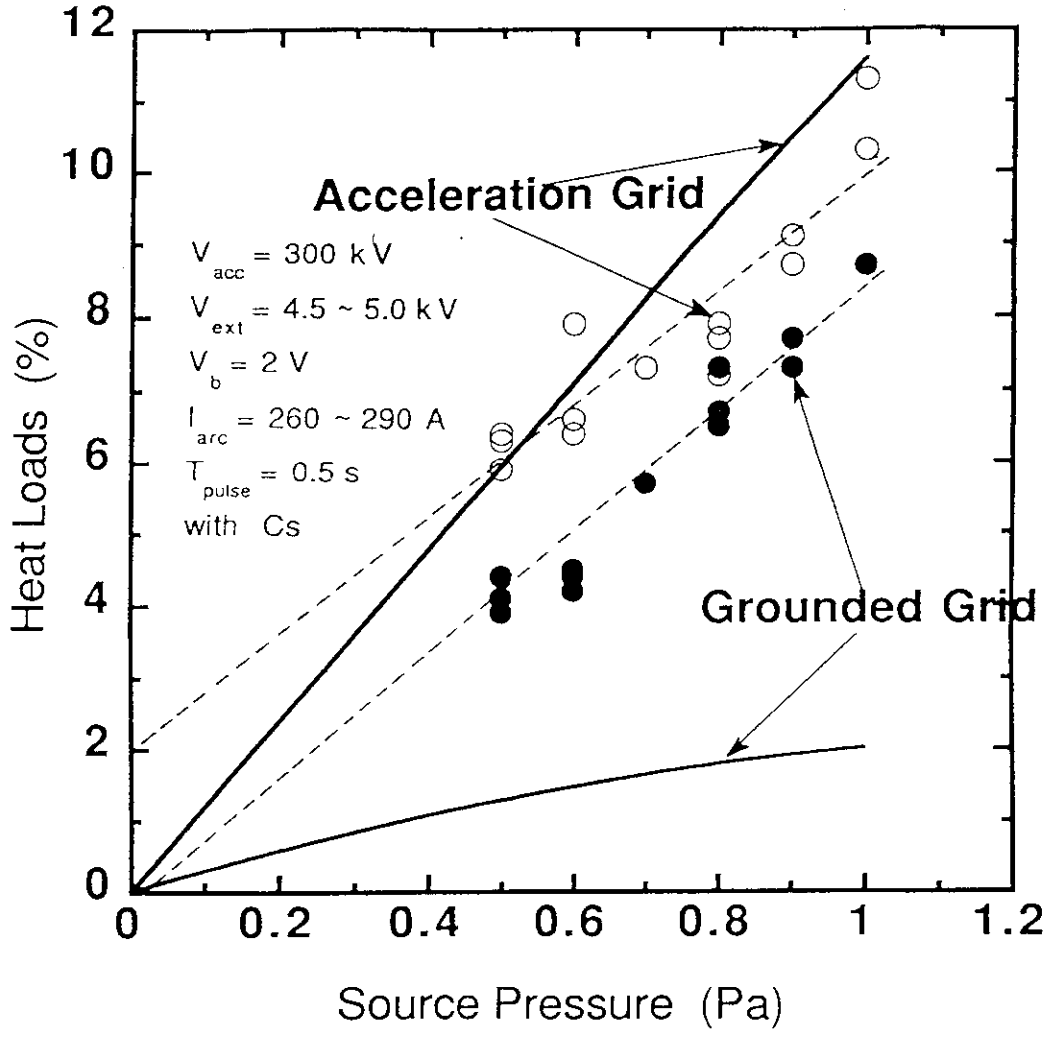

Fig.2.3-13 The heat load on the grids in a two-stage acceleration as a function of the operational gas pressure

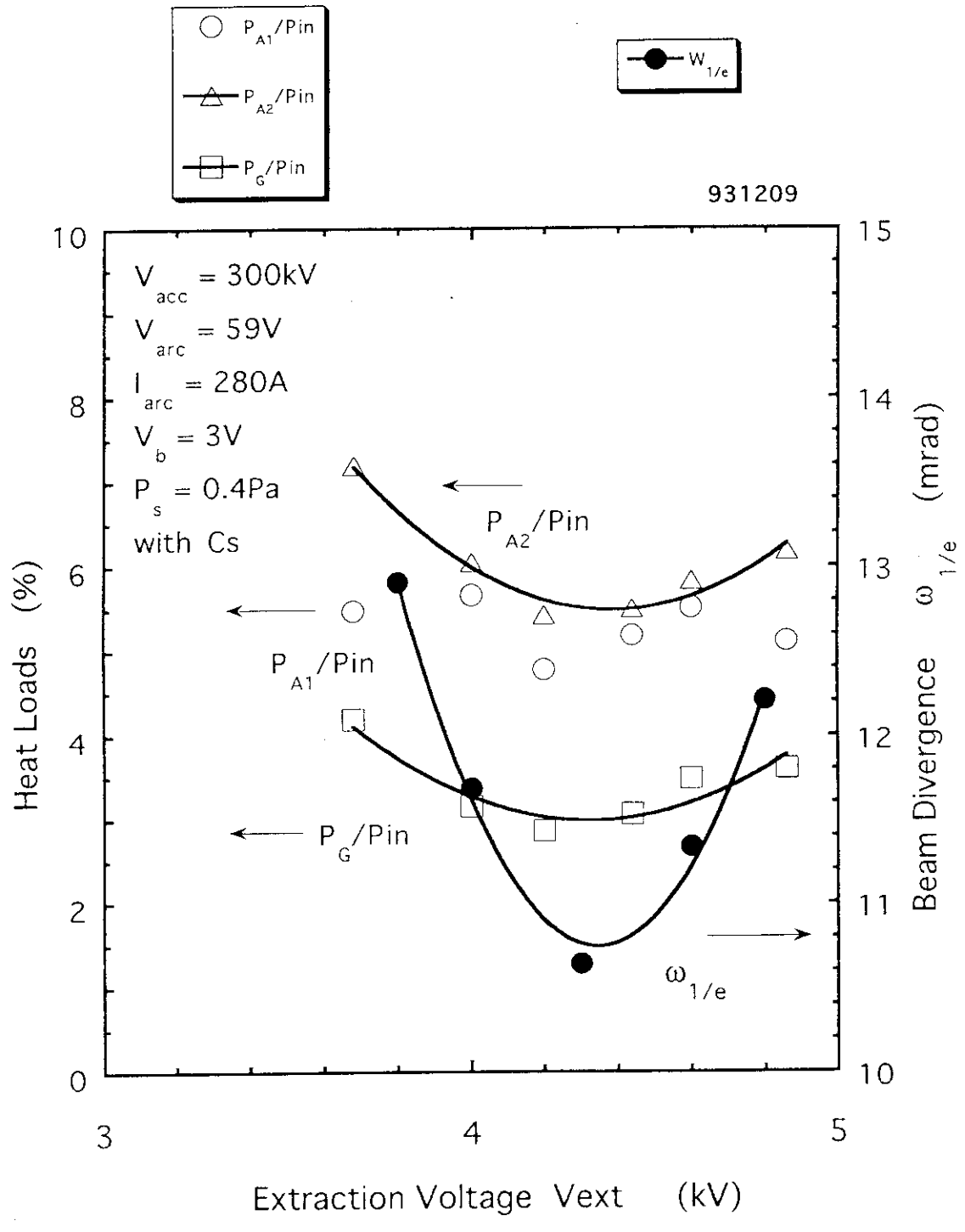

Fig.2.3-14 The heat load on the grids in a three-stage acceleration as a function of the extraction voltage

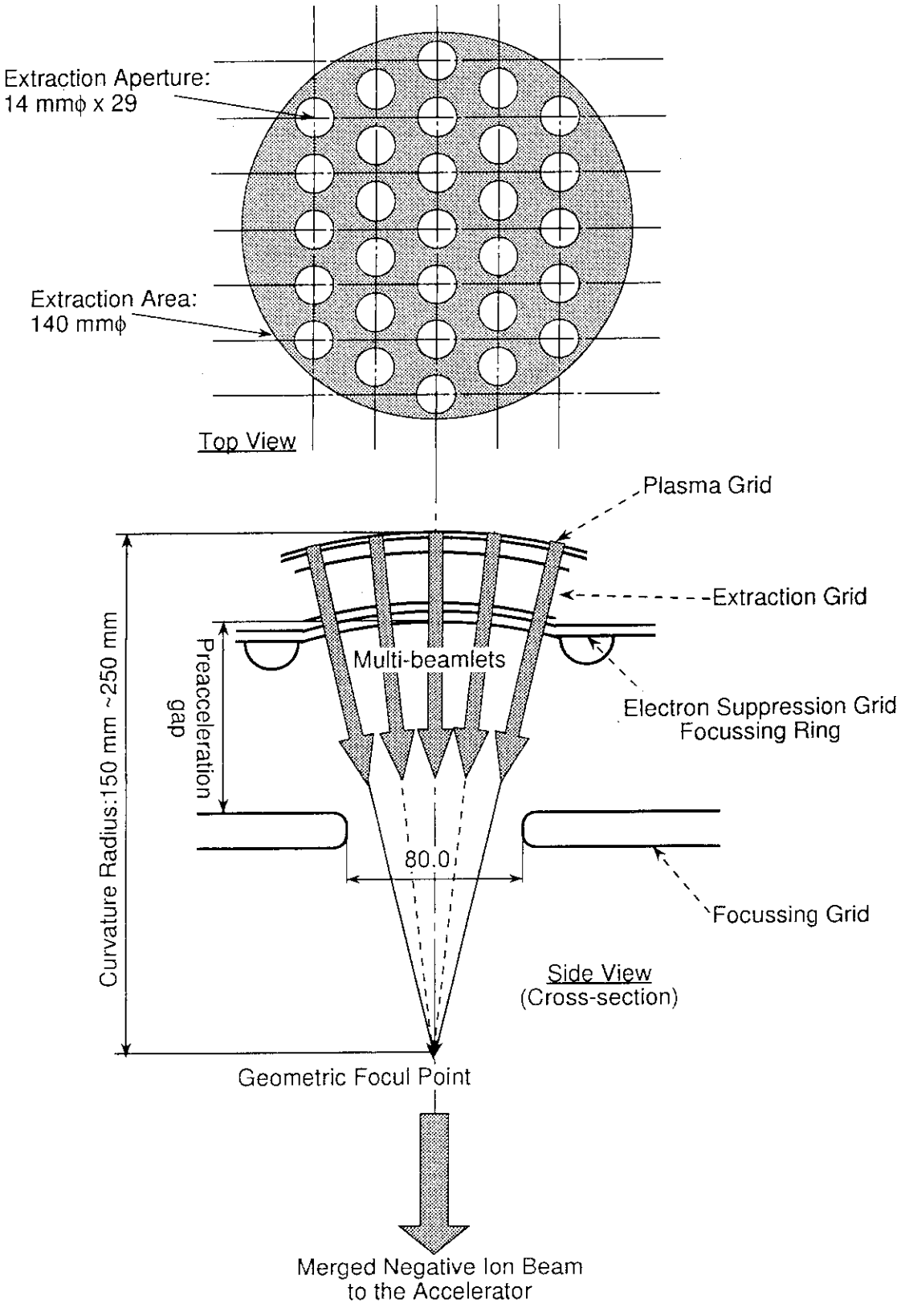

Fig.2.3-15 A schematic of the one ampere class beam merging system

2.4 High Voltage Insulator

The insulator should have enough voltage holding capability and enough strength to support the total weight of the ion source, the extractor and the accelerator. The major specifications are as follows;

1. Diameter:	1.9 m OD, 1.8 m ID
2. Height:	24 cm
3. Material:	Voidless FRP
4. Weight:	
5. Voltage Holding in the Air:	100 kV
6. Voltage Holding in SF6 Gas:	220 kV
7. Outgas:	$< 10^{-3}$ Pa.m^3/s

Figure 2.4-1 shows a crosssectional and a plain views of the insulator. The accelerator column is made of 5 insulators and 6 flanges. The insulators are jointed with the flanges by clamps attached outside the insulators. Figure 2.4-2 shows the detailed design of the clamps.

Figure 2.4-3 shows the electric field in the accelerator column. The field near the clamps is shown in detail in Figure 2.4-4. The highest electric fields inside and outside the vacuum are 4.3 kV/mm and 3.8 kV/mm, respectively.

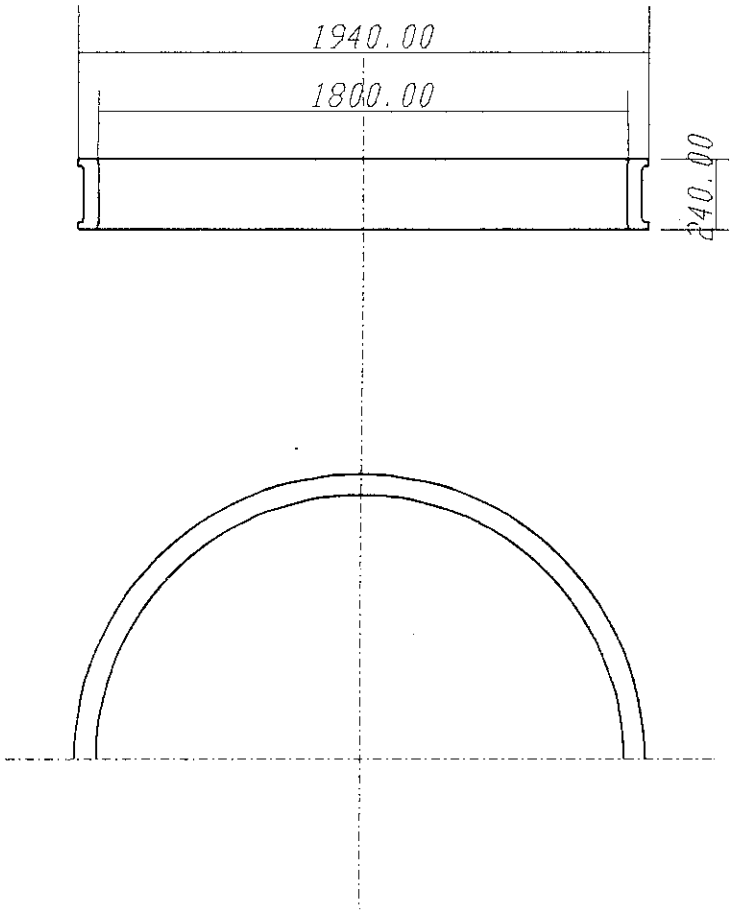

Fig.2.4-1 Insulator for the Prototype Accelerator

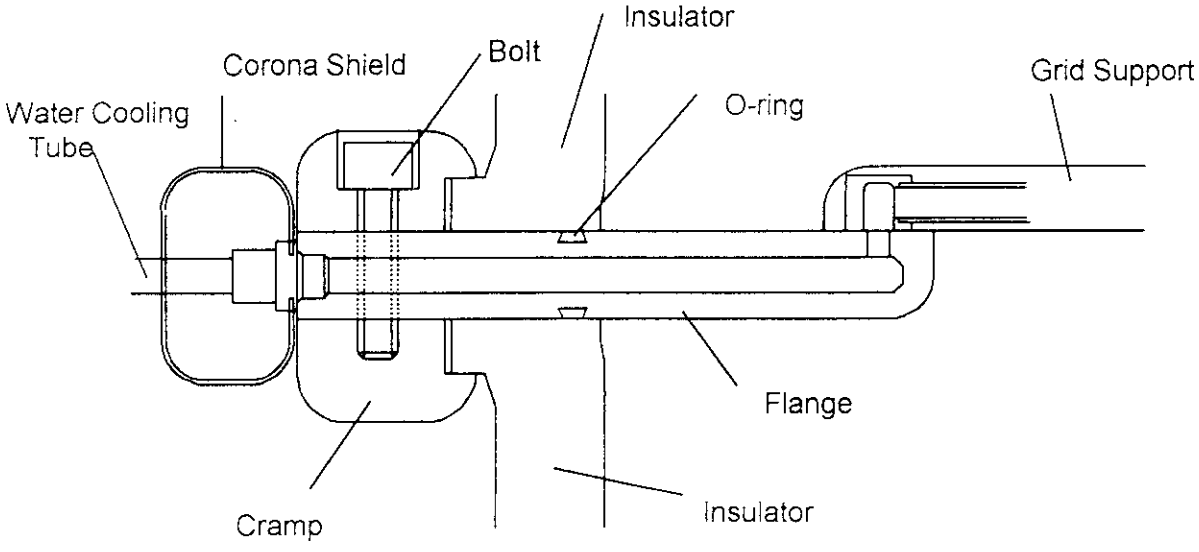

Fig.2.4-2 Junction of an Insulator and a flange

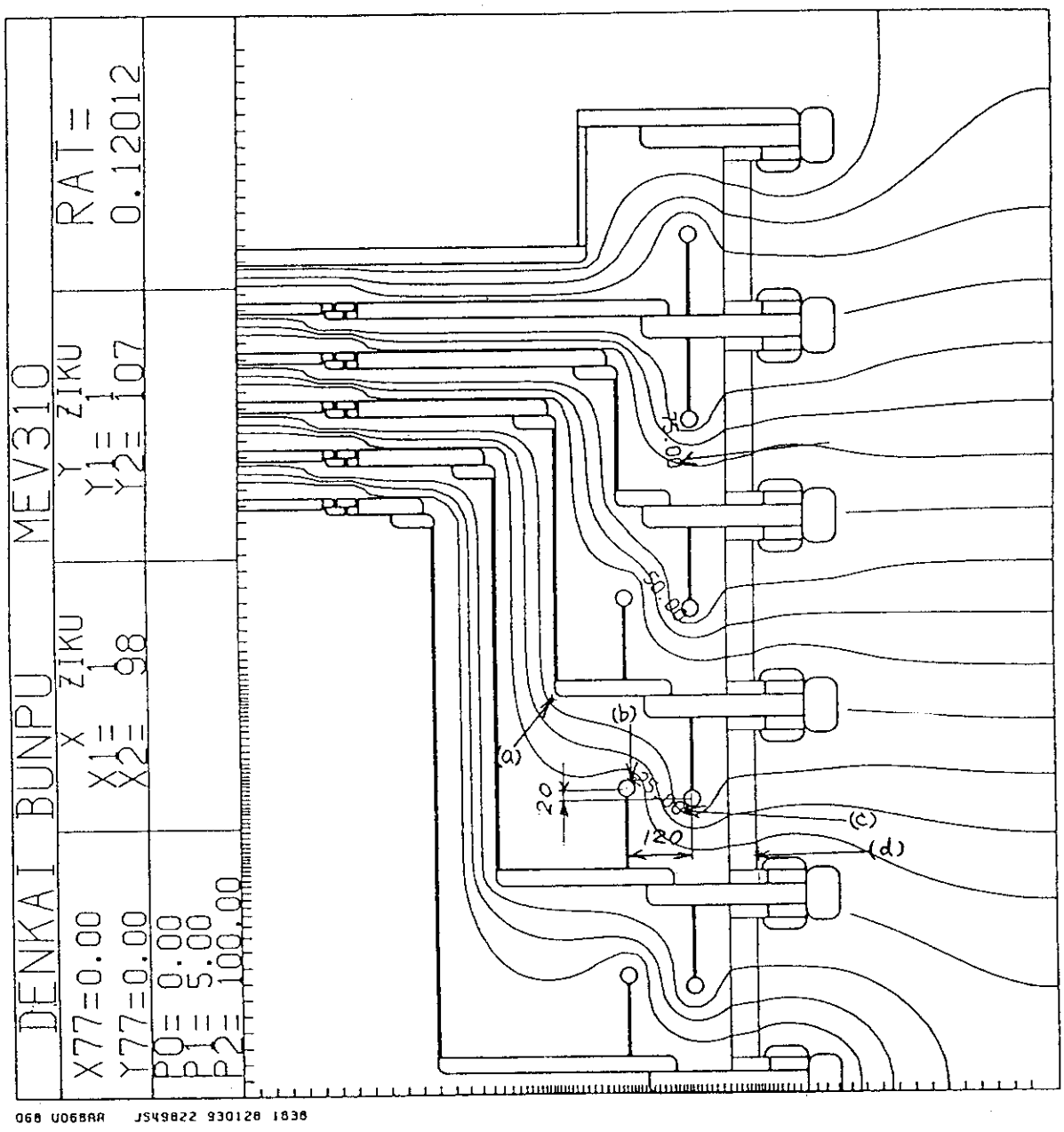

Fig.2.4-3 Electric field in the accelerator column

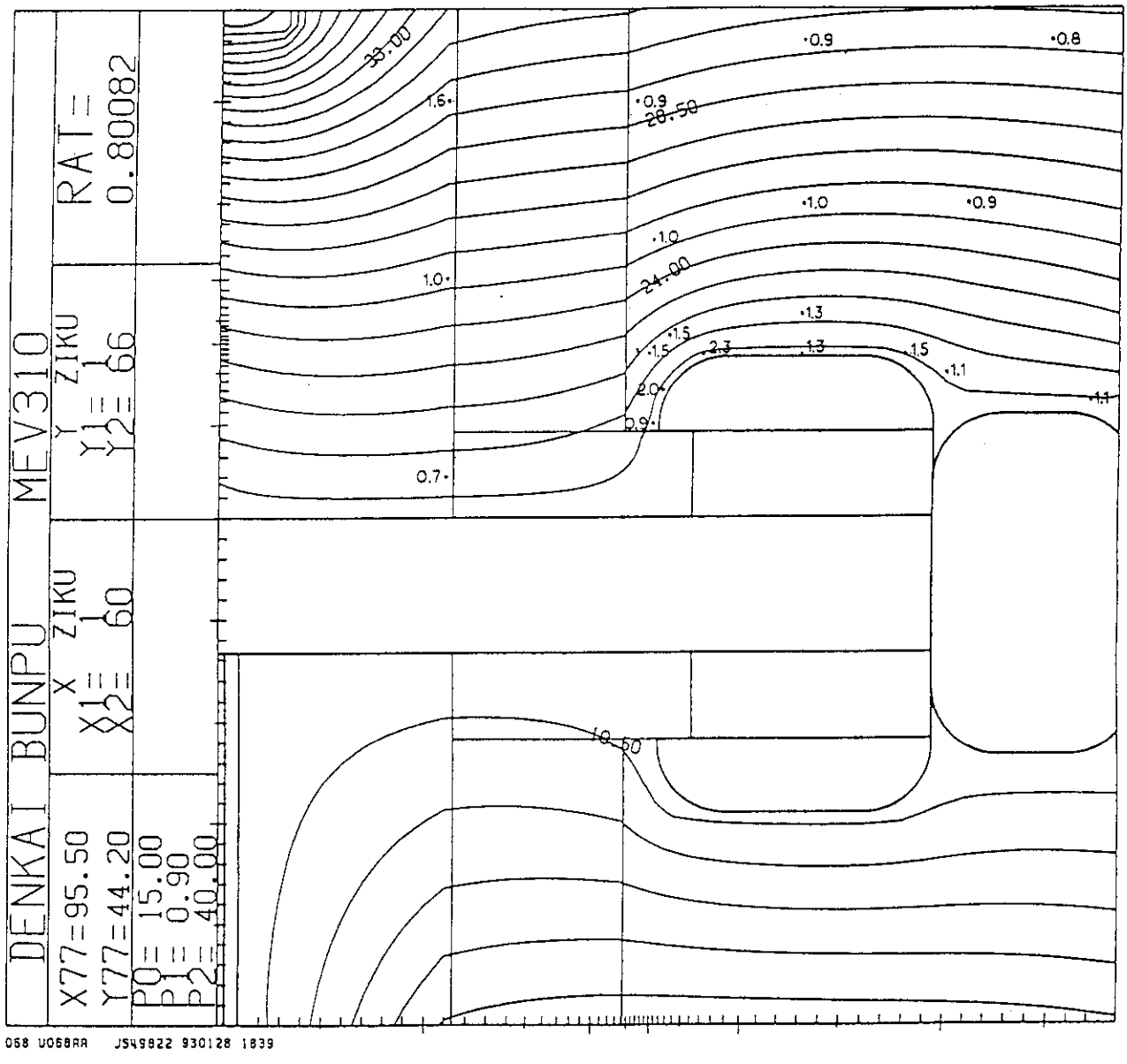

Fig.2.4-4 Electric field near the junction of an insulator and a flange

3. Design of MeV Test Facility

3.1 Overview

MeV Test Facility (MTF) has been designed as a test bed for the Prototype Accelerator. It consist of power supplies sufficient to operate the Prototype Accelerator, and beam line components such as a vacuum system and a beam target, and auxiliary systems such as a cooling water system and a diagnostic system. Radiation shield is necessary for shielding the X-rays which are emitted in case the electrons are accelerated to high energies. Major specification of the MeV Test Facility are listed in Table 3.1-1.

Table 3.1-1 Specifications of the MeV Test Facility

Type of High Voltage Power Supply:	Cockcroft-Walton Type
Voltage:	1 MV (200kV x 5 stages)
Current:	1 A
Pulse Length:	60 s
Duty:	1/60
Electric Power for Negative Ion Production:	100 kVA (Motor Genertor)
X-ray Shield:	80-100 cm concrete
Vacuum System:	100 m3/s Cryo-Sorption Pump
	20 m3/s Turbo-molecular Pump
Cooling Water System:	1000 l/min, 1.2 MPa

Figure 3.1-1 shows a bird's-eye view of the MeV Test Facility. Two SF_6 gas vessels are installed inthe X-ray shield; one is for the Cockcroft-Walton high voltage circuit (Accel. Power Supply Vessel -AP Vessel), and the other is for the power supplies for negative ion production (Source PowerSupply Vessel - SP Vessle). Both vessels are connected by a tube, through which the Cockcroft-Walton circuit and the power supplies for negative ion production are linked together at the high voltage potential. The AP Vessel is 3.2 m in diameter and 11 m in length, and SP Vessel is 3.6 m in diameter and 8 m in length. The vessels are filled with SF_6 gas for the high voltage insulation. When the vessels are pressurized at 0.6 MPa, the power supplies sustain at the high voltage of up to 1.5 MV.

Installed in the AP Vessel is the Prototype Accelerator, which produces the negative ion beams in the vertical direction. The beamline is attached to the AP Vessel under the Prototype

Accelerator. This configuration has following advantages;

1) Access to the Prototype Accelerator is easy; since the accelerator is installed on a holizontal plate, it is easy to replace the components for various experiments,
2) Electrons are accelerated downwards, which makes the X-ray shielding easy.

Figure 3.1-2 shows a schematic diagram of the MeV Test Facility. High voltage (1 MV) and intermediate voltages (800,600,400,200 kV) created by the Cockcroft-Walton Circuit are connected to each stage of the acclerator. Power supplies for negative ion production and extraction are at the high potential, and the high voltage cables from these power supplies are connected with the negative ion source via a surge block core, which is a critical element for surge protection. Source of the electric power of these power supplies is a motor generator, which insulates the high voltage of up to 1.5 MV.

Auxiliary system of the MeV Test Facility consists of a cooling water system, a vacuum system, a gas feed system, a diagnostic system, and a beamline. Cooling water system has a water choke for high voltage insulation in the SF6 gas vessel. Hydrogen gas is fed to the negative ion source via a long insulator tube. A beam target is installed at the end of the beamline, on which maximum beam power of 1 MW is to be dissipated.

The MeV Test Facility is to be built by re-constructing the test bed for the present NBI units for the JT-60U. It is to be installed in the NBI Test Building in Naka Fusion Research Establishment, JAERI. The X-ray shield can be constructed using an old pit, which has enough size for the two SF6 gas vessels. The cooling water system will be provided as an additional part of the present cooling water system for the NBI test bed.

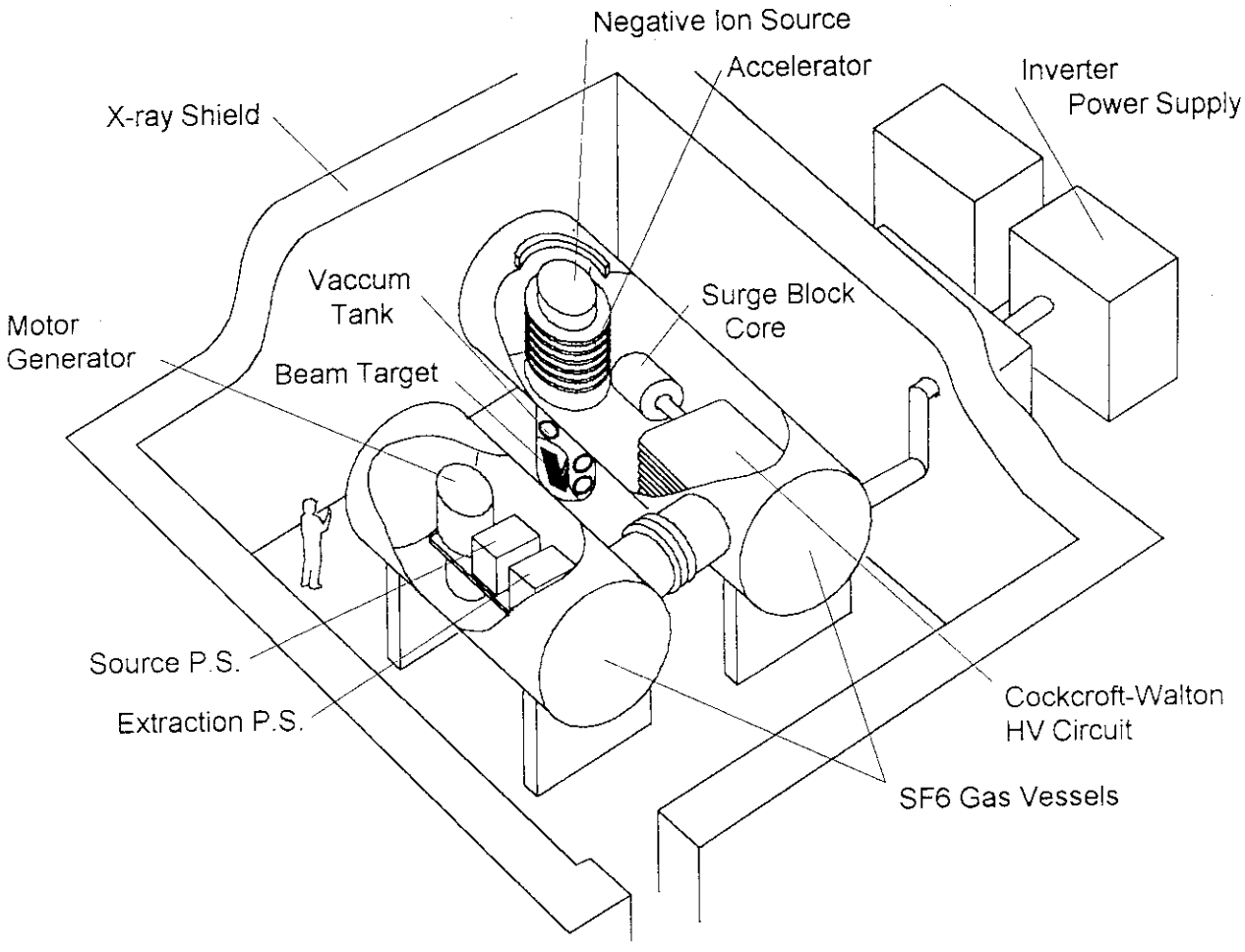

Fig.3.1-1 Bird's-eye view of MeV Test Facility

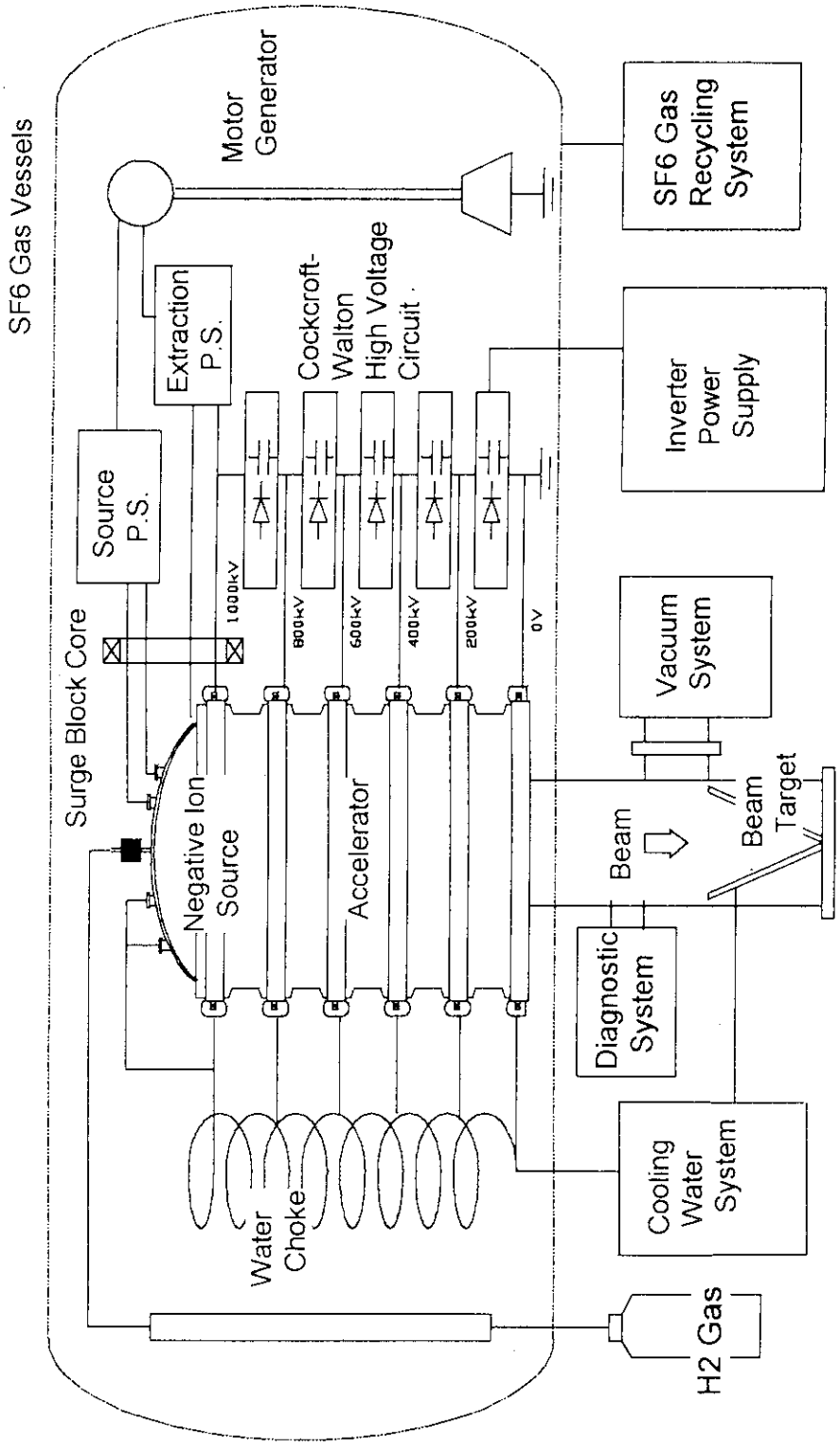

Fig.3.1-2 A schematic diagram of MeV Test Facility

3.2 Power Supply System

3.2.1 System Requirements

A proof of principle for an ampere class beam acceleration up to an energy of MeV is one of the most important subjects to realize an one-MeV class NBI system[1]. The power supply system which is utilized for the experiment on high energy beam acceleration of negative ions has been designed.

A schematic diagram of the power supply system is shown in Fig. 3.2-1. The power supply system consists of source power supplies for negative ion production and a high voltage power supply for beam acceleration. Capacity of the power supply system was designed to produce high energy negative ion beams up to 1 MeV, 1 A for 60 s pulse with a duty cycle of 1/60. Specifications of the power supply system is shown in Table 3.2-1.

Table 3.2-1 Specifications of the system

Acceleration Voltage:	1 MV
Acceleration Current:	1 A
Pulse Length:	1 min
Duty Cycle:	1/60
Surge Current:	<2kA

A plasma generator is mounted on the high potential and produced H^- ions are extracted and accelerated from the negative high potential to the ground. Therefore, the source power supplies are mounted on the high voltage platform insulated from the ground. Electric power for the power supplies is generated at the high potential by a motor-drive generator with an insulator shaft (M-G). The high voltage power supply is a Cockcroft-Walton DC high voltage generator driven by a 3 kHz inverter system. Surge suppression system is adopted for protection of the ion source and the power supply itself from electric breakdowns in the accelerator. The power supply system is installed in SF_6 gas pressurized tanks (SP vessel : Source Power Supplies Vessel, AP vessel : Acceleration Power Supply Vessel). The prototype accelerator is mounted in the AP vessel.

Layout of the power supply system is shown in Fig. 3.2-2. The SP vessel and the AP vessel are installed in a X-ray shield pit. The dimensions of the SP vessel and the AP vessel are 3.6 m in

inner diameter, 6.7 m in inner length and 3.2 m in inner diameter, 10.6 m in inner length, respectively. These two vessels are connected by a coaxial duct. Other components of the power supply system are mounted in the power supply room. These are a distribution transformer, a converter system, an inverter system, compensating reactors, a high frequency transformer, a M-G starter, a SF6 gas recovering system and a SF6 gas recycling system. Out put of the high frequency transformer is fed to the Cockcroft-Walton by a coaxial duct that is installed in a labyrinth duct. The power supply system is operated from a control room which is placed at next room to the power supply room.

3.2.2 Source Power Supplies

The source power supplies consist of a cathode power supply, an arc power supply and a bias power supply for a plasma generator. An extraction power supply and an electron suppression power supply are utilized for negative ion extraction and electron suppression from the source plasma. These power supplies are mounted on a high voltage platform insulated from the ground. The motor-drive generator, which has an insulator shaft made by fiber reinforcement plastic (FRP), feeds the electric power to the source power supplies. The capacity of the generator is 100 kVA. Reasons for using the M-G system are that the power supply system should be compact and the stray capacitance should be reduced as low as possible to prevent the damages on the accelerator from the breakdowns. The specifications of the power supply system is shown in Table 3.2-2.

It is necessary to cut off with high speed to protect the cathode and the anode surface from the arcing phenomena in the plasma generator. Therefore, the arc power supply has a GTO switch whose cut off speed is shorter than 100 ms. A snubber circuit which is a commutation circuit composed of IGBTs and resistors is applied to the arc power supply to reduce the rise time of the out put. Optimum value of the resister can be selected by a remote control system for a certain arc discharge current in the plasma generator.

The high speed switching is also required to the extraction power supply and the electron suppression power supply to protect a plasma grid, an extraction grid and an electron suppression grid from the breakdowns. These power supplies have inverter system which can switch the out put and control the voltage at AC side instead of the DC switch like the GTO. A frequency of the inverter is 10 kHz. Cut off speed is shorter than 100 ms which is enough for protection of grids.

It is very important to reduce surge voltage between each power supplies when the breakdowns occur in the main accelerator. Voltage clump circuit composed of capacitors or non-

linear resistors are used between each circuit.

3.2.3 Acceleration Power Supply

A diagram of the acceleration power supply is shown in Fig. 3.2-3. The acceleration power supply is the Cockcroft-Walton DC high voltage generator(CW). The CW circuit is driven by the 3kHz inverter system. AC 420 V, 50 Hz is converted to DC by a converter system. Then the inverter system produces 3 kHz AC up to 1500 V. High frequency transformer is connected to boost the AC voltage up to 95 kV. This AC high voltage is supplied to the CW through the coaxial feed through. High voltage out put of the CW is controlled by controlling of the out put of the converter and the inverter. PWM control is adopted to the system for voltage regulation.

Suppression of voltage ripple and voltage drop at the beam initiation are required to produce good beam optics. Therefore, the elements of the CW circuit were designed to suppress the ripple smaller than 2 % p-p and the voltage drop smaller than 15 %.

The voltage ripple of the CW is shown by equation (1).

$$V = \frac{I}{fC} \frac{n(n+1)}{2} \qquad (1)$$

V: voltage ripple (V)
I: out put current (A)
f: frequency of input power to the CW (Hz) (f=3kHz)
C: capacitor of the circuit (F) (C= 3.4x10-7 F)
n: number of stages (n = 5)

Therefore, the voltage ripple is described as follows

$$V = \frac{1.0}{3\times10^{3}\ \ 3.4\times10^{-7}} \frac{5(5+1)}{2} \qquad (2)$$

$$= 1.5\times10^{4}\ \text{V}\ \ (1.5\%)$$

Voltage drop at the initiation of the beam was designed to be lower than 15%. The voltage drop is shown as follows.

$$dV = \frac{I}{fC}\left\{\frac{2n^3}{3} + \frac{n^2}{2} + \frac{n}{3}\right\} \qquad (3)$$

Therefore, the voltage drop dV is

$$= 9.6 \times 10^4 \text{ V}$$
$$=(9.6 \%)$$

The ion source has a five stages electrostatic accelerator. There are four intermediate electrodes between the extractor and the grounded electrode. Generally, a bleeder resistance is used to get intermediate potentials for a small current accelerator. A higher current beam acceleration requires a large bleeder current to keep a stable potential distribution. The high power bleeder resistance is not available from the limitation of the temperature of the SF6 gas in the tanks and power loss. Therefore, the intermediate potentials are supplied from the each stage of the Cockcroft-Walton generator.

3.2.4 Surge Protection

Surge protection is one of the most important keys to make a stable beam acceleration system. In order to avoid not only malfunctions of the power supply system but also degradation of voltage holding characteristics of the accelerator, the breakdown surge should be suppressed as low as possible. It is necessary to reduce the stray capacitance which is an energy source of the surge, and to suppress the inflow of the surge to the ion source accelerator by using a surge blocker.

Generally, an insulated transformer which is utilized for the source power supplies has a large stray capacitance[2]. Therefore, in order to reduce stray capacitance, the M-G system has been introduced instead of the insulating transformer

Further, newly developed magnetic cores are adopted to the surge blocker. The surge blocker consists of FINEMET[3,4] (Fe Based Soft Magnetic Alloys Composed of Ultrafine Grain Structure) cores which have a saturation magnetic flux density of 1.35 T that is about 4 times higher value than that of a former ferrite core. A schematic view of the core is shown in Fig.3.2-4. Dimensions of the core are 900 mm in outer diameter, 400 mm in inner diameter and 25.4 mm in thickness. The FINEMET tape is rolled with insulation layer of SiO_2 coating.

Suppression of the surge current peak is more important than the energy input to the accelerator grid to prevent degradation of voltage holding in the Neutral Beam Injection system which has an ion source with a shorter gap accelerator of about 10 mm for each gap[2]. According to the experimental results using parallel electrodes in the vacuum, we can say that damages of the electrodes by large current discharge is considered to be severe at shorter gap length. In the case of a longer gap, the electrode damage is not so strong, even a high current discharge[5]. Longer gaps of around 90-50 mm are applied in the MeV class accelerator. Considering feasibility of the surge suppression system and high voltage of 1 MV, we fixed that the target value of the surge current is lower than 2 kA.

Stray capacitance between the high voltage part and the ground was calculated to be 402 pF. The surge current to the accelerator was simulated by using a circuit simulation code of SPICE with a simplified equivalent circuit that is shown in Fig.3.2-5. Thirteen cores are used for the surge blocker. Specifications of the surge blocker are shown in Table 3.2-3. A resistor of 570 ohm is connected in parallel to the surge blocker to dissipate the surge energy at the breakdown. A biasing current of 55 A is supplied to the opposite direction of the beam current. A twice higher value of the V.S. can be utilized by the effect of biasing current.

A simulated wave form of the surge current at the accelerator is shown in Fig. 3.2-6. The peak of the current can be suppressed to lower than 2 kA by the surge blocker whose capacity is 0.288 V·s with the biasing. An input energy to the accelerator was estimated to be smaller than 0.06 J by assuming that an arcing voltage is 100 V.

It is necessary to suppress surge voltage on the grounded line to prevent malfunctions of the system. In this system, all the high voltage parts are covered by the SP vessel and the AP vessel, which are connected to the ground by one point grounding circuit. The high voltage parts are shielded completely by the vessels. Therefore, the surge voltage on the grounded line is considered to be negligible low.

3.2.5 High Voltage Insulation

For the insulation of the high voltage power supply and the ion source, the SP vessel and the AP vessel are filled with a pressurized SF6 gas. The theoretical breakdown voltage V in the SF6 gas is given by the following equation[6].

$$V = 89pd\eta(1 + 0.175 / \sqrt{pr}) \qquad (4)$$

p : gas pressure (atm. abs)

d : gap length (cm)

h : field utilization factor (ratio of average to maximum electric field)

r : radius of curvature (cm)

In the uniform field, the breakdown voltage is about three times higher than that of the air. Breakdown voltages in SF6 gas under uniform field electrodes are shown in Fig. 3.2-7[7]. The breakdown voltages. are almost linear to the pressure of lower than about 0.3 MPa. However, it tends to saturate at higher pressure region. From the data in ref[7], we can expect that the voltage holding characteristics in the pressurized tanks with 0.6 MPa SF6 gas is nine times higher than that of air with 0.1 MPa.

The shortest gap is 38 cm between the surge blocker and the AP vessel. The breakdown voltage is estimated to be 10.2 MV. This value is enough for insulation. The high voltage platform is insulated from the ground by epoxy support. The CW is also insulated by epoxy support.

A water choke is mounted under the surge blocker in the AP vessel to supply cooling water to the ion source. The water choke consists of nylon tubes winded on two FRP posts which are built with a separating distance of 1.2 m. Height of the water choke is 1 m. Length of the tubes per one turn is 3 m. Six turns are adopted and total length of the tubes is 18 m. For the intermediate electrodes, the water is distributed from the intermediate points of the water choke. Resistivity of the water is 2 MW·cm. Ten tubes are connected to the part of 1MV. Every two tubes are connected to each intermediate electrode. Total leak current is estimated to be lower than 6 mA.

3.2.6 Controls and Diagnostics

The control system of the power supply is set up in the control room. Control signals for high voltage power supplies are insulated by optical fibers to prevent malfunctions of the system by surge propagation to the control system. Blockdiagrams of the control system for the power supply system are shown in Fig.3.2-8 and Fig.3.2-9. The beam out put is controlled by the computer and sequence controller. The typical time chart of the operation is shown in Fig. 3.2-10. Diagnostics for the out put of the power supplies can be monitored at the control room.

Reference

[1] Y.Ohara et.al.,"Development of high power negative ion sources for fusion researches at JAERI", ICIS`93, Peking,1993.
[2] K.Watanabe et.al.,"Surge suppression in a power supply of a neutral beam injector", J. of Plasma and Fusion Research, vol.69, No. 10 (1993), pp.1229-1241(in Japanese).
[3] Y.Yoshizawa et al.,"Fe-Based Soft Magnetic Alloys Composed of Ultrafine Grain Structure", Materials Transaction, JIM, vol.31,No.4(1990), pp.307-314.
[4] S.Nakajima et. al.,"Development of a surge blocker core using a material of Fe-Based Soft Magnetic Alloys Composed of Ultrafine Grain Structure", National Convention Record IEE Japan 14-58 (1991)(in Japanese).
[5] K.Watanabe et.al.,"dc voltage holding experiments of vacuum gap for high-energy ion sources",J.Appl.Phys. 72(9),(1992),pp3949-3956.
[6] The Committee of V-t Characteristic of SF_6 Gas of IEE of Japan,"Voltage-time characteristics of SF_6 gas", CIGRE Meeting SC-15(WG-03), Paris, 4th Sep.(1982).
[7] Hitachi Research Laboratory, Hitachi, Ltd,"breakdown characteristics in SF_6 gas gap".

Table 3.2-2 Specifications of the Power Supply System

1. Source Power Supplies

	V (V)	I (A)	Pulse (s)	Rise Time	Cut Off Time	Ripple p-p(%)
Cathode	15	800	61	0.2-3 s soft-start	~10ms	3
Arc	120	400	60	~10μs	100μs	3
Bias	5	100	61	1s	~10ms	3
Extraction	10kV	2	61	0.2s	100μs	2
Electron Supression	10kV	0.5	61	0.2s	100μs	2

2. Acceleration Power Supply

(Cockcroft-Walton DC high voltage generator)

V (kV)	I (A)	Beam Pulse Length (s)	Rise Time	Ripple p-p(%)
1000	1	60	1min	2

Table 3.2-3 Specifications of Surge Blocker

Dimension	ϕ 900- ϕ 400 x t 25.4 mm
Saturation Magnetic Flux	1.35 T
Effective Cross Section	4.45×10^{-3} m^2
Average Magnetic Path	1.94 m
Number of Core	13
Volt.Second	0.144(0.288 with Bias)

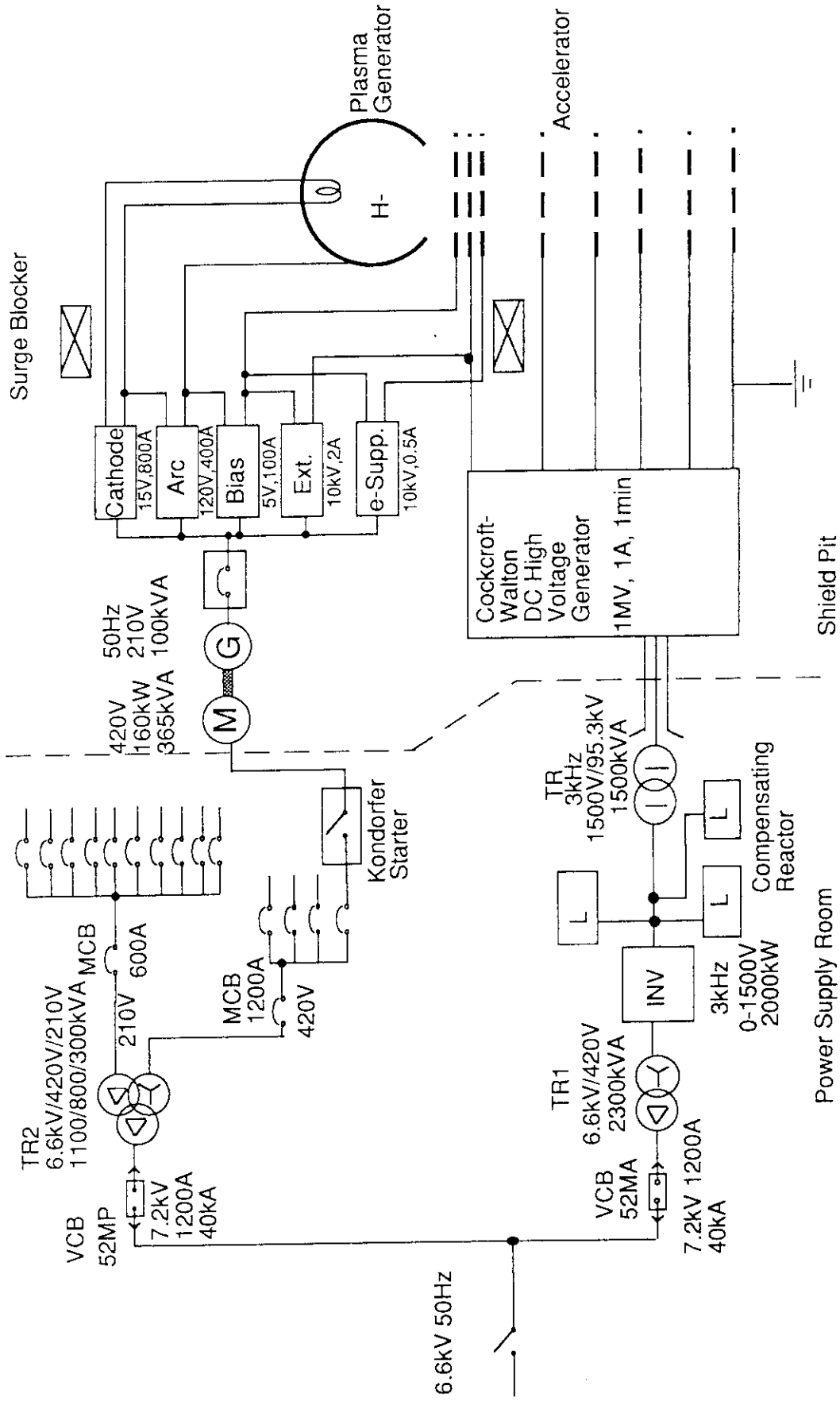

Fig.3.2-1 Schematic Diagram of Power Supply System

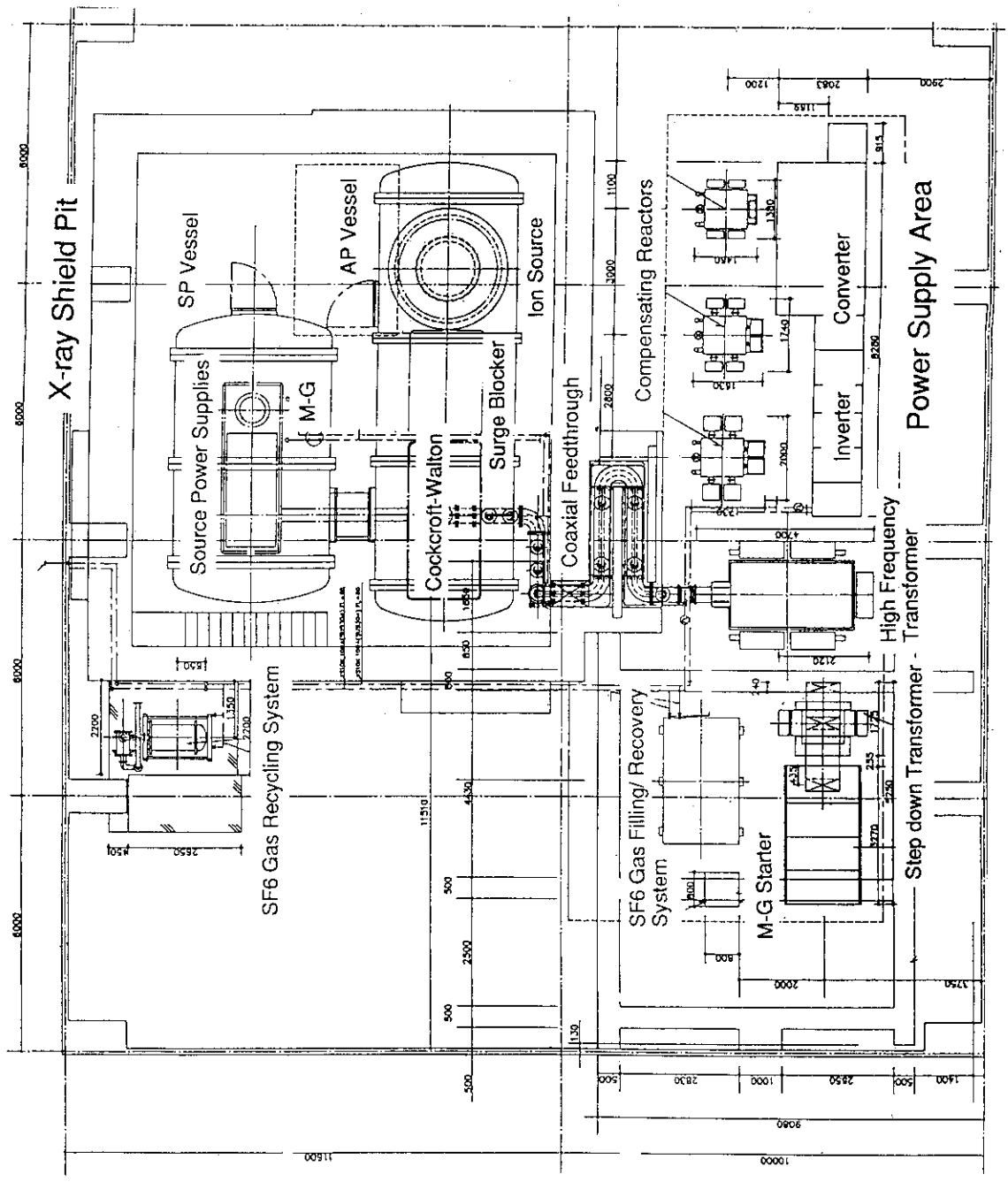

Fig.3.2-2 Layout of Power Supply System

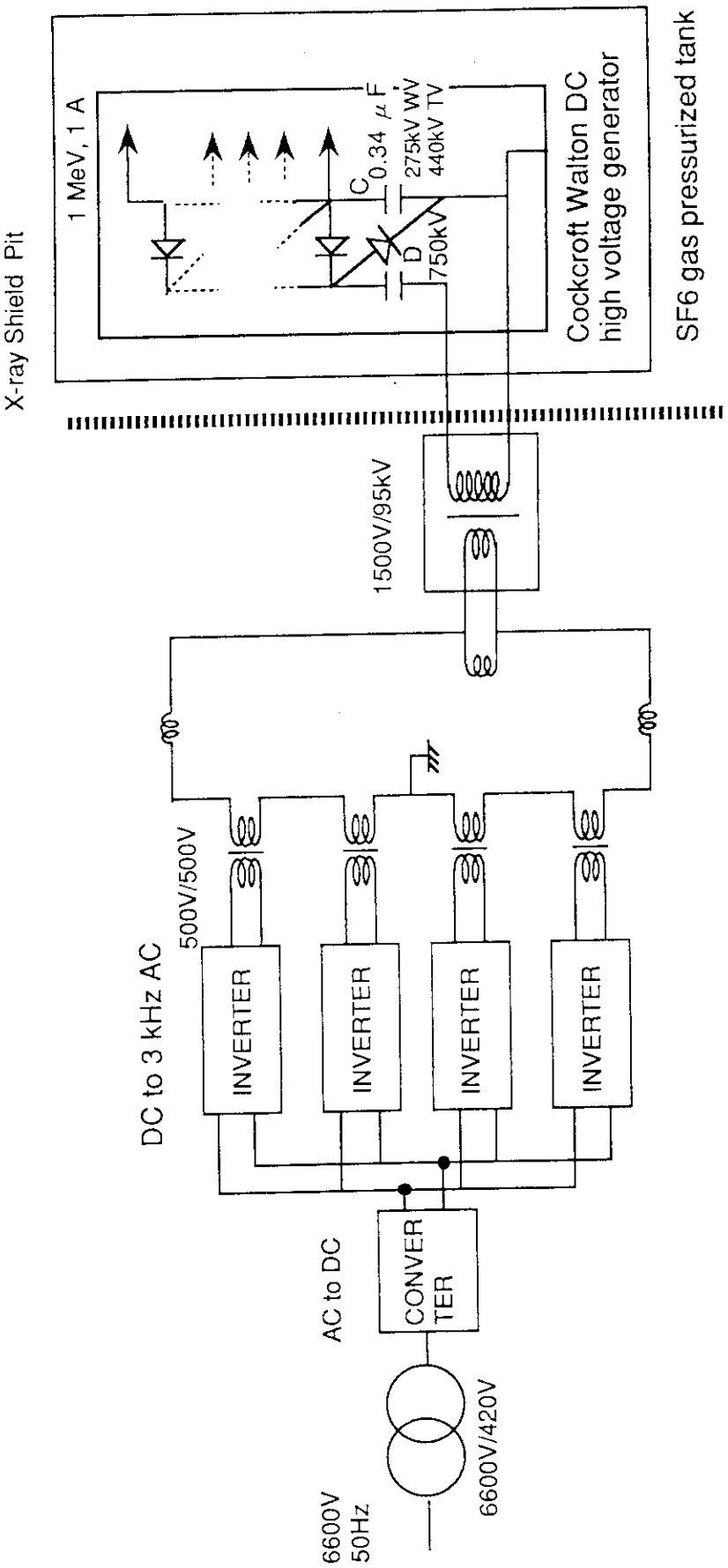

Fig.3.2-3 Schematic Diagram of Accelerator Power Supply

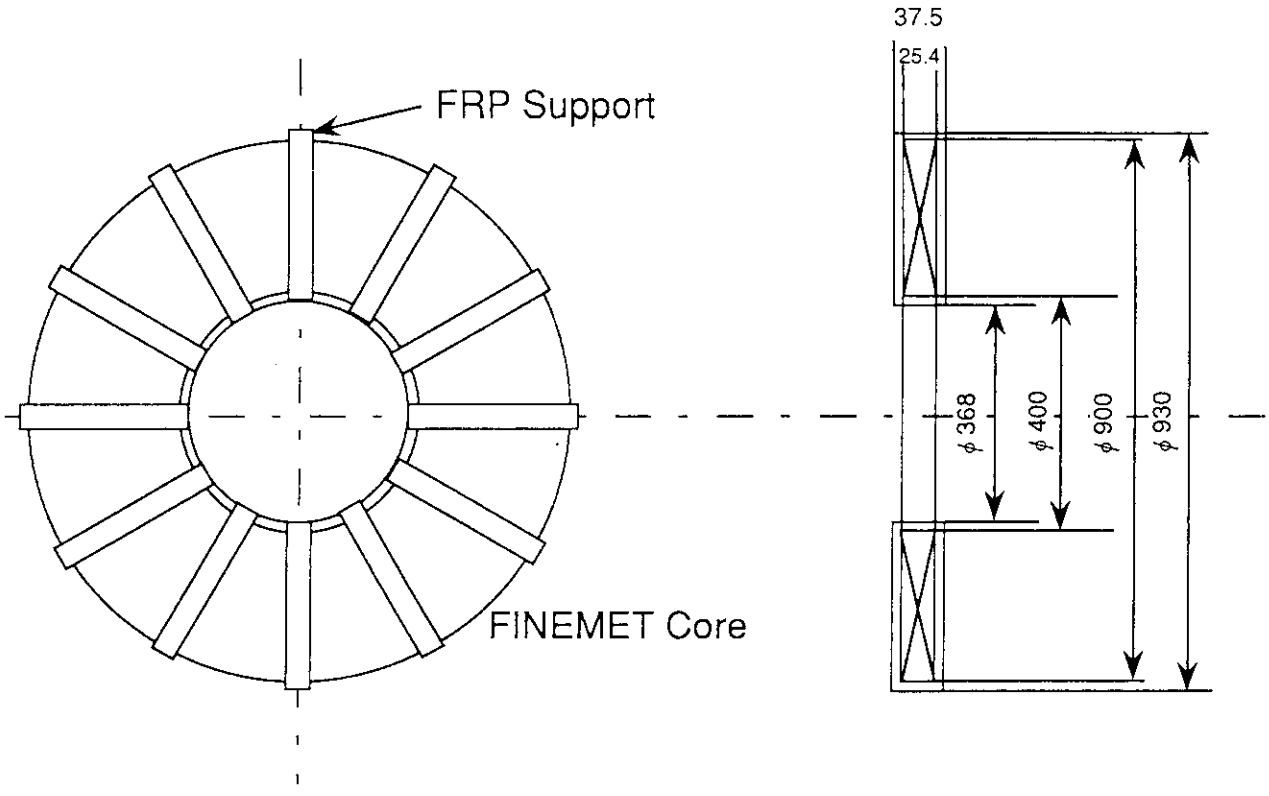

Fig.3.2-4 Dimensions of the FINEMET Core

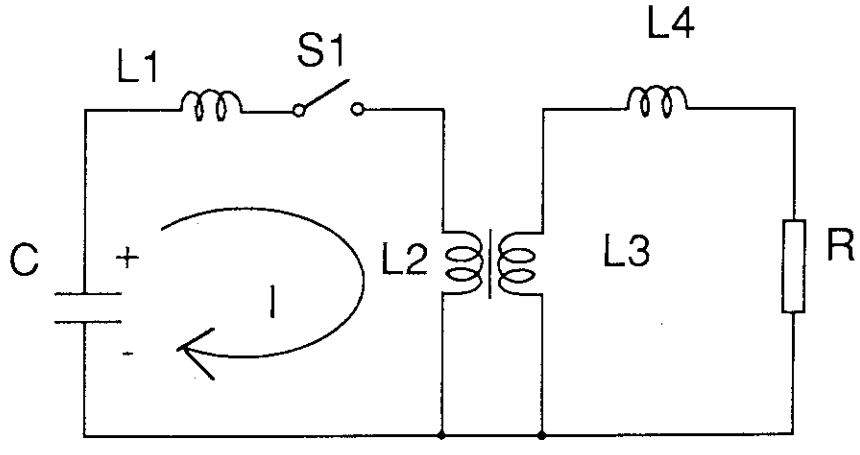

C=450pF　　L1=2.5 μ H
L4=2.5 μ s　　L2,L3=74.5 μ H
R=570 Ω

Fig.3.2-5 Equivalent Circuit of the Power Supply with Surge Blocker

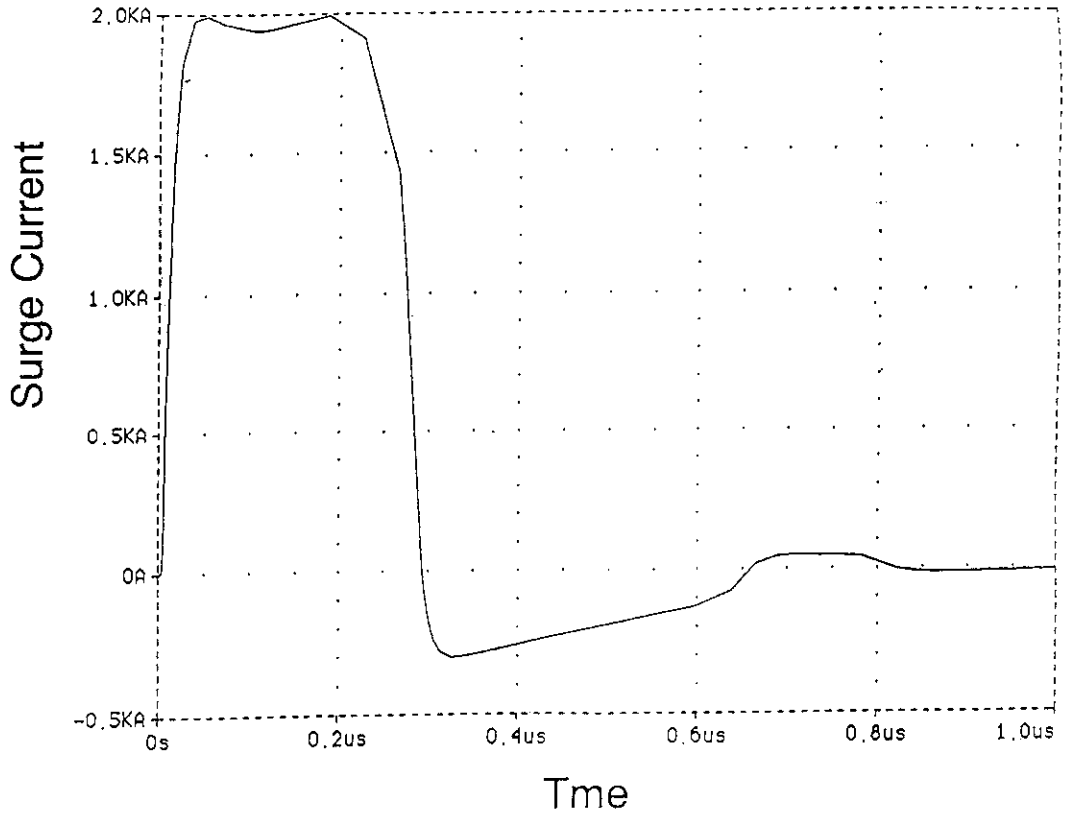

Fig.3.2-6 Surge Current Wave form Simulated with SPICE

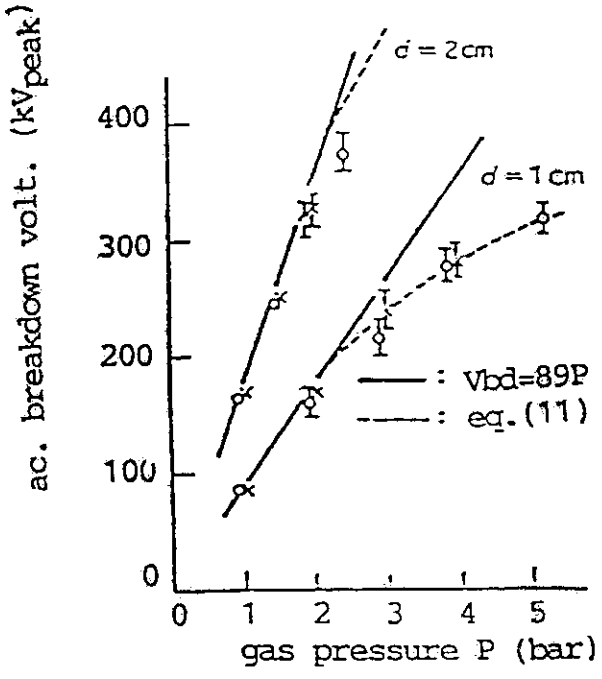

Fig.3.2-7 Breakdown Voltages in SF_6 Gas for Uniform Field Electrodes (200mm in dia.)(Ref.8)

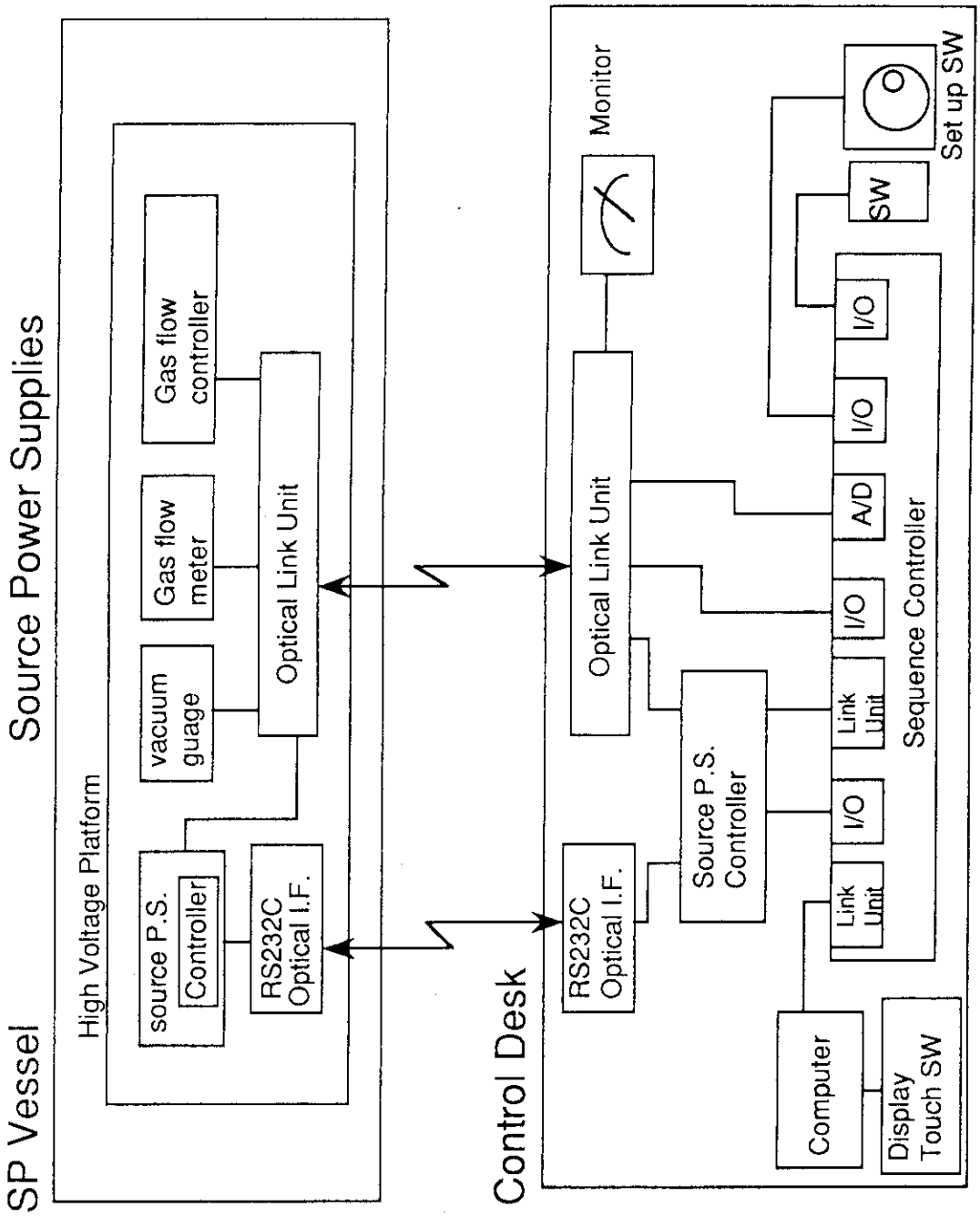

Fig.3.2.8 Block Diagram of the Source Power Supply Control System

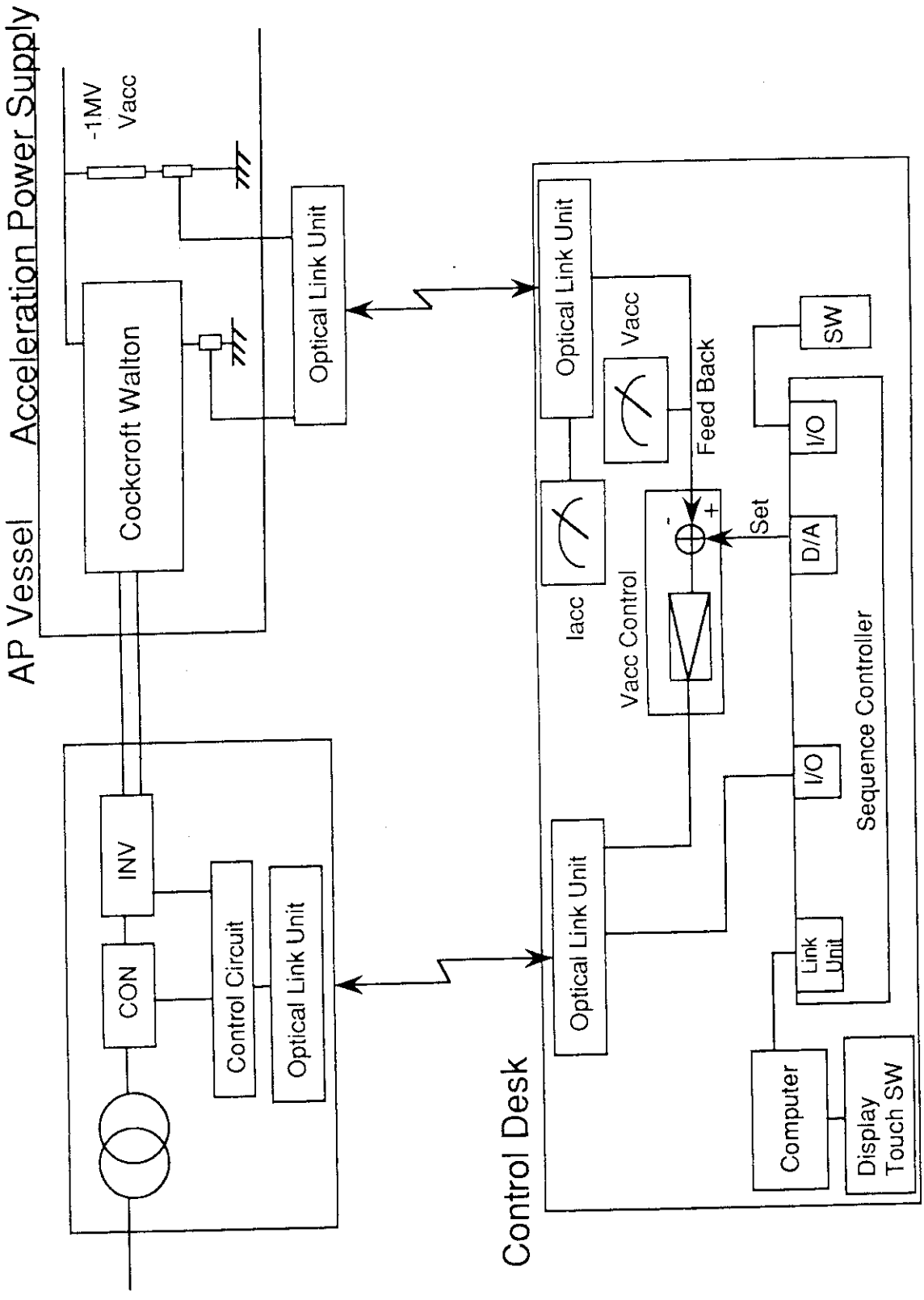

Fig.3.2.9 Block Diagram of the Acceleration Power Supply System

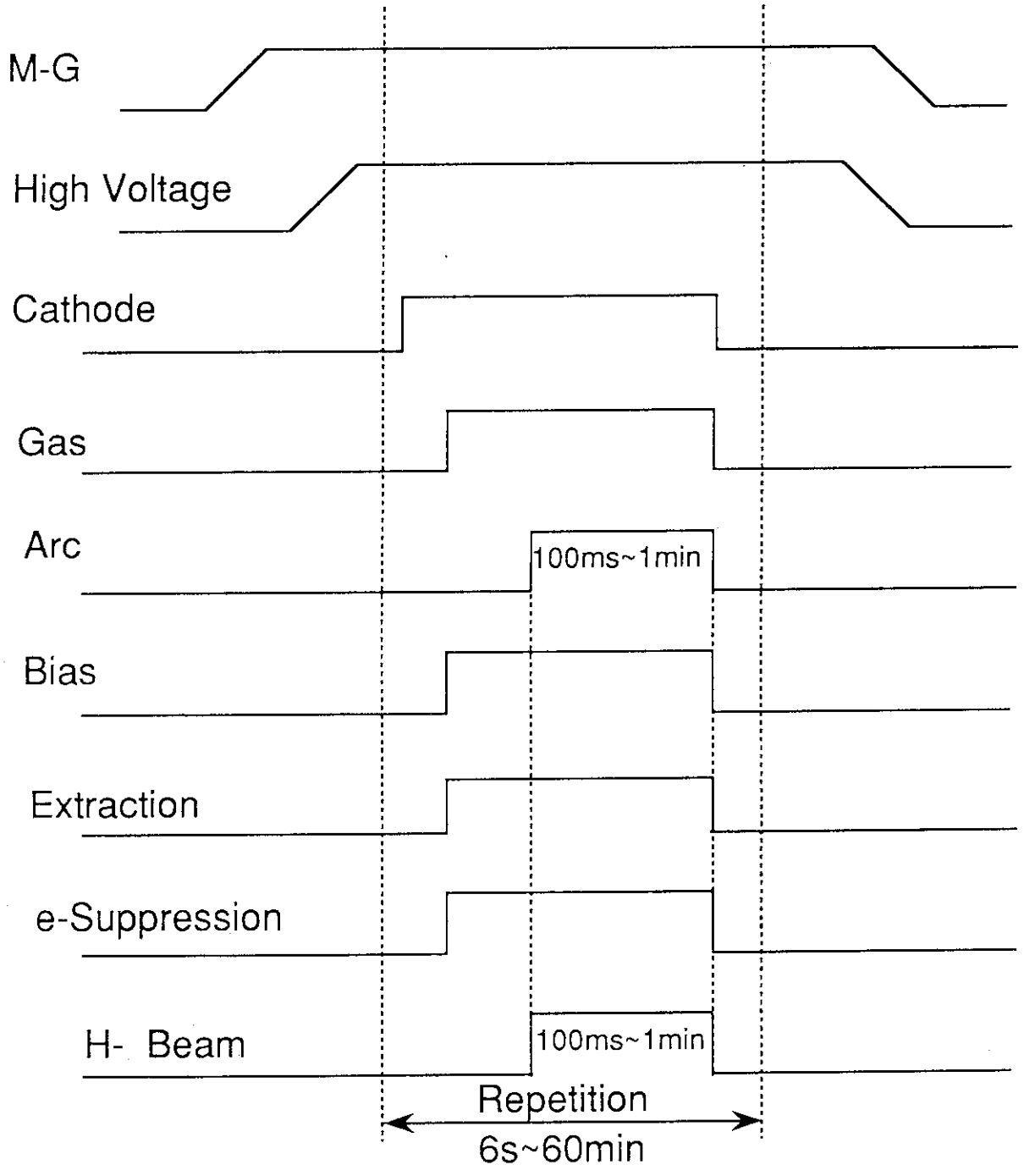

Fig.3.2.10 Time Chart of Operation

3.3 Auxiliary System

3.3.1 System requirements

Auxiliary system of the MeV test facility consists of a beamline systemwith a diagnosis system and a beam target, cooling water system, vacuum system. The beamline is vertically attached beneath the ion source equipped in the AP vessel. To create clean vacuum in the beamline and ion source/accelerator, two pumps, i.e. the cryo-sorption pump and the compound molecular pump are utilized. Even when the cryo-sorption pump is regenerated, the clean vacuum in the ion source/accelerators can be maintained by closing a gate valve. The cooling water system is mainly for supplying pure water with a resistivity of more than 1 MΩ cm to the ion source electrically isolated from ground potential. To keep the high voltage insulation, tubes of the cooling water originated from the header with ground voltage are connected to the ion source/accelerator with high voltage via a water chock. The pure water is also supplied so as to cool the beam target, the compressor of the cryo-sorption pump, and the diagnosis system. Especially, water flow rate of 480 l/min is prepared for the beam target. In operating the ion/accelerator at full power, the total heat load is 1 MW (1 A x 1 MeV). Assuming the beamlet divergence to be 5 mrad, the peak heat flux reaches around 5 kW/cm^2. To reduce the permissible level, the beam target is leaned by 30 degree against a beam axis.

3.3.2 Beamline

Figure 3.3-1 shows the beamline of the MeV Test Facility (MTF). The beamline is 2560 mm in length and 500 mm in inner diameter. The beamline is vertically connected with the AP vessel via a bellow flange in order to absorb a quake. Two oil free pumps evacuate the beamline so as to create the clean vacuum, which is achieved even during the regeneration of the cryo-sorption pump by closing a gate valve mounted beneath the ion source. To observe the high energy beams and to equip the diagnosis devise such as a beam profile monitor, there are many ports on the beamline. At the end of the beamline, there is a beam target with an area of 240 mm x 260mm , where the delivered ion beams are dissipated.

3.3.3 Cooling Water System

The water header of the MTF is placed in the shielding pit, which is connected with 1 MPa line of Particle Beam Engineering Facility. The specifications of the cooling water system are as follows;

(1) pressure :1 MPa

(2) total water flow rate:850 l/min

(3) resistivity : less than 2 MΩ cm

As shown in Table 3.3-1, the water header has 18 feeding lines. The feeding lines of 12 are utilized for the ion source, is connected with ion source via a water chock. In order to measure the heat loads of ion source, Platinum resistance thermometer are also equipped in lines.

3.3.4 Vacuum System

A compound molecular pump and a cryo-sorption pump are mounted on the beamline. The features of each pump are as follows;

The compound molecular pump:

(1) Pumping speed : 1.3 m^3/s in hydrogen

(2) Oil free (magnetic bearing mechanism)

(3) Operational region : from 133 Pa to 10^{-8} Pa.

The cryo-sorption pump:

(1) Pumping speed : $10m^3/s$

(2) Molecular sheave : charcoal

(3) Pumping capacitance : 310 Pa m^3

In a typical operation, i.e. at the pressure of 0.13 Pa, the pressure in the beamline is 0.007 Pa., and the gas flow rate is as low as 0.19 Pam^3/s.

3.3.5 Beam Target

Figure 3.3-2 shows the beam target. The specifications of the beam target are summarized as follows;

(1) Area: 240 mm x 260 mm

(2) Cooling tube: 12 externally-finned tube

(4) Water flow rate: 480 l/min

(5) Angle against the beam axis : 30 degree

Assuming a beamlet profile to be Gaussian with a beam divergence of 5 mrad, the peak heat flux in normal incident is estimated to be around 5 kW/cm^2. This heat load is so high that the externally-finned cooper tube can not endure 1). To reduce the heat load down to permissible value of 2.5 kW/cm^2 (critical heat flux), the beam target is leaned by 30 degree against the beam axis. The accepted beam power can be measured by platinum resistance thermometer. The temperature rise of the beam target at the water flow rate of 480 l/min as a function of beam power is shown in Fig. 3.3-3.

3.3.6 SF6 Gas Recycling System

SF6 gas filled in the tanks is heated by the power supply system. Therefore, a gas recycling and cooling system is required. The gas recycling system is shown in Fig.3.3-4. During the operation of the power supply system, the gas is circulated and cooled by the recycling system with water cooling system. Specifications of the circulator is shown in Table 3.3-2. The moisture content in the SF6 gas is monitored.

Table 3.3-2. Specifications of SF6 Gas Recycling System

Cooling Capacity:	40.1 kW
Pressure of SF6 Gas:	0.6 MPa
Recycling Rate:	12 m^3 / min
Gas Temperature:	10 deg C

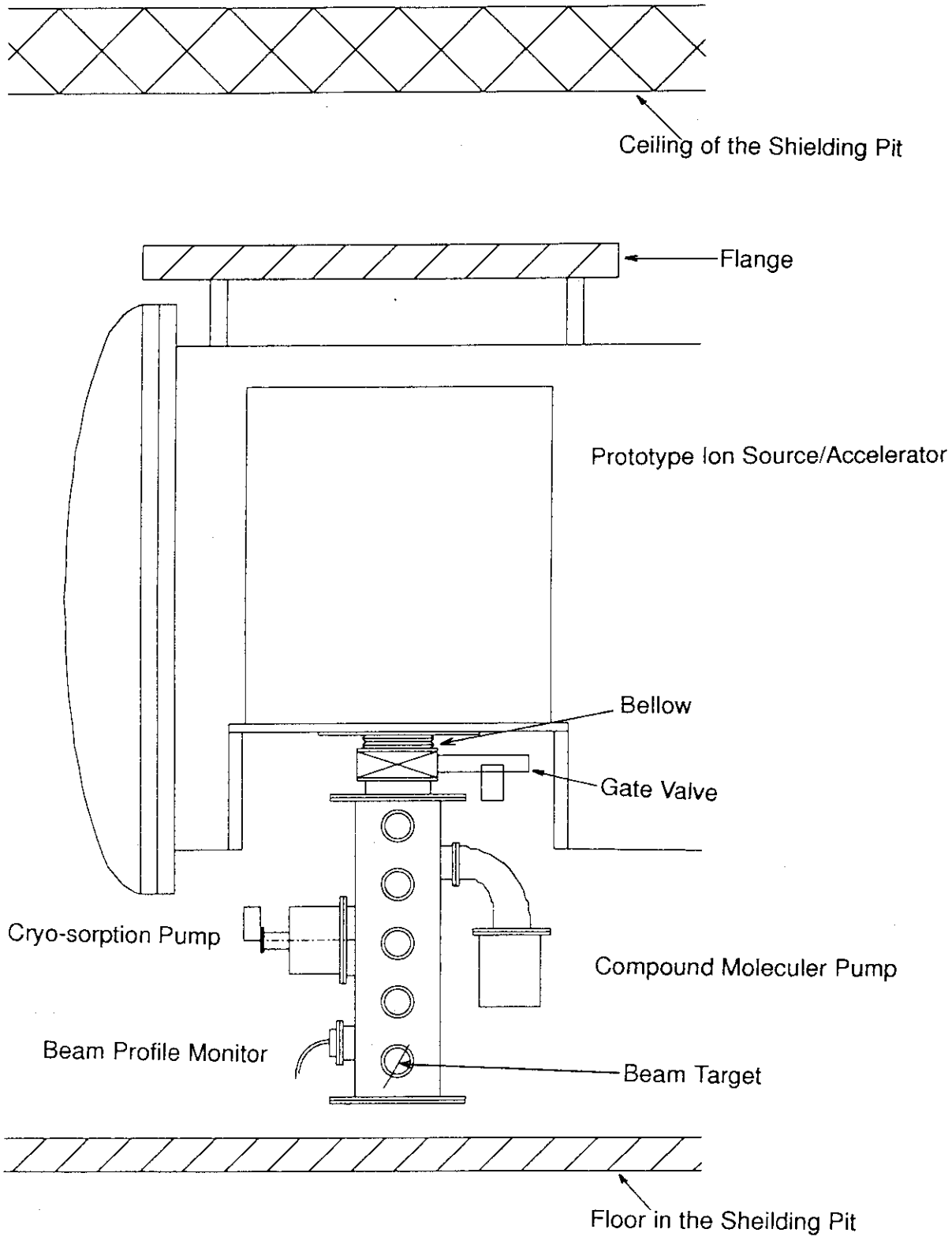

Fig.3.3-1 The beamline of MeV Test Facility

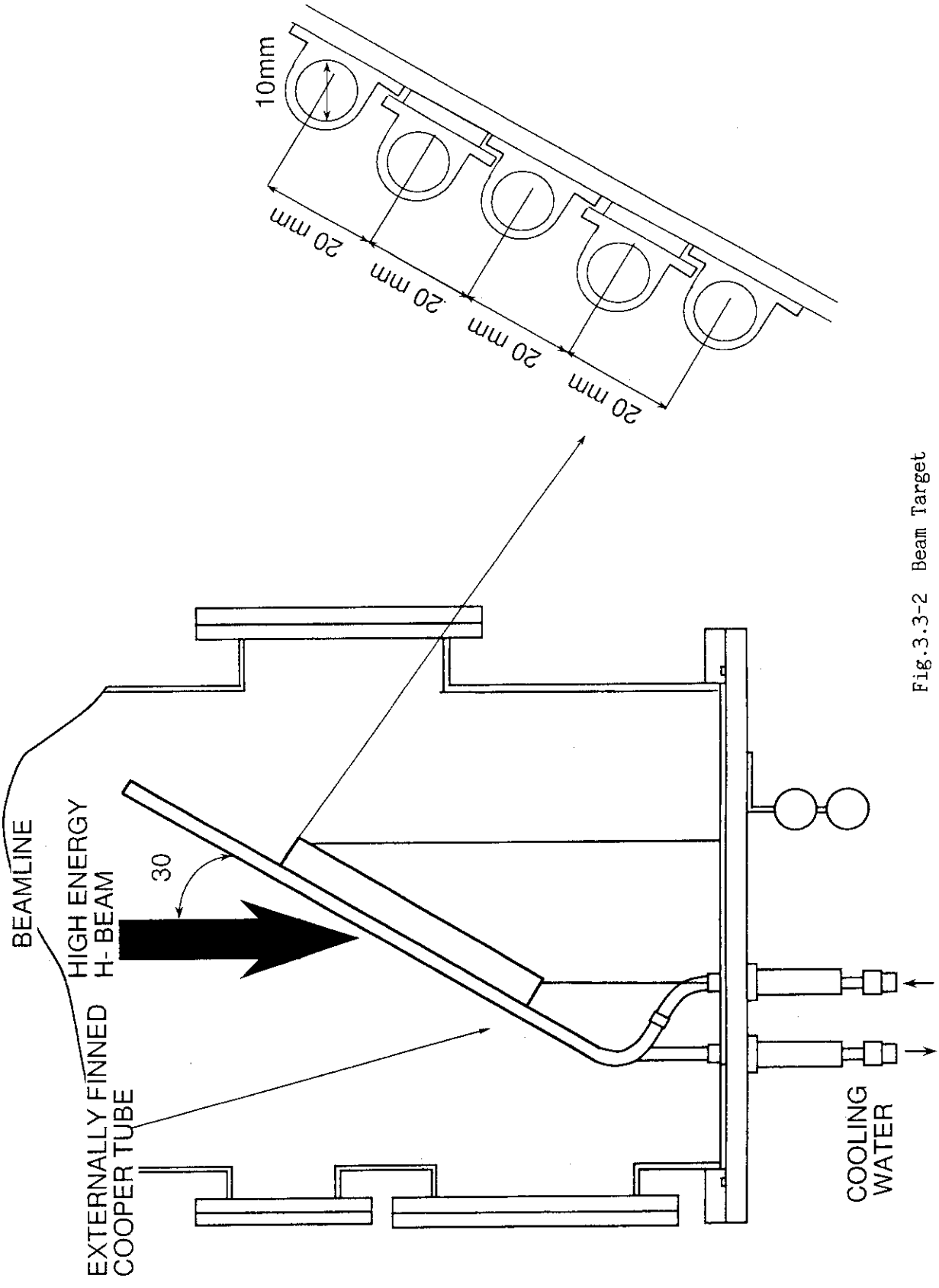

Fig.3.3-2 Beam Target

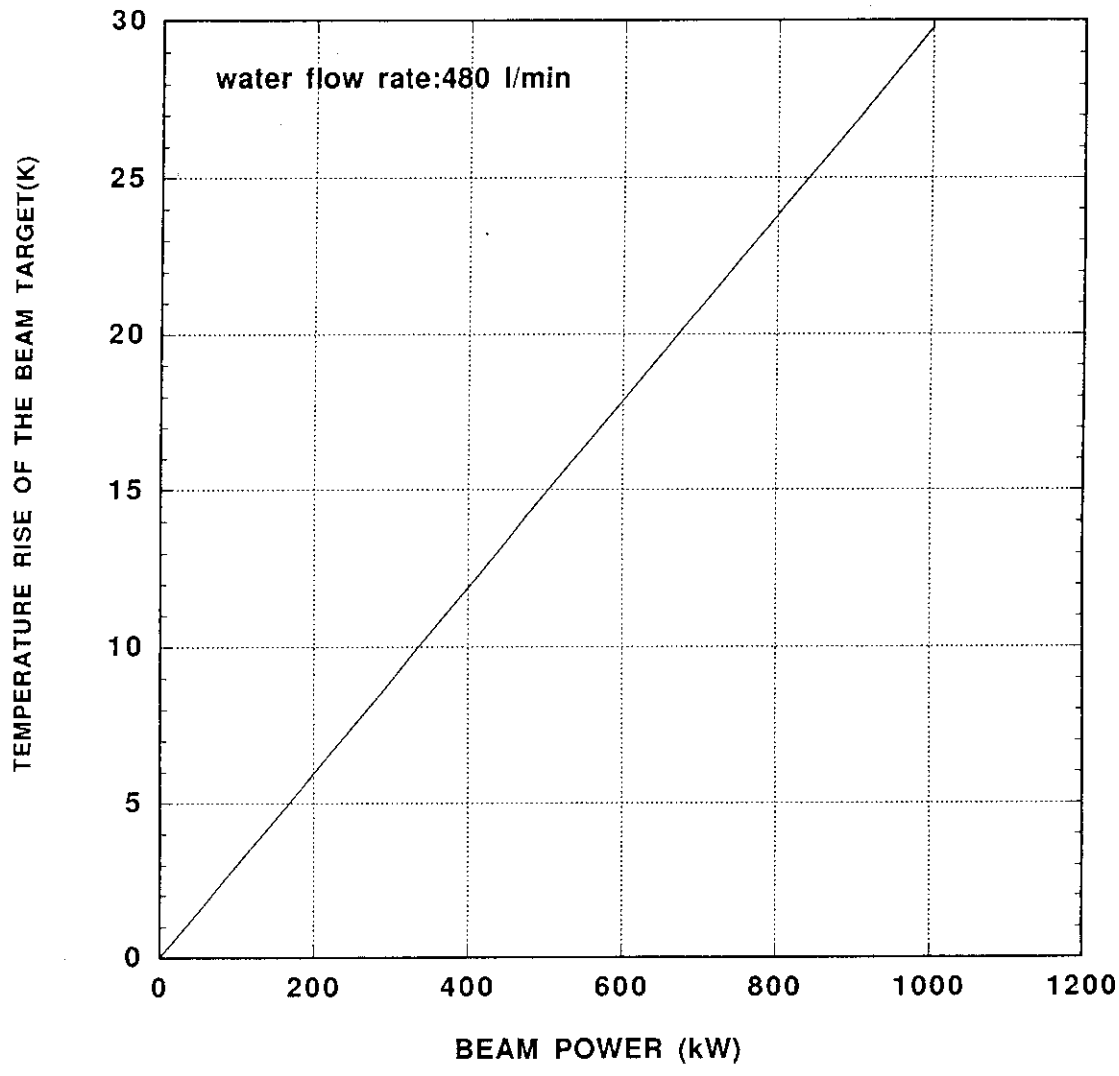

Fig.3.3-3 Temperature rise of the beam target

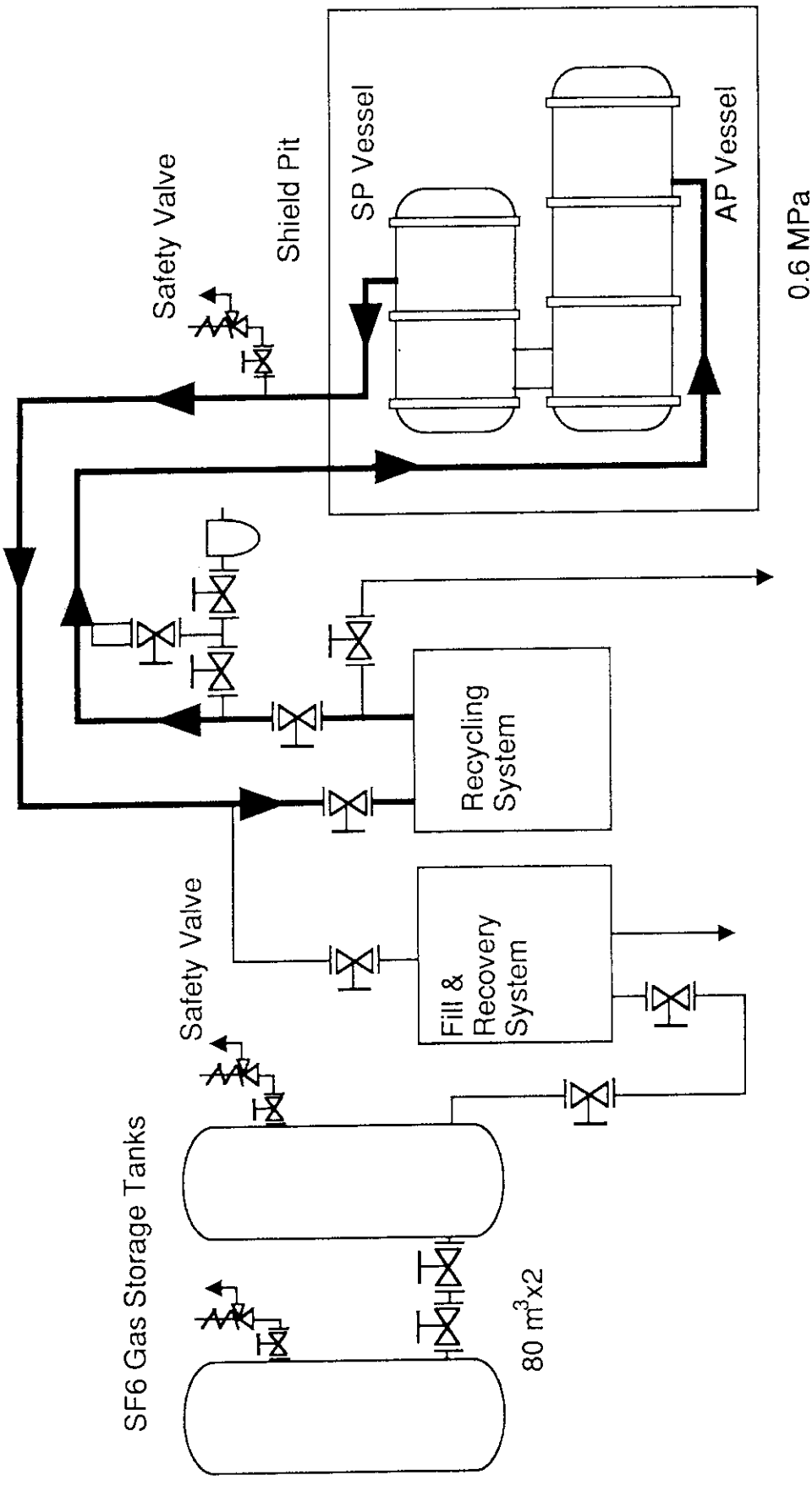

Fig.3.3-4 SF_6 Gas Recycling System

3.4 X-ray Shield

3.4.1 Basis of shield design

Deuterium negative ion beam is used in the ITER NB system. Although an isotope effect is reported in the production process of hydrogen and deuterium negative ions, the difference of negative ion currents obtained with hydrogen and deuterium is already examined in US-Japan[1] and CEA-JAERI[2] collaboration experiments. Performance of the deuterium NB system can be evaluated from the results obtained in the test facility with hydrogen. Hence only production and acceleration of hydrogen negative ion is considered in the present design. Accordingly neutron generation and subsequent activation in the test facility are not considered.

In the course of hydrogen negative ion beam production, there is no generation of radiant ray or radioactive substant in the operation of concern. However, if electron is accelerated together with the negative ion, bremstrahlung X-ray is emitted by collision of high energy electron with accelerator grids or beam dump. Mechnism of electron and subsequent X-ray generation as a basis of shield design are evaluated in the following section 3.4.2.

The MeV Test Facility is classified as a Cockcroft-Walton type accelerator in Japanese law of radiation protection. Here the specification related to the law is summarized as below:

Ion Species:	H^-
Ion Beam Energy:	1 MeV
Ion Beam Current:	1.0 A
Beam Pulse:	1 minute at maximum, duty 1/60
Operation:	48 hours/week
Radiant:	X-ray (maximum energy: 1 MeV)
Location:	NBI test Building, JAERI Naka

Some safety devices, such as interlock systems, alarm lamps, automatic indicator of operational condition, are equipped for the radiation safety.

For the X-ray shield the main components of the test facility, such as the ion source / the accelerator, the acceleration power supply, and the source power supply, are installed in the basement pit in the room as shown in Fig. 3.4-1, 2, and 3. Ground level of the pit is covered with concrete for the X-ray shield. The concrete shield are designed so as to reduce the X-ray dose of radiation workers and general staffs. The design considerations are described in sections 3.4.3 and 3.4.4 for X-ray penetration and streaming, respectively. Thickness of the concrete is listed in Table 3.4-1.

Table 3.4-1 Thickness of the concrete shield

Shield wall (E, W, N):	90 cm
Shield wall (S):	100 cm
Shield wall (Ceiling):	80 cm

Layout of the MeV Test Facility in the building is shown in Fig. 3.4-4. Inside, near the shielding pit and power supply area is prohibited to trespass during the operation. The NBI test room is set up to be a radiation controlled area. Evaluation of these results are described in section 3.4.5.

3.4.2 X-ray Production

X-ray in the MeV Test Facility is generated only by bremstrahlung of electron accelerated together with the negative ion. Amount of electron produced in the accelerator is estimated first in this subsection. Then a method of X-ray generation computation is described. The amount of X-ray to be generated and the energy spectra is shown in the end of this subsection.

In the course of extraction/acceleration free electron is stripped and produced from The negative ion by collision of the ion with residual gas molecule. Through a gas flow calculation[3] in the source/accelerator and the MeV Test Facility vacuum chamber, the stripping loss of The negative ion is evaluated to be 8.3 % of the ion current at the source pressure of 0.15 Pa. The stripping loss of the ion was also evaluated in an acceleration experiment with "350 keV source" [4], which has a similar structure in the electrostatic accelerator. Assuming that all the heat load in the accelerator grids were generated by the stripped and accelerated electron, the electron production was estimated to be 4.7 % of the ion. Here we assume that the electron of 10 % , i.e. 0.1 A, is accelerated up to full energy of 1 MeV for the X-ray generation.

A computer code "EGS-4[5]" was used in the calculation of X-ray generation from the electron beam. The code compute electro-magnetic cascade of electron in a solid substrate by Montecarlo method. Assumptions used in the calculation is summarized as follows:

1) The multi-group energy structure:

	Lower boundary (MeV)	Upper boundary (MeV)
group 1:	1.0×10^{-2}	5.0×10^{-2}

group 2:	5.0×10^{-2}	1.0×10^{-1}
group 3:	1.0×10^{-1}	1.5×10^{-1}
group 4:	1.5×10^{-1}	2.0×10^{-1}
group 5:	2.0×10^{-1}	3.0×10^{-1}
group 6:	3.0×10^{-1}	4.0×10^{-1}
group 7:	4.0×10^{-1}	6.0×10^{-1}
group 8:	6.0×10^{-1}	8.0×10^{-1}
group 9:	8.0×10^{-1}	1.0×10^{0}
group 10:	1.0×10^{0}	1.5×10^{0}

2) The 1 MeV electron is impinged virtically on a beam dump as the electron target.

3) The beam dump was assumed as a copper plate of 10 mm thickness.

The angular distribution and energy spectra of the generated X-ray is shown in Fig. 3.4-5 and 3.4-6. The X-ray is generated almost uniformly on the surface of the beam dump, i.e. beam injection side. The maximum X-ray generation rate in this side is 0.0386 photon/electron Sr^{-1}.

3.4.3 X-ray Penetration

From a results obtained by the X-ray generation calculation dose rate of the X-ray penetrating the shield on the MeV Test Facility was calculated. The assumptions and calculaion conditions are summarized as follows:

1) X-ray generation: Total X-ray generation was assumed from the maximum value obtained in 3.4.2 (0.0386 photon / electron in unit steradian). The total X-ray generation is;

$$0.0386 \times 4\pi = 0.485 \text{ (photon / electron)}$$

2) A similar energy group structure was used. The energy stectrum obtained in 3.4.2 was conserved.

3) The average dose in a week was evaluated for the full test facility operation, i.e. 48 hours/week with the duty factor of 1/60.

4) Shield considered in the calculation is:

Shield wall (E, W, N):	90 cm thick concrete
Shield wall (S):	100 cm thick concrete
Shield wall (Ceiling):	80 cm thick concrete
AP Vessel	2 cm thick iron (cylinder part)
and SP Vessel:	2.5 cm thick iron (barrel head)
Auxilary shield:	4 cm thick lead

X-ray penetrating underground was neglected since the conrete base and soil has enough thickness for the shield. Shielding effect of power supplies, the source and the accelerator etc. were also neglected.

5) The dose rate was evaluated on points shown in Fig. 3.4-7.

The calculation was carried out in two methods; computation by "QAD[6]" code for bulk shielding, and an analytical calculation for detail evaluation at the points.

Folmurla used in the analysis is as below.

$$H_U(X) = \frac{48}{60}\sum_{E=1}^{10}\left\{\frac{S(E)}{4\pi r^2}\exp\left[-\sum_{i=1}^{3}(\mu_i(E)\,d_i)\right]X_1(E)\,B(E)\,X_2\,f_{X1cm}\right\} \qquad (1)$$

Here,
$H_U(X)$: Dose rate at point X (Sv/week)
48: weekly operation time (hours)
1/60: duty factor
E: Energy group
S(E): Number of X-ray photon
Number of 0.1 A Electron is;
$0.1\ A \times 1/(1.60 \times 10^{-19}\ A/Coulomb) = 6.25 \times 10^{17}$ electrons
(number of X-ray photon)$= 6.25 \times 10^{17} \times$ photon generation in 3.4.2
r: distance between beam dump and the evaluation point (cm)
$\mu_i(E)$: attenuation coefficient of shield (/cm)
di: Thickness of the shield (cm)
$X_1(E)$: Conversion factor from photon flux to irradiation dose rate (R/hr(p/cm^{2}s))
B(E,d): Build up factor of conrete
X_2: Conversion factor from irradiation dose rate to absorption dose rate of air
(= 0.00873 Gy / R)
f_{X1cm}: Conversion factor from absorption dose rate of air to dose equivalent at 1 cm depth (Sv / Gy)

An example of the results obtained by the code QAD is shown in Fig. 3.4-8. The result of the analytical is summarized in Table 3.4-2 and 3.4-3 for the evaluation points.

3.4.4 Duct Streaming

An entrance cave, rf feed line, auxiliary power / gas / water lines, and hatch on the ceiling are ducts penetrating the shield of the MeV test stand. These ducts have thicknesses more than 80 cm concrete for direct X-ray. Also all these ducts are provided labyrinth structure to attenuate X-ray streaming passing through the ducts.

A ratio of doses due to the X-ray streaming at inside and outside of the shield are estimated by the following fomula;

$$\frac{D_{out}}{D_{in}} = C\left(\frac{d_0^2}{8l_0^2}\right)\left(\frac{\alpha d_1^2}{8l_1^2 \sin\theta_1}\right)\cdots\cdots\left(\frac{\alpha d_j^2}{8l_j^2 \sin\theta_j}\right)\cdots\cdots\left(\frac{\alpha d_n^2}{8l_n^2 \sin\theta_n}\right) \qquad (1)$$

Here for a duct:

Dout:	Dose rate at the duct outside of the shield
Din:	Dose rate at the duct inside of the shield
dj:	Equivalent duct diameter, dj $= \sqrt{4/\pi}$ aj bj
lj:	Duct length
θ j:	Angle of the duct bend
α :	Albedo (= 0.1 for the X-ray)
C:	Safety factor = 1
aj,bj:	Dimension of the duct opening

The results of the estimation for the ducts are summarized in Table 3.4-4.

As shown in the table, X-ray streaming through the ducts are attenuated more than 11 order of magnitude in each duct. Comparing the attenuation of streaming with that of penetrating the shield concrete, the attenuation factor is four order larger in the streaming X-ray attenuation. In the present evaluation of the X-ray shield the dose due to the streaming is negligible with respect to that of the concrete shield for the X-ray penetration.

3.4.5 Evaluation

From the result obtained in section 3.4.4, Effect of streming X-ray through the ducts are neglected in the evaluation.

As be shown in Table 3.4-2, the dose rate in the radiation controlled area is 0.068 mSv/week at the maximum at the evaluation point A. This value is well below equivalent dose calculated from

annual dose of ICRP recommendation No. 60 for the radiation workers. The radiation safety in the controlled area is secured.

The dose rate on boundary of the radiation controlled area is summarized in Table 3.4-3. The highest dose rate is 5.6 μSv/week at the evaluation point J. This value is well below equivalent dose calculated from annual dose of ICRP recommendation No. 26 for general workers. The radiation safety outside the controlled area is secured.

Reference

[1] T. Inoue et.al., Rev. Sci. Instrum. 61/1, 496 (1990).
[2] K. Watanabe et.al., Proc. 6th Int. Symp. on Production and Neutralization of Negative Ions and Beams, AIP Conf. Proc. No. 287, 326, (1992).
[3] Y. Okumura, Memorandum "Evaluation of accelerated electron in the MeV Test Facility" (in Japanese).
[4] K. Watanabe et.al., "Production of a Hydrogen Negative Ion Beam of 350 keV, 0.2 A, 1 s by an electrostatic accelerator", EP-93-48, Society of Electric Engineers of Japan (in Japanese), (1993).
[5] W. R. Nelson, H. Hirayama, and D. W. Rogers, SLAC-265 (1985).
[6] Y. Sakamoto, S. Tanaka, "QAD-CGGP2 and G33-GP2: Revised versions of QAD-CGGP and G33-GP", JAERI-M 90-110 (1990).

Table 3.4-2 Summary of dose rate at evaluation points in the radiation controlled Area

	Evaluation Point (Coordinate (Origin: X-ray source)) and Position	Distance (cm)	Shield (Thickness: cm)	Dose Rate (mSv/week)	
	Point A (0, 340, 420) Shield Pit North Side Outer Wall Surface	540	Iron (4.5) Concrete (90)	6.1×10^{-2}	
	Point B (-803.5, 0, 410.5) Shield Pit West Side Outer Wall Surface (Inside of Power Supply Area)	902	Lead(4) Concrete (90)	4.6×10^{-3}	
	Point C (0, -990, 420) Shield Pit South Side Outer Wall Surface (Inside of Power Supply Area)	1075	Iron (7) Concrete (100)	9.3×10^{-4}	
	Point D (370, 0, 430) Shield Pit East Side Outer Wall Surface (Inside of Power Supply Area)	568	Iron (4.5) Concrete (90)	5.3×10^{-2}	
	Point E (-400, 0, 620) Shield Pit Roof (Inside of Power Supply Area)	738	Iron (2) Concrete (80)	5.3×10^{-1}	

Table 3.4-3 Summary of dose rate at evaluation points on the radiation controlled area boundary

	Evaluation Point (Coordinate (Origin: X-ray source)) and Position	Distance (cm)	Shield (Thickness: cm)	Dose Rate (mSv/week)	
	Point F (0, 1190, 1460) Loading Room wall surface	1884	Iron (4.5) Concrete (90)	4.9×10^{0}	
	Point G (-880, 0, 450) PBEF power Supply Area	988	Lead (4.0) Concrete (90)	3.8×10^{0}	
	Point H (0, -1890, 790) Building South Side Wall	2048	Iron (4.5) Concrete (100)	2.6×10^{-1}	
	Point I (1350, 0, 1570) Building East Side Wall	2071	Iron (4.5) Concrete (90)	4.0×10^{0}	
	Point J (-880, 0, 1580) 2F PBEF Controll Room	1809	Lead (4.0) Concrete (80)	5.6×10^{0}	

Table 3.4-4 Attenuation of X-ray streaming through ducts

Duct	Number of Bend	Equivalent Diameter (cm)	Duct length (cm)	Bending Angle (degree)	Attenuation in Each Bend	Total Attenuation
HF Power Feed Line	0	67.7	110	—	4.73×10^{-2}	5.18×10^{-12}
	1	67.7	280	90	7.31×10^{-4}	
	2	67.7	80	90	8.95×10^{-3}	
	3	67.7	280	90	7.31×10^{-4}	
	4	67.7	50	90	2.29×10^{-2}	
Entrance Cave	0	128	120	—	1.42×10^{-1}	1.03×10^{-11}
	1	137	95	90	2.60×10^{-2}	
	2	137	140	90	1.20×10^{-2}	
	3	137	90	90	2.90×10^{-2}	
	4	137	133.5	90	1.32×10^{-2}	
	5	207	220	90	1.11×10^{-2}	
	6	143	68.5	90	5.45×10^{-2}	
Auxiliary Power, Gas, Water Line	0	20	106	—	4.45×10^{-3}	2.10×10^{-13} x 16Ducts $= 3.36 \times 10^{-12}$
	1	20	275	90	6.61×10^{-5}	
	2	20	40	90	3.13×10^{-3}	
	3	20	148	90	2.28×10^{-4}	

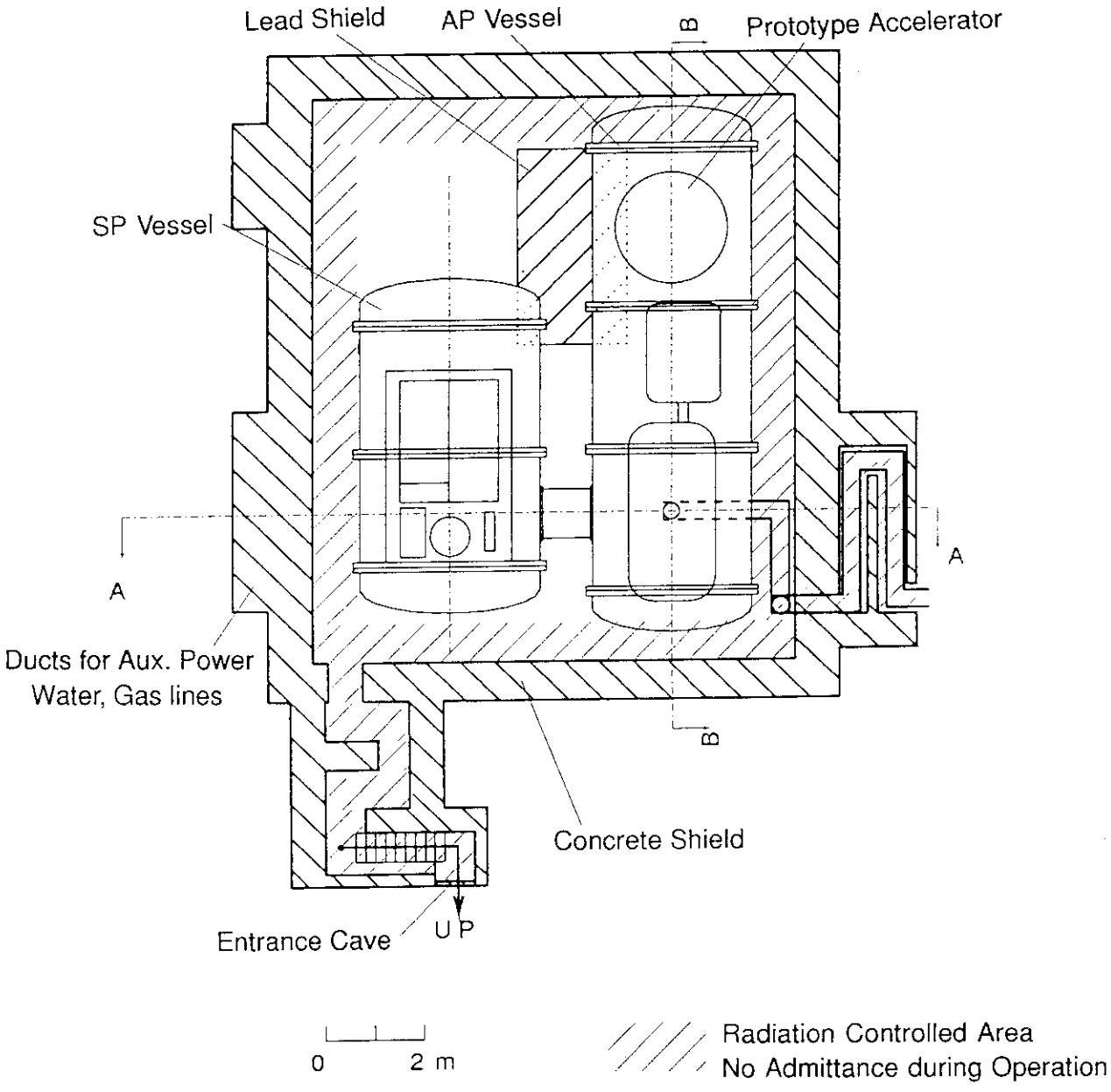

Fig.3.4-1 A plan view of MeV Test Facility in shielding pit (B1F)

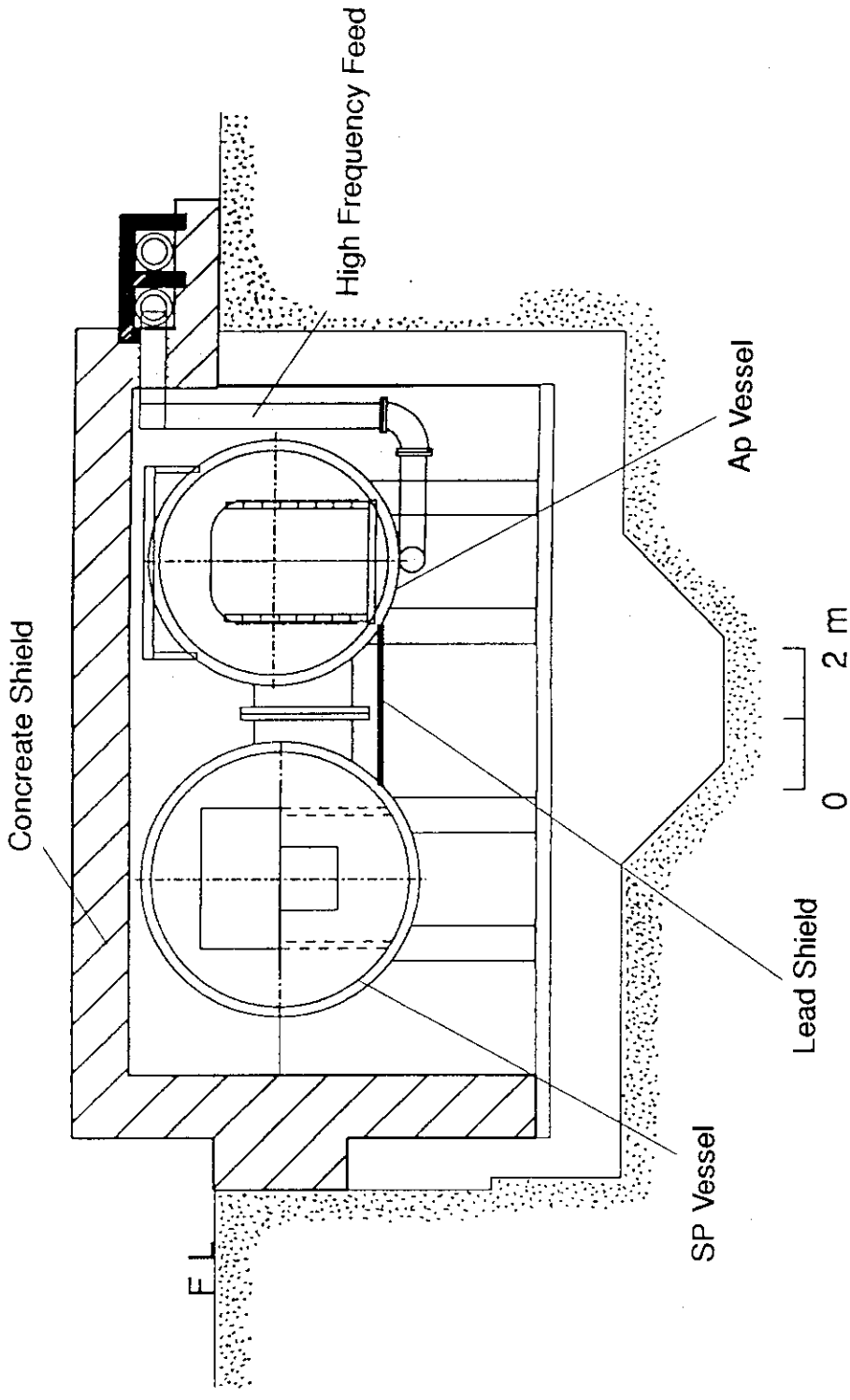

Fig.3.4-2 A cross-sectional veiw of MeV Test Facility.
(Cross-section A-A', E-W direction)

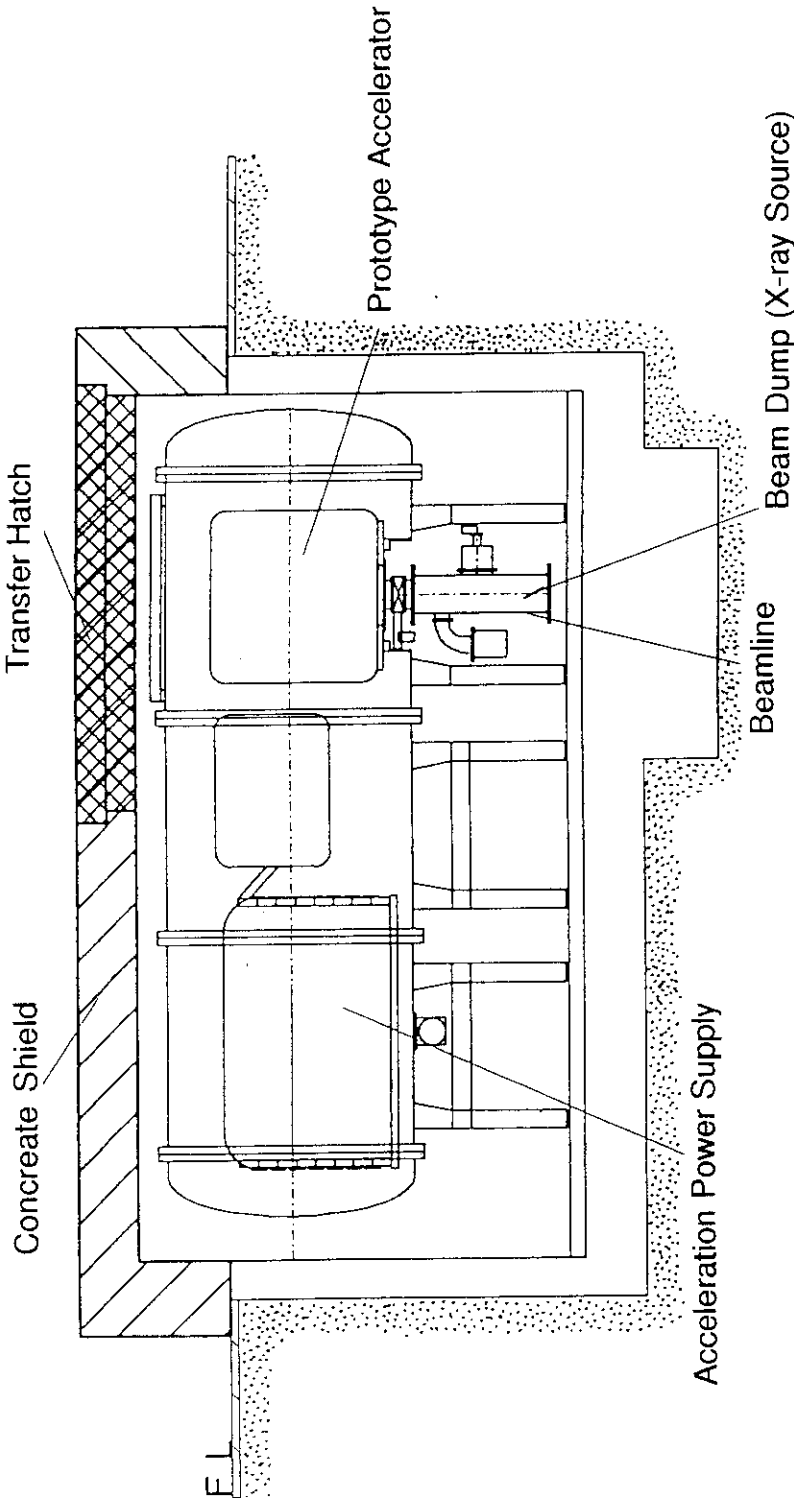

Fig.3.4-3 A cross-sectional view of MeV Test Facility
(Cross-sectional B-B', S-N direction)

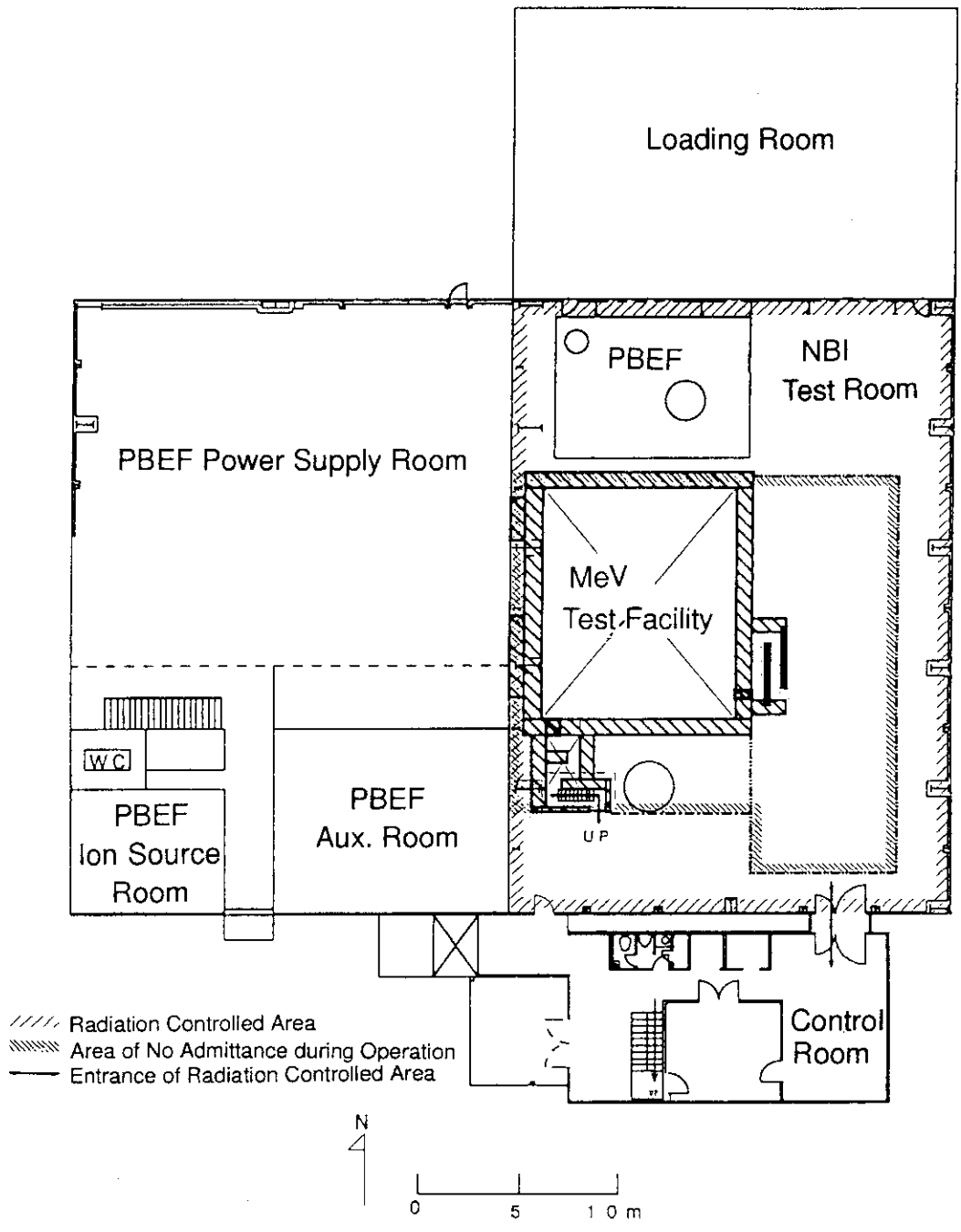

Fig.3.4-4 A Plan view of the building (ground level).

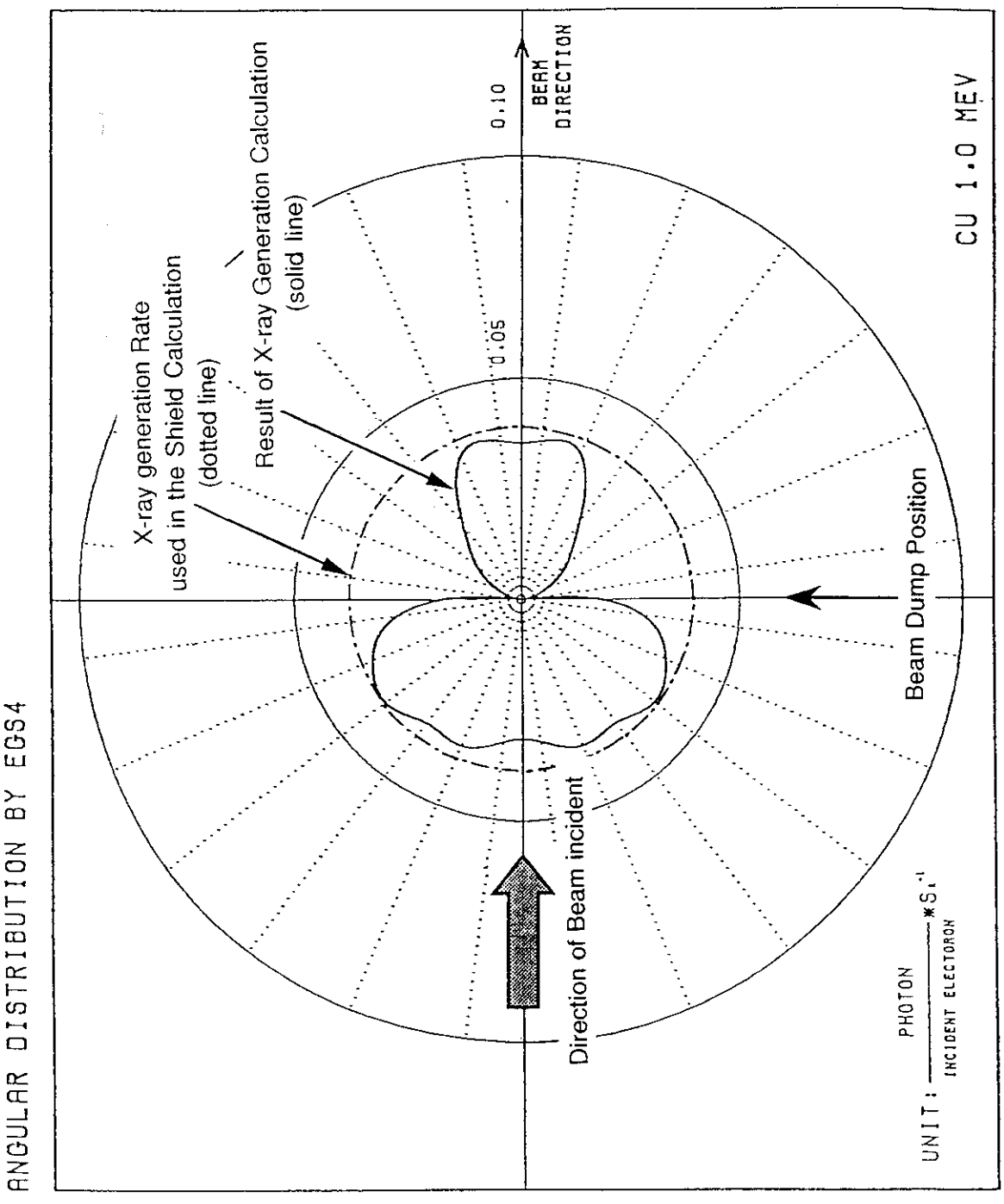

Fig.3.4-5 The angular distribution of the X-ray generated by 1 MeV electron incident on the beam dump.

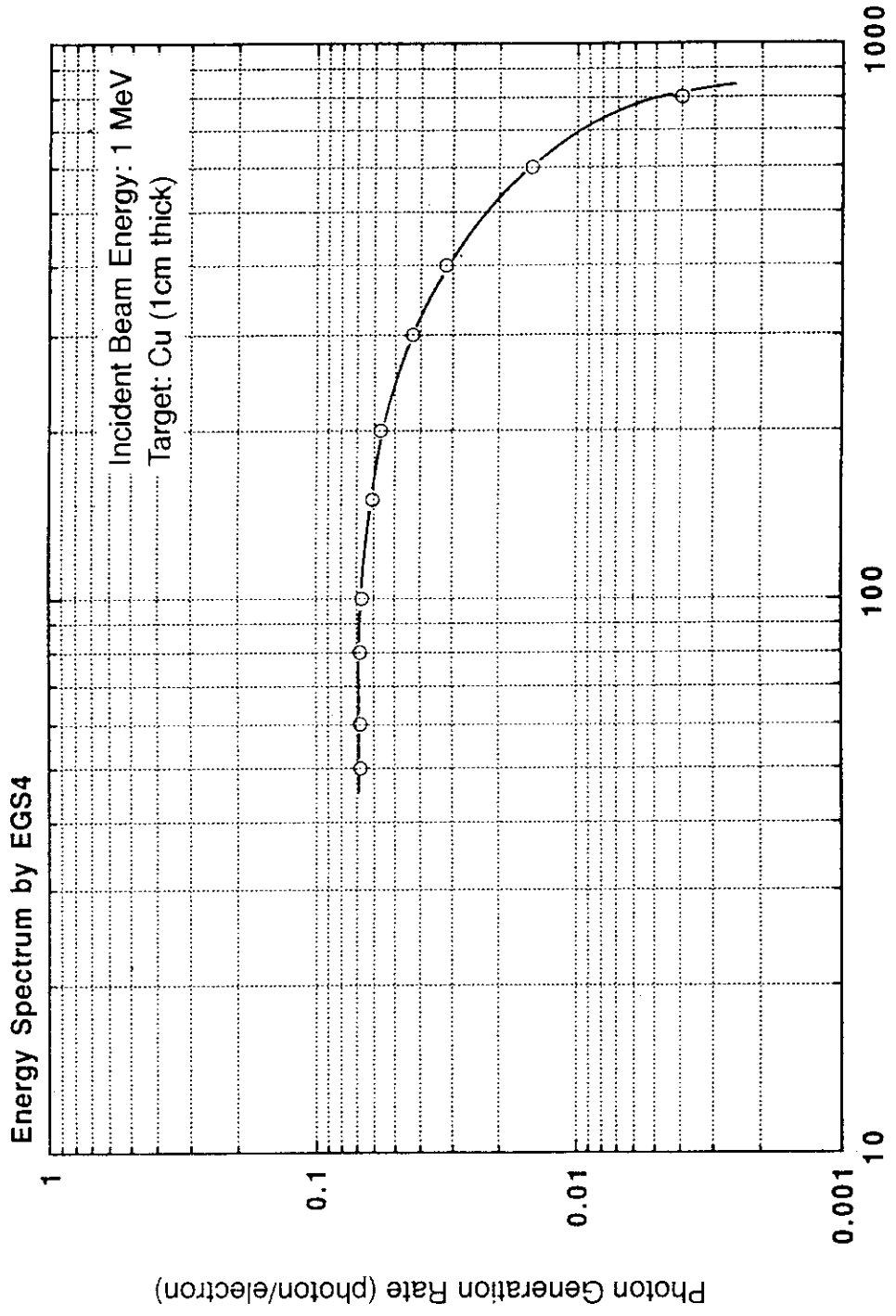

Fig.3.4-6 The energy spectra of the X-ray generated by 1 MeV electron incident on the beam dump.

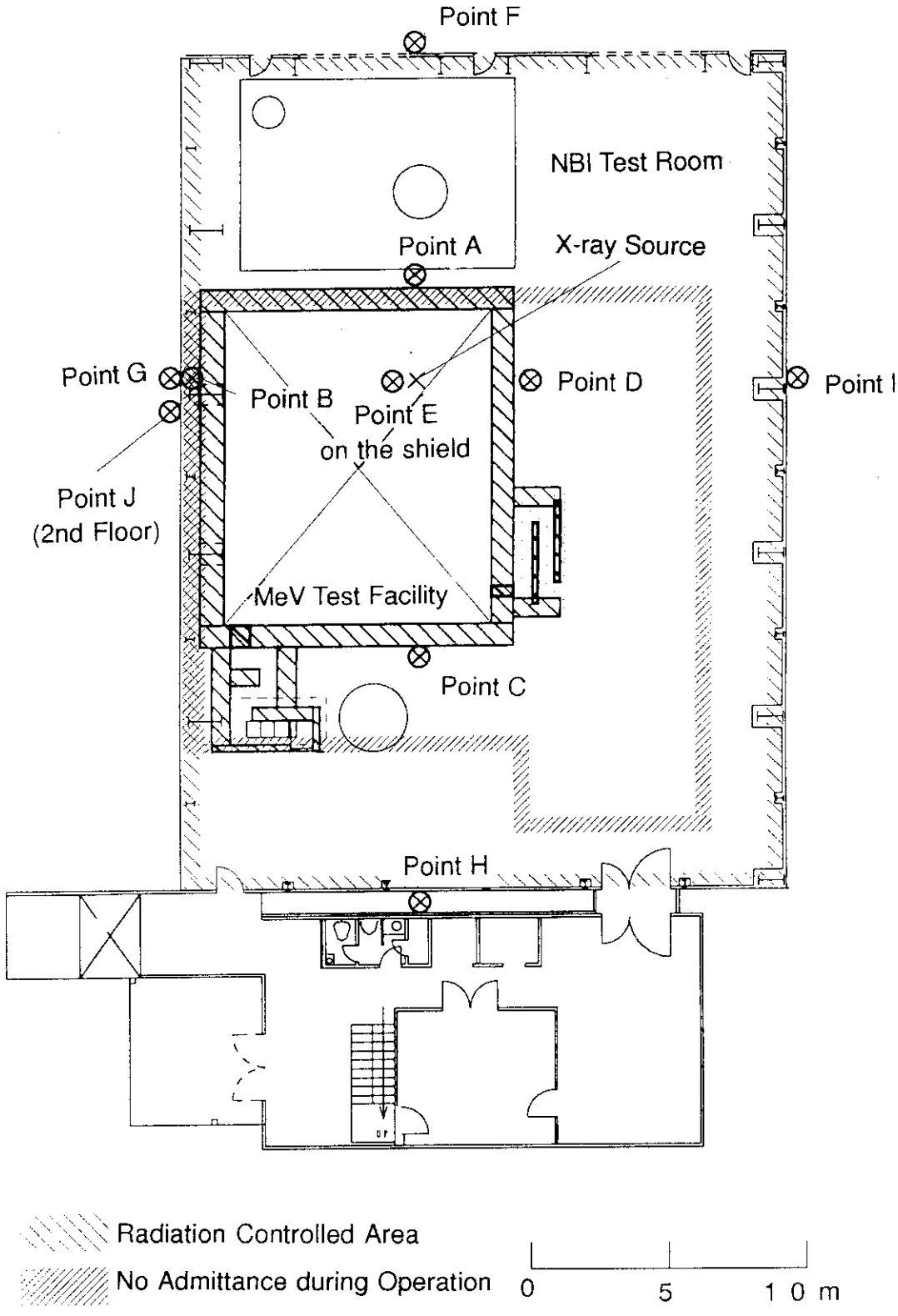

Fig.3.4-7 The position of the X-ray generation and the evaluation points.

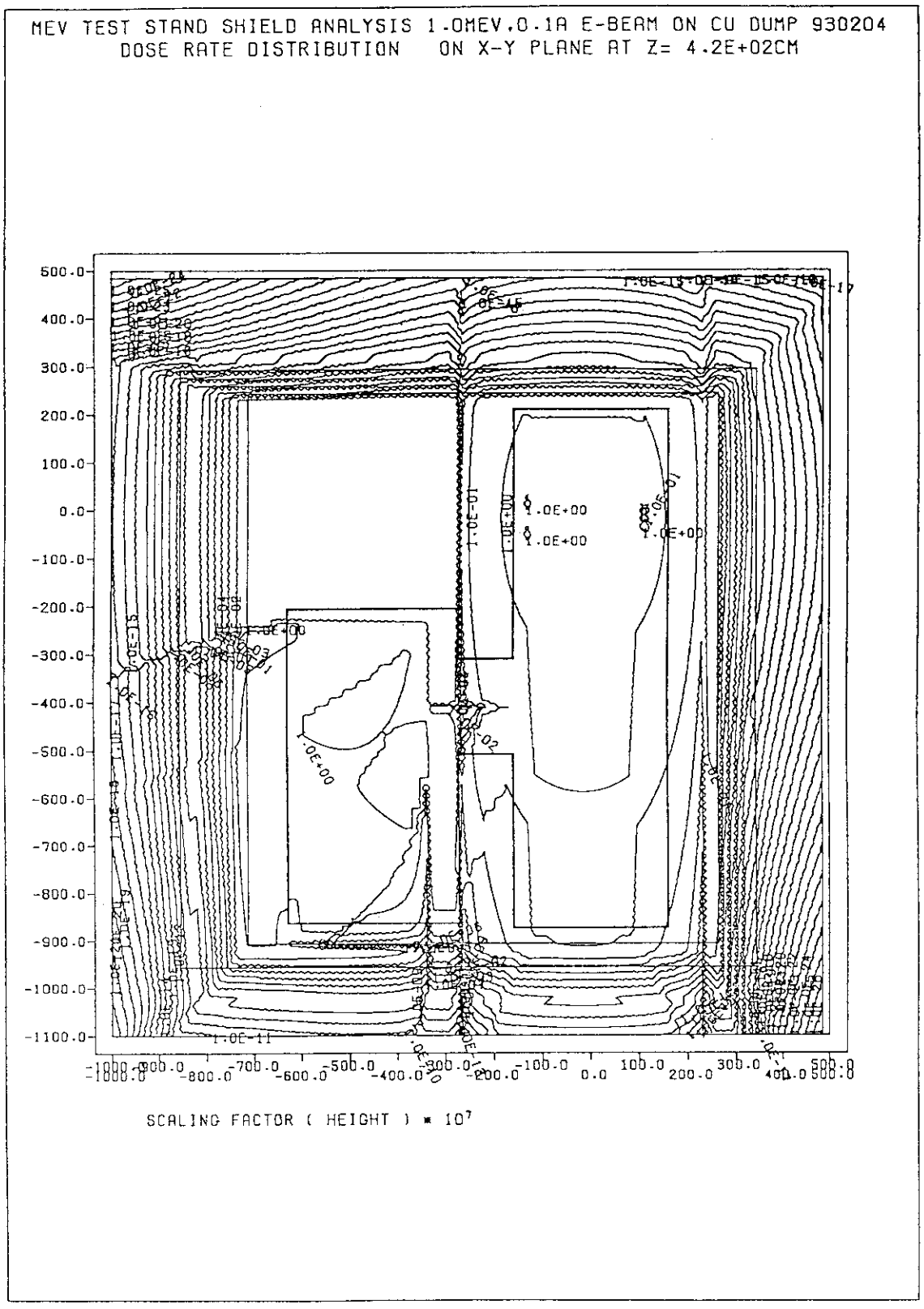

Fig.3.4-8 The contour map of the dose rate in MeV Test Facility at ground level. (unit : 10^7mSv/hr)

3.5 Layout of MeV Test Facility (MTF)

Figure 3.5-1 shows a layout of MTF. There are two vessels pressurized by a 0.6 MPa SF6 gas in the shielding pit (9.8 m in width x 11.5 in length, 4.5 m in height) : one is for the Cockcroft-Walton DC generator (AP vessel), and the other is for ion source power supply system (SP vessel). The AP vessel is 3.2 m in diameter and 10.7 m in length, and SP vessel is 3.6 m in diameter and 6.7 m in length. The beamline evacuated by two pumps is vertically connected with the AP vessel. The cooling water is supplied from the header placed beside the AP vessel to the ion source/accelerator and the beam target. Especially, the tubes of the cooling water are connected to the ion source/accelerator via the water chock placed inside the AP vessel for high voltage insulation. After drawing into a metal clad placed on the intermediate floor, a commercial electrical line of 50 Hz, 6.6 kV is transformed to 420 V, and then connected with inverter system of 3kHz so as to drive the Cockcroft-Walton DC generator. The inverter system is placed on the power supply room surrounded by fence, from which the high frequency output is supplied to the Cockcroft-Walton DC generator via a coaxial duct. In the power supply room , a circulator recycling the SF6 gas to the vessels is also placed. In opening the vessels, the SF6 gas is stored in two storage tanks placed outdoor. All the instructions is operated in a control room , which is newly constructed. Also, the data acquisition system is in the control room.

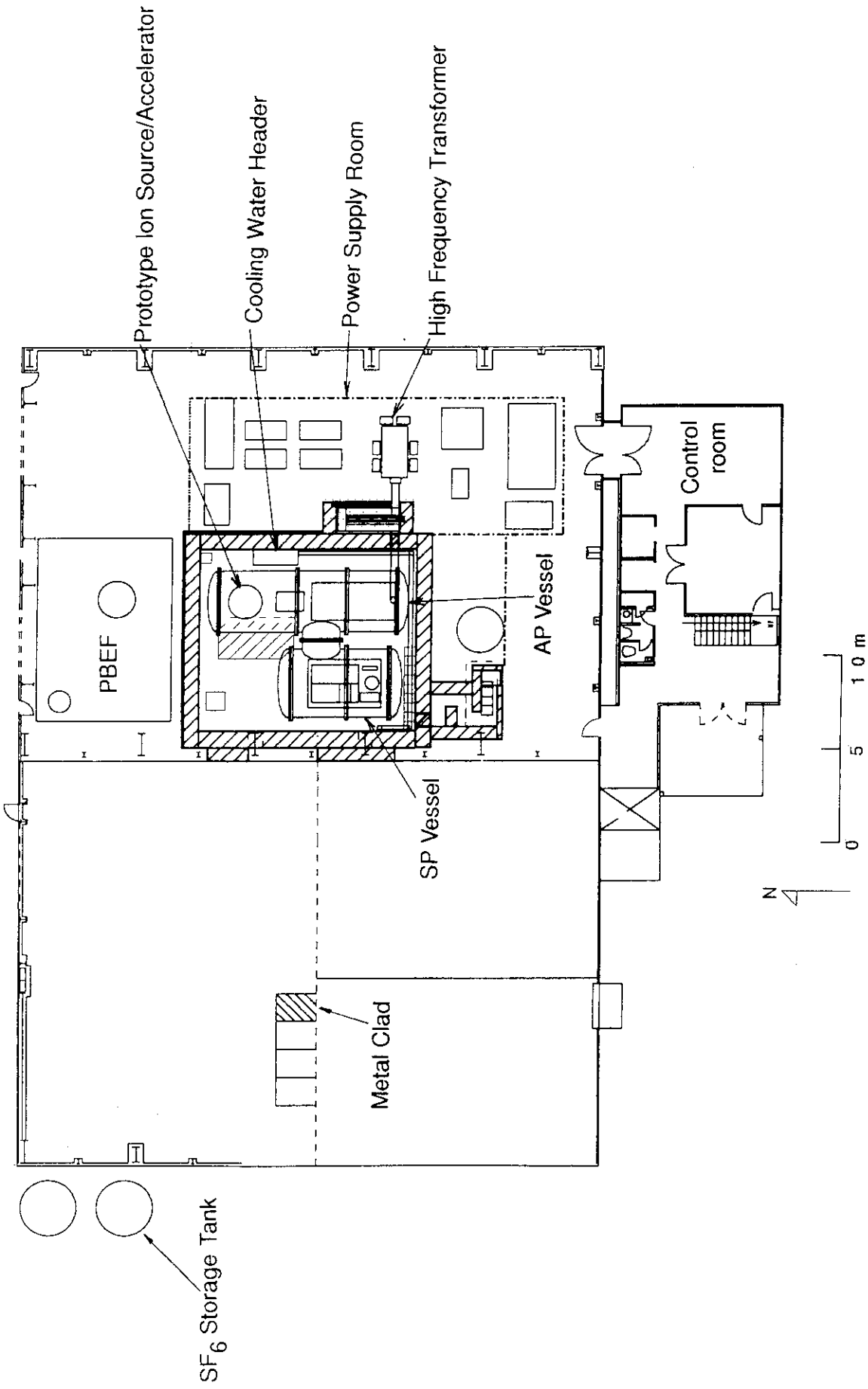

Fig.3.5-1 A layout of MeV Test Facility in the building

4. SUMMARY

(1) Design of the Prototype Accelerator

For a stable acceleration of negative ions, it is important to suppress the ion stripping loss and free electron production due to the collisions of beam ions with gas molecules. Hence, the ion source is designed to operate at a low pressure around 0.1 Pa. The source is a magnetic multipole plasma generator with magnetic filter field, with a semi-cylindrical shape of 34 cm in diameter and 34 cm long. A small amount of cesium vapor is seeded in the source to reduce the operation gas pressure at high negative ion current density.

The electrostatic (ES) accelerator is designed with a capability of accelerating 1 A negative ion beams up to 1 MeV. Two types of acceleration systems have been designed, namely, a multi-multi type and a multi-single type. The overall dimension of the cylindrically-shaped accelerator is approximately 2 m in diameter and 1.5 m high. The negative ion beam is accelerated in five stages. The insulator columns are made of Voidless FRP, of which hight is 240 mm for 200 kV insulation.

(2) Design of the MeV Test Stand

The major components of the Test Stand consist of a Cockcroft-Walton type dc high voltage generator for negative ion acceleration, an ion source power supply system, a surge protection system, auxiliary systems and a X-ray shield. The dc generator is composed of 5 stages and capable of delivering 1 A at 1 MV (1 MW) for 60 s. From each stage, the intermediate acceleration voltages are supplied to the accelerator. The frequency of AC power to the Cockcroft-Walton circuit is 3 kHz. The ion source power supply system is composed of five power supplies, i.e., the cathode, the arc, the bias, the ion extraction, and the electron suppression power supply, which are used to produce 1 A negative hydrogen ions with the energy of up to 10 keV. These power supplies are placed at a high potential which corresponds to the output voltage of the dc generator. The total input power for these power supplies is 100 kVA, which is supplied by a motor-generator driven by an insulated shaft. The surge protection system is designed to suppress the peak current below 2 kA. These major components including the Prototype Accelerator are installed in a SF_6 vessel pressurized at 6 kg/cm^2 to overcome high voltage gradients.

ACKNOWLEDGEMENT

The present design work has been completed through the discussions with other staffs in NBI Heating Laboratory, JAERI Naka. The authors would like to thank S. Shimamoto, the director of Department of Fusion Engineering Research at JAERI, S. Matsuda, the ITER EDA Home Team Leader of Japan and Dr. S Tamura, director of Naka fusion Research Establishment for their continuous encouragement and supports. They are also grateful to Nissin Electric Co. Ltd. and Hitachi Ltd. for their cooperation in the design task.